การสกัดไอออนทองที่ภาวะจุดเริ่มขุ่นโดยใช้พอลิออกซีเอทิลีนโนนิลเฟนิลอีเทอร์

นางกานดา ว่องไวลิขิต

วิทยานิพนธ์นี้เป็นส่วนหนึ่งของการศึกษาตามหลักสูตรปริญญาวิทยาศาสตรดุษฎีบัณฑิต
สาขาวิชาเคมีเทคนิค ภาควิชาเคมีเทคนิค
คณะวิทยาศาสตร์ จุฬาลงกรณ์มหาวิทยาลัย
ปีการศึกษา 2544

ISBN 974-03-1618-2

CLOUD POINT EXTRACTION OF GOLD (III) ION WITH POLYOXYETHYLENE NONYL PHENYL ETHER

Mrs. Kanda Wongwailikhit

A Dissertation Submitted in Partial Fulfillment of the Requirements
for the Degree of Doctor of Philosophy in Chemical Technology
Department of Chemical Technology
Faculty of Science
Chulalongkorn University
Academic year 2001

ISBN 974-03 -1618 -2

Thesis Title	CLOUD POINT EXTRACTION OF GOLD (III) ION WITH POLYOXYETHYLENE NONYL PHENYL ETHER
By	Mrs. Kanda Wongwailikhit
Field of Study	Chemical Technology
Thesis Advisor	Professor Pattarapan Prasassarakich, Ph.D.
Thesis Co-advisor	Professor Makoto Aratono, Ph.D.

Accepted by the Faculty of Science Chulalongkorn University in Partial Fulfillment of the Requirements for the Doctor's Degree

…….. Dean of faculty of Science
(Associate Professor Wanchai Photiphichitr, Ph.D.)

THESIS COMMITTEE

…….. Chairman
(Associate Professor Tharapong Vitidsant, Ph.D.)

……..……. Thesis Advisor
(Professor Pattarapan Prasassarakich, Ph.D.)

…….. Thesis Co-advisor
(Professor Makoto Aratono, Ph.D.)

…….. Member
(Professor Somsak Damronglerd, Dr.Ing.)

…….. Member
(Associate Professor Pornpote piumsomboon, Ph.D.)

…….. Member
(Assistant Professor Solot Suwanayuen, Ph.D.)

กานดา ว่องไวลิขิต : การสกัดไอออนทองที่ภาวะจุดเริ่มขุ่นโดยใช้พอลิออกซีเอทิลีนโนนิลเฟนิลอีเทอร์. (CLOUD POINT EXTRACTION OF GOLD (III) ION WITH POLYOXYETHYLENE NONYL PHENYL ETHER) อ. ที่ปรึกษา : ศ. ดร. ภัทรพรรณ ประศาสน์สารกิจ, อ.ที่ปรึกษาร่วม : Prof. Dr. Makoto Aratono 147 หน้า. ISBN 974-03-1618-2.

งานวิจัยนี้เป็นการศึกษาการสกัดที่ภาวะจุดเริ่มขุ่นของไอออนทองด้วยพอลิออกซีเอทิลีนโนนิลเฟนิลอีเทอร์ (ออกซีเอทิลีน = 9) สารละลายของสารลดแรงตึงผิวนอนไอโอนิกพอลิออกซีเอทิลีน แสดงปรากฏการณ์จุดเริ่มขุ่น ซึ่งเป็นผลจากการไฮเดรชันน้อยลงที่อุณหภูมิสูงขึ้นที่ทำให้การละลายลดลง ที่อุณหภูมิสูงกว่าจุดเริ่มขุ่น สารละลายจะแยกเป็น 2 ชั้น ได้แก่ ชั้นของสารลดแรงตึงผิวและชั้นของน้ำ ตัวถูกละลายใด ๆ ที่เกิดแรงยึดเหนี่ยวกับไมเซลล์ จะถูกทำให้เข้มข้นขึ้นในชั้นของสารลดแรงตึงผิวเมื่อทำให้สารละลายมีอุณหภูมิสูงกว่าจุดเริ่มขุ่น วิธีสกัดสารด้วยจุดเริ่มขุ่นสามารถใช้แยกไอออนทองออกจากไอออนโลหะอื่น เนื่องจากความสามารถเลือกจำเพาะกับทองในไมเซลล์ของพอลิออกซีเอทิลีนโนนิลเฟนิลอีเทอร์ งานวิจัยนี้ทำการศึกษาผลของเวลา อัตราส่วนระหว่างพอลิออกซีเอทิลีนต่อทอง อุณหภูมิการแยกชั้น และ ความเป็นกรดเบสของสารละลาย ต่อร้อยละของการสกัดทอง ผลที่ได้นำไปใช้ในการออกแบบกระบวนการสกัดทองจากไอออนโลหะชนิดอื่น กระบวนการประกอบด้วยการสกัดที่จุดเริ่มขุ่น 2 ขั้น ขั้นแรกสกัดที่ พี-เอช 3 เพื่อสกัดทองออกจากไอออนโลหะอื่น ขั้นที่ 2 ทำการสกัดที่พี-เอช 7 เพื่อแยกทองออกจากสารลดแรงตึงผิว แล้วตกตะกอนโลหะทอง ร้อยละของการสกัดทองที่ได้สูงกว่า 63 โดยความบริสุทธิ์ของทองเท่ากับร้อยละ 98 นอกจากนี้ได้ศึกษาสมการเทอร์โมไดนามิกส์เพื่ออธิบายความแรงของพันธะระหว่างไอออนทองและพอลิออกซีเอทิลีนโนนิลเฟนิลอีเทอร์ ความแรงของพันธะในสารละลายมีลำดับความแรงคือ ที่ พี-เอช 3 มากกว่า พี-เอช 10 และ พี-เอช 7 ตามลำดับ ซึ่งสอดคล้องกับร้อยละของการสกัดทองที่ได้จากการสกัดที่ภาวะจุดเริ่มขุ่น

ภาควิชา	เคมีเทคนิค	ลายมือชื่อนิสิต .....
สาขาวิชา	เคมีเทคนิค	ลายมือชื่ออาจารย์ที่ปรึกษา .....
ปีการศึกษา	2544	ลายมือชื่ออาจารย์ที่ปรึกษาร่วม.....

4173802223 : MAJOR CHEMICAL TECHNOLOGY
KEY WORD: CLOUD POINT EXTRACTION / GOLD EXTRACTION / PH-SWITHCHING / INTERACTION BETWEEN GOLD (III) ION AND PONPE-9 / POLYOXY ETHYLENE NONL PHENYL ETHER

KANDA WONGWAILIKHIT : CLOUD POINT EXTRACTION OF GOLD (III) ION WITH POLYOXYETHYLENE NONYL PHENYL ETHER. THESIS ADVISOR : PROF. PATTARAPAN PRASASSARAKICH, Ph.D., THESIS COADVISOR : PROF. MAKOTO ARATONO, Ph.D., 147 pp. ISBN 974-03-1618-2.

The cloud point extraction (CPE) of gold (III) ion with polyoxyethylene nonyl phenyl ether (oxyethylene =9) was investigated. A solution of polyoxyethylenated nonionic surfactant exhibits cloud point phenomena as a result of less hydration at elevated temperature with subsequent decrease in aqueous solubility. Above the cloud point temperature, the solution seperates into two phases: the surfactant-rich phase and the water-rich phase. Any analytes that can interact with and bind the micellar entity will become concentrated in the surfactant-rich phase upon heating the solution over CP. The CPE methodology can be utilized for separating gold (III) ion from other metals because of the selectivity of gold ion into the micellar of PONPE-9. In this study, the effect of equilibration time, ratio of PONPE-9 to gold, settling temperature, and pH of the solution on extraction efficiency were investigated. The results obtained had been applied to design the process schemes for recovering gold (III) ion from other metal ions. The process consists of two batches of CPE. The first batch was performed at pH 3 for extracting gold (III) ion from other metal ions. The second was conducted at pH 7 for separating gold ion from surfactant. Metallic gold can be precipitated out. Greater than 63% of gold with 98% purity can be recovered. Moreover, the thermodynamic equations for describing the interaction between gold (III) ion and PONPE-9 were proposed. The comparative of that interaction in the solutions is in the order of pH 3> pH 10> pH 7 which is in accordance with the percent extraction of gold obtained by CPE.

Department Chemical Technology Student's signature.....
Field of study Chemical Technology Advisor's signature.....
Academic year 2001 Co-advisor's signature.....

ACKNOWLEDGEMENTS

The author wishes to express her deepest gratitude to her advisors, Professor Pattarapan Prasassarakich and Professor Makoto Aratono for their guidance, encouragement and support given throughout the course of this study.

The author wishes to thank Associate Professor Tharapong Vitidsant, Professor Somsak Damronglerd, Associate Professor Pornpote piumsomboon, and Assistant Professor Solot Suwanayuen for their participation on the dissertation committee; and the National Metal and Materials Technology Center for financial support. The author also wishes to thank the Department of Chemistry, Faculty of Science, Kyushu University for financial support of the thermodynamic study and Department of Chemistry and Physics, Faculty of Science, Rangsit University for this opportunity of this study.

A great thank is expressed to Prof.Kinsi Motomura for his encouragement love like a father, and Prof.Yoshiteru Hayami for his understanding during this period of study. Sincerest appreciation is also extended to Dr.Takanori Takiue for their invaluable suggestions and generous help during this research in Kyushu University, Japan. Here my teacher, Hiroki Matsubara sense, sticks on forever memorial. Many thanks are due to the people in the research group of Professor Makoto Aratono, Ryo Murakami, Yoshimori Kikuchi, Yumi, Akiko, Soichiro, Takata, Ruri, Tamura, Takahara, Eriko, Nami, Matsuda, Tasi, Shin, Ben for their friendly help. Thank also go toward the master students of department of chemistry, faculty of sciences, Kyushu University, Fukuoka, Japan: namely, Akio Ohta, Koichiro Seno, Akiko Nomura, Takahiro Shinozuka who provide the data for thermodynamic study in Chapter 2.

Moreover, the author would like to say thank to all of friends, Dr.Jirawan Teinsuwan, Dr.Marasri Reungjitchchawara, Dr.Nundh Tavarangkul, Mrs.Kamolwan Wongsiri, Mrs.Hataiporn Yamsa-ngapan Mr.Somnuk Bunyasastapan, Mr.Watcharasak Subanpong for their hospitality and standing beside.

Finally, and most of all, the author would like to express her deep gratitude to her family, her friends for their love, inspiration, and endless encouragement throughout this entire study.

CONTENTS

PAGE

CONTENTS (Continued)

PAGE

CONTENTS (Continued)

PAGE

LIST OF TABLES

TABLE **PAGE**

LIST OF FIGURES

FIGURE **PAGE**

LIST OF FIGURES (continued)

FIGURE **PAGE**

LIST OF FIGURES (continued)

FIGURE **PAGE**

LIST OF FIGURES (continued)

FIGURE **PAGE**

LIST OF FIGURES (continued)

FIGURE **PAGE**

LIST OF FIGURES (continued)

FIGURE **PAGE**

NOMENCLATURE

V	: the volume of the actual system
n_i	: total amount (mole) of component i in the system
C_i	: molar concentration of component i
A	: surface area
q	: heat
w	: work
p	: pressure
X_i	: mole fraction of component i
γ	: surface tension
Γ	: surface density
μ	: chemical potential
m_i	: molality of component i
M	: molarity
C	: cmc, critical micelle concentration
g	: gravity
V	: drop volume
ℓ	: plunged distance of needle
r	: radius of capillary
F	: correction factor
m_1	: surfactant molality
Γ_1^{H}	: surface excess density at the interface
T	: absolute temperature
R	: gas constant
$\Delta s(1)$	: entropy associated with the adsorption from the monomeric state in the aqueous solution
s^{H}	: surface excess entropy per unit surface area
s_1	: partial molar entropy of the monomeric surfactant in the aqueous solution
$\Delta s(\mathrm{M})$	: entropy change of the adsorption of surfactant from the micellar state per unit surface area

N_1^{M} : excess number of surfactant molecules in a micelle particle

s^{M} : excess molar entropy of micelle particle

$\Delta_{\mathrm{W}}^{\mathrm{M}} s$: entropy of micelle formation per mole of surfactant from the monomeric state in aqueous solution

$\Gamma_1^{\mathrm{H},C}$: surface density at the cmc

Δs^{C} : entropy change per mole at the cmc

$\Delta_{\mathrm{W}}^{\mathrm{M}} h$: enthalpy change associated with the micelle formation

C_p^{mic} : heat capacity of micellar state of surfactant

C_p^{mono} : heat capacity of monomeric state of surfactant

T_c : critical temperature

X_c : critical surfactant concentration

%E : percent extraction

C_s : concentration of gold (III) ion in surfactant-rich phase

C_w : concentration of gold (III) ion in water-rich phase

M_s : mass of gold (III) ion in surfactant-rich phase

M_w : mass of gold (III) ion in water-rich phase

V_s : volume of surfactant-rich phase

V_w : volume of water-rich phase

$C_{Au,w}$: concentration of gold ion in the water-rich phase

$C_{Au,o}$: initial concentration of gold ion in the solution

m : total molarity

m_{Au} : molality of $HAuCl_4$

m_{PO} : molality of PONPE-9

X_{PO} : mole fraction of PONPE-9 in the mixture

X_{Au} : mole fraction of HAuCl4 in the mixture

C : total molality at cmc of the mixture

C_{Au} : molality of $HAuCl_4$ at cmc of the mixture

C_{PO} : molality of PONPE-9 at cmc of the mixture

C_{PO}^{o} : molality of PONPE-9 at the cmc of the reference

γ^{C} : surface tension at the cmc

Γ^{H} : total surface density in the adsorbed film in the mixture

X_{PO}^{H} : mole fraction of PONPE-9 in the adsorbed film in themixture

$\Gamma_{AuCl_4}^{H}$: surface density of $AuCl_4^-$ in the adsorbed film in the mixture

$\Gamma_{Au(OH)_3}^{H}$: surface density of $Au(OH)_3$ in the adsorbed film in the mixture

$\Gamma_{PO}^{H,o}$: surface density of PONPE-9 in the adsorbed film of the reference

X_{PO}^{M} : mole fraction of PONPE-9 in micelle in the mixture

$X_{PO}^{H,C}$: mole fraction of PONPE-9 in the adsorbed film in the mixture at cmc.

Acronyms

CP : Cloud Point Temperature

CPE : Cloud Point Extraction

C_iE_j : polyetylenegylcol monoalkyl ether

PONPE : Polyoxyethylene Nonyl Phenyl Ether

EG : Ethylene Glycol

EDTA : Ethylenediamine Tetraacetic acid

PEG : Polyethylene Glycol

DMG : Dimethyl Glyoxime

PVA : Polyvinyl Chloride

SLS : Sodium Lauryl Sulfate

SEM : Scanning Electron Microscope

HPLC : High Performance Liquid Chromatography

Superscripts

w : water phase

A : air phase

H : interface, in the adsorbed film

M : micelle

CHAPTER 1

INTRODUCTION

1.1 Introduction

Increasing demand for gold in recent industrial products such as electronic device and catalysts makes it crucial to recover gold from the inevitably increasing waste products from the viewpoint of resource conservation. Since conventional selective dissolution-conditioning and precipitation process for recovering precious metals are labor-intensive, more flexible hydrometallurgical ones such as solvent extraction and ion exchange have attracted special attention. Therefore, the possibility of other alternatives is of interest to turn the ecological waste into valuable commodities.

Cloud point extraction (CPE) is a relatively novel separation method based on an aqueous two-phase system with polyoxyethylenated nonionic surfactant. CPE has been applied for separating some organic compounds and some metals from aqueous media [1,2]. For comparison purposes, the cloud point procedure is superior to or very competitive with all the approaches for the extraction of target analytes. In the CPE approach, no volatile organic solvent is required, which is an important advantage. Other advantages of CPE are that 1) wide variation of the initial analyte concentration does not appreciably alter the extraction recoveries achieved, 2) only a small amount of nonionic surfactant is required to generate the two phases and 3) an affinity cosurfactant can be incorporated into the system to increase the extraction selectivity. Moreover, CPE is potentially industrial process because of its ease of scale up. Instead of using an organic solvent or a water-soluble polymer, a nonionic surfactant can also be employed to form two liquid phases for extraction.

However, nonionic surfactants are not available as pure homogeneous materials. They have a high background absorbance in the ultraviolet region due to the presence of the aromatic moiety in the surfactants employed to date. Also thermally labile analytes can undergo degradation at the temperatures required for phase separation to occur with some of these surfactants.

On the other point of view, thermodynamic approaches are often used for the study of surface properties of the surfactant solution [3]. Recently, there are many

successful reports on the study of the interaction between components in the surfactant solution by applying the developed thermodynamic equation to the experimental surface tension data [4,5]. By use of the excess thermodynamic quantities, some conclusions can be drawn regarding the interaction between components in the solution at different pH conditions.

1.2 Theory

1.2.1 Nonionic Surfactant

In recent years nonionic surfactants have become increasingly important in many applications, such as, pharmaceutical technology, cosmetics, food products, and chemical technology. Similarly, these have found applications as ordered media and used in virtually all fields of analytical chemistry in order to improve existing methods and to develop new analytical procedures [6,7].

Surfactant has two parts in a molecule; a hydrophobic part (tail part) which is a long chain of hydrocarbon, it functions as water hating group. The other is a hydrophilic part (head part) which has a polar group, this part is water liking (e.g. sulphonate, carboxylate, sulphate, phosphate, quarternary ammonium) as shown in Figure 1.1. For nonionic surfactant, the hydrophilic part contains the electronegative atoms such as oxygen and nitrogen which are capable of associating with the hydrogen-bond networking.

Important behaviors of surfactants that explain the majority of observed phenomena are solubilization, adsorption of a surfactant at a surface, and the formation of micelles in a solution. These three phenomena differentiate a surfactant from other chemical entities. It is the abnormal solubility characteristics of surfactants that give adsorption and form micelles. It is the adsorption on the surfaces that gives the surface active effects of foaming, wetting, emulsificating, and dispersing of solids and detergency. It is the micellar properties that give the solution and bulk properties of surfactants such as viscosity and solubilisation.

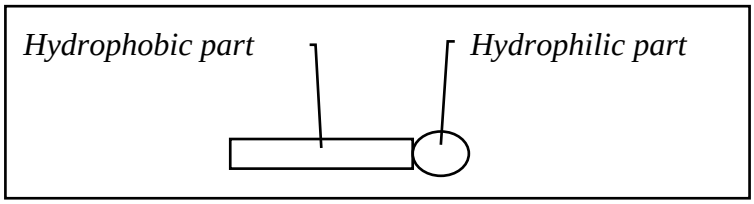

Figure 1.1 Basic structure of a surfactant.

1.2.1.1 Solubility of Surfactants in Water

In the surfactant solution, the water molecules wrap around the hydrophilic part of the surfactant molecules by hydrogen bonding. Then, the more hydrophilic groups in surfactant molecule, the more water molecules extend to make more water-soluble. Surfactant in water has two important effects, hydrophobic and hydrophilic effects [8].

a) The hydrophobic effect

The hydrocarbon chain is insoluble in water. The mechanism involves both enthalpic and entropic contributions and results from the unique multiple hydrogen-bonding capability of water. There is a restructuring or re-orientation of water around nonpolar solute that imposes more ordered structure on the surrounding water molecules, giving a decrease in entropy. Then hydrophobic groups tend to increase the degree of order on water molecules around them.

b) The hydrophilic effect

The hydrophilic group gives disordering effect of water molecule. Polar groups with a highly electronegative character show strong electrophilic properties and make the surfactant molecules soluble in water. The aqueous solubility of surfactant molecule depends upon the relative strengths of the hydrophobic and hydrophilic effect.

Because nonionic surfactants do not ionize in aqueous solution, they have many advantages as detergents and emulsifiers. The inverse temperature-solubility relation of polyoxyethylene surfactants indicates that the over-all solubility of these

materials depends on the extent of hydration of hydrophilic moiety. The water molecules are affixed to the ether oxygens by hydrogen bonding. Consequently, depending on the nature of the hydrophobic group, at least four to six ethylene oxide units per molecule are required to produce a water-soluble surfactant.

1.2.1.2 Adsorption and Critical Micelle Concentration (cmc)

The major characteristics of surfactant is that it is at a higher concentration at the surface than that in the bulk of a liquid. This phenomenon is known as adsorption and occurs at a liquid/solid interface, at a liquid/liquid interface and at a air/liquid interface.

The important properties of surfactant are their properties of being adsorbed at interface and of micelle formation. The adsorption of a surfactant from solution to a surface depends upon the concentration. At very low concentration, there is no orientation and the molecule lies flat on the surface. As the concentration increases, they begin to orient depending on the nature of hydrophilic group and the surface. The orientation of surfactant molecules is going up to a specific concentration of surfactant where the micelle has been formed in the solution. The concentration is known as the critical micelle concentration (cmc).

The cmc of surfactant indicates the point at which monolayer adsorption is almost complete and the surface active properties are at an optimum. Hence, there is considerable practical interest in cmc as it represents, in practice, the lowest concentration need to get the maximum benefit.

The determination of the value of the cmc can be made by use of any of physical properties, but most commonly the breaks in the electrical conductivity, surface tension, light scattering, or refractive index concentration curves have been used for this purpose. In this work, cmc was evaluated by the extinct break point obtained from the surface tension versus surfactant concentration.

1.2.1.3 Effect of Head Size of Surfactant to Micelle Shape

At the concentration higher than cmc, surfactant molecules aggregate to form a colloidal-sized cluster in solution, called micelle. In aqueous media, the surfactant molecules in micelle are oriented with their hydrophilic heads toward the aqueous

phase and their hydrophobic groups away from it. It is important to understand that the structure and shape of the micelle can change and that the micelle is a dynamic entity [8]. Depending upon the conditions, micelles can form spherical, rod shape or lamellar shape, neat structure (see Figure 1.2).

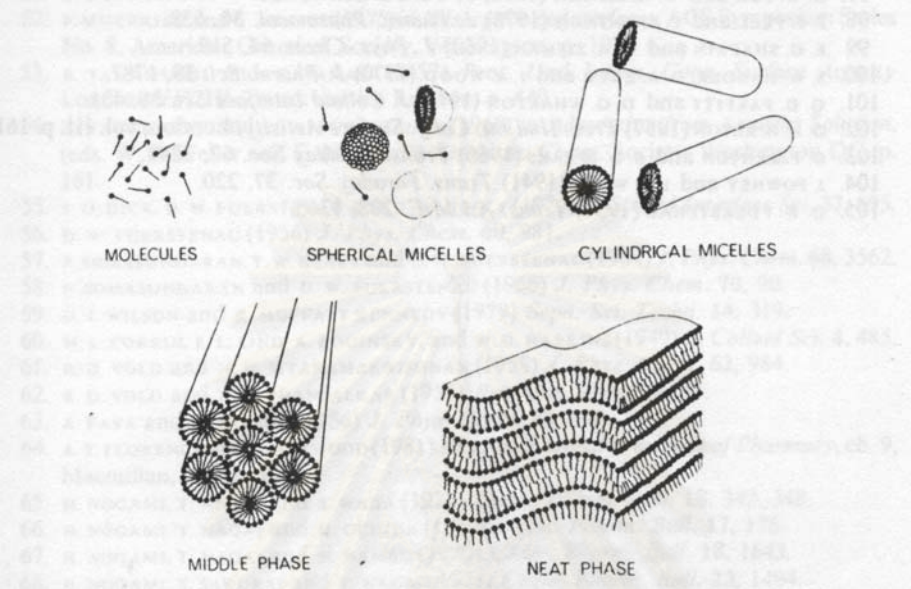

Figure 1.2 Schematic representation of idealized structure of surfactant [9].

Changes in temperature, concentration of surfactant, additives in the liquid phase, and structure groups in the surfactant may all cause changing in size, shape, and aggregation number of micelle, with the structure varying from spherical through rod- or disklike to lamellar in shape [9,10].

A theory of micellar structure, based upon the geometry of various micellar shapes and the space occupied by the hydrophilic and hydrophobic groups of the surfactant molecules, has been developed by Israelachvili et al. [8]. The area occupied by the hydrophobic group and the hydrophilic group was defined by:

Hydrophilic group area = a_o

Hydrophobic group area $a_h = v/l_c$ where v is the alkyl chain volume and l_c its maximum length

Micelle shape can be approximately determined by the relation of surfactant number ($a_h/a_o = v/a_o l_c$) as in Table 1.1

Table 1.1 Relation between surfactant number and micellar structure

$v/a_o l_c$	Predicted micellar structure
≤ 1/3	Spherical micelles
1/3 – ½	Cylindrical micelles
½ - 1	Bilayers, vesicles, lamellar in aqueous media
≥ 1	Inverse structures

In general, the head size affects on the shape of micelle in the order that the smaller head size, the higher the surfactant number and the micellar shape changes downward the table. Parameters, that affect the head size of surfactant such as solution temperature and electrolyte concentration, change micellar shape.

In aqueous solutions, micelle likes to be in form O/W (oil in water) where its heads are outer around micelle as in Figure 1.3b. An increase in temperature appears to cause dehydration of the polyoxyethylene chain, then to yield a decrease in head size, consequently to accompany a change in micellar structure toward the lamellar structure. It may turn o/w structure to water in oil (W/O) structure as shown in Figure 1.3c.

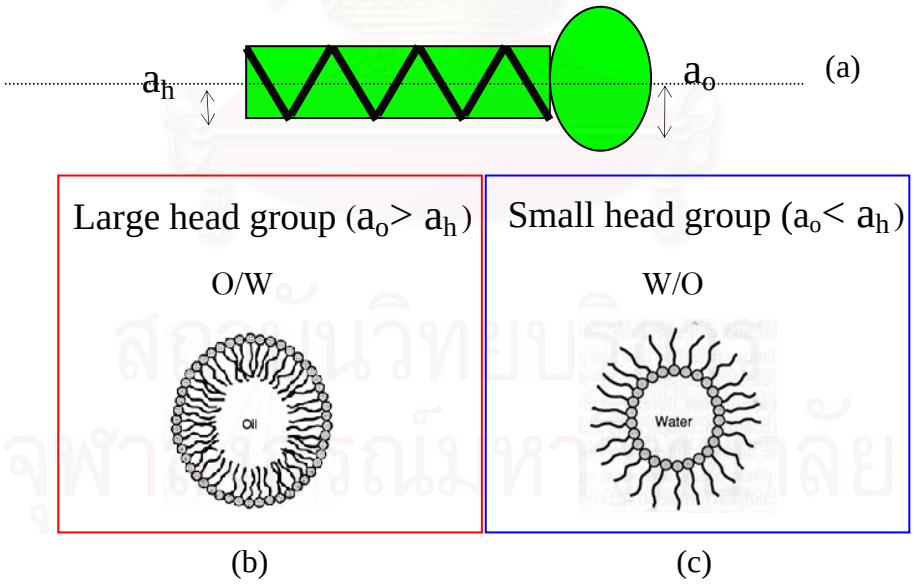

Figure 1.3 Schematics of micelle shape of different head size [8].

1.2.1.4 Polyoxyethylene Nonyl Phenyl Ether Surfactant

Polyoxyethylenated nonionic surfactant posses the series of ethylene oxide group as the hydrophilic part of the molecule. Polyoxyethylene nonyl phenyl ether (PONPE) is one of the worldwide products due to the stability to hot dilute acidic, alkali, and oxidizing agent [10]. Its hydrophobic part composes of a nonyl hydrocarbon chain and the polyoxyethylene series as a hydrophilic part in addition to a phenyl group between those two parts. The structure of PONPE is shown in Figure 1.4. In this work, PONPE-9 is employed as the media for phase separation in which the number of oxyethylene (n) is about 9.

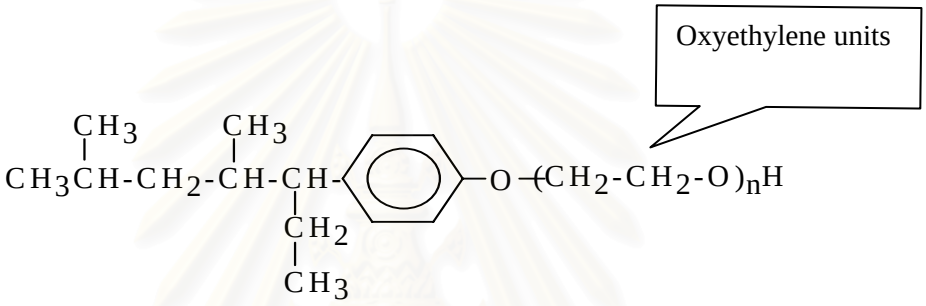

Figure 1.4 Polyoxyethylene nonyl phenyl ether (PONPE).

Polyoxyethylenated nonionic surfactant shows abnormal solubility characteristics compared to most other chemical compounds. The solubility of most common chemical compounds in water increases as the temperature rises and furthermore the solubility of ionic surfactants increases dramatically above a certain temperature known as the krafft point. In contrast to this, the solubility of polyoxyethylenated nonionic surfactant decreases dramatically above a certain temperature known as the cloud point. The increasing temperature diminishes the hydrogen bonding between water molecules and hydrophilic groups of surfactant, causing dehydration, and then results in a smaller head size of the surfactant. Then, micelle shape is changed to get lamellar shape where aggregation numbers get high enough that can not be dissolved in water. The micelle shape can be in form of water in oil (W/O) at a higher temperature as in Figure 1.5

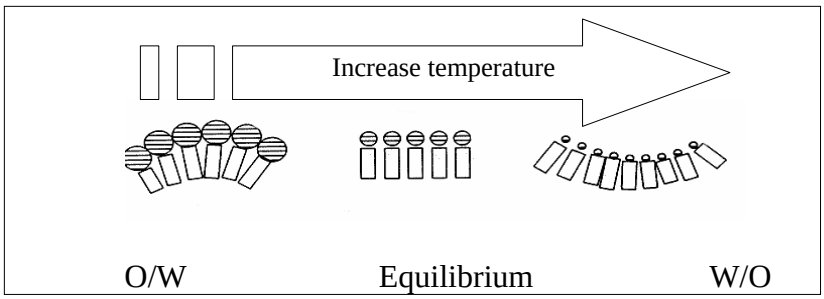

Figure 1.5 Temperature effect to micelle shape of polyoxyethylenated nonionic surfactant [8].

1.2.2 Cloud Point of PONPE

The solubility of polyoxyethyleneated surfactants in water is related to the hydration of ether oxygens of polyoxyethylene groups. An increase in temperature causes dehydration owing to the decrease in a number of hydrogen bonds, which raise the micellar weight and decrease the cmc.

If the temperature continues to increase, the micelles become so large and the number of intermicellar interactions increases to such an extent that a sudden onset of turbidity is perceptible even to the naked eyes. This temperature is called the cloud point (CP) (see Figure 1.6). A further rise in temperature causes the solution to begin to separate into two phases: One surfactant-rich phase (surfactant-coacervage phase) and the other water-rich phase (surfactant-depletion phase) in which containing the surfactant at the concentration close to cmc (see Figure 1.7).

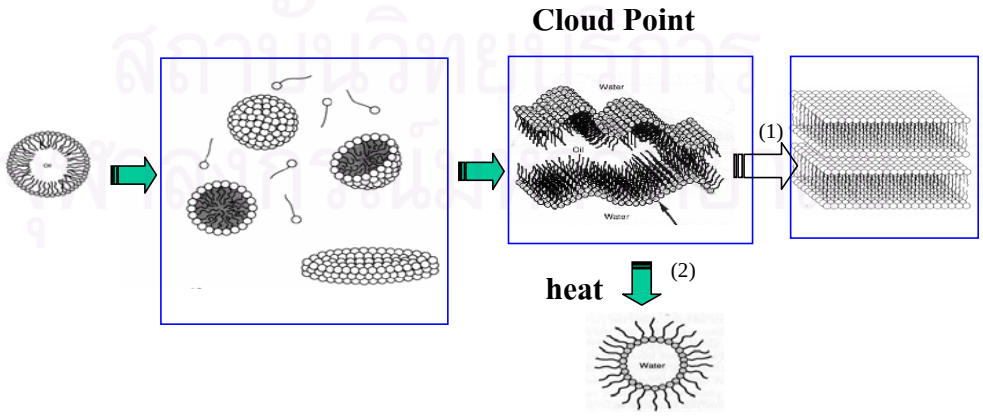

Figure 1.6 Schematic representations of cloud point phenomena of polyethoxylated nonionic surfactant [8].

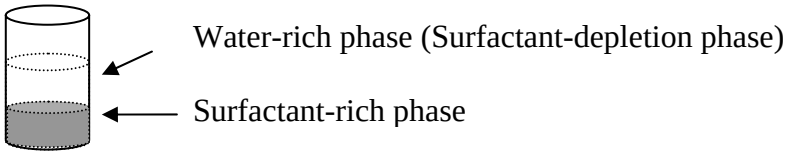

Figure 1.7 Representation of surfactant-rich phase and water-rich phase.

The separation is believed to be due to the sharp increase in the aggregation number of the micelles and the decrease in intermicellar repulsion resulting from the decreased hydration of the oxyethylene oxygens in the polyoxyethylene hydrophilic group with increase in temperature. As the temperature increases, micellar growth and increased intermicellar attraction cause the formation of particles that are so large that the solution becomes visibly turbid. Phase separation occurs because of the different in density of the surfactant-rich and the water-rich phases [11]. Generally separation into two phases is achieved by increasing the temperature. By decreasing temperature below the cloud point, the surfactant and water mixture becomes homogeneous again, since the system is reversible.

1.2.3 Effects on Cloud Point

The cloud point temperature depends on the length of hydrophilic group (oxyethylene units) and hydrophobic group (alkyl chains) groups. For a particular hydrophilic group, the larger the percentage of oxyethylene in the surfactant molecule, the higher the cloud point, although the relation between oxyethylene percentage and cloud point is not linear.

Surfactant concentration has an influence to cloud point temperature depending on types and structure of surfactant. However, surfactant concentration has less influence compared to the concentration of the additives, which are usually inorganic salts and polyalcohols.

The concentration of salts and some additives affect in a great extent on the alternation of CP. In general, the effect of adding electrolytes to nonionic systems seems to result in droping in the CP whereas the addition of some organic compounds results in an increase. The change in the CP of nonionic surfactant due to the addition of electrolyte has been attributed mainly to the “salting out” or “salting in” of the hydrophobic groups in the aqueous solvent by the electrolyte, rather than to the effect

of the latter on the hydrophilic groups of the surfactant [10]. This results in a change in the activity coefficients of the solute.

Polyoxyethylenated surfactant also shows a variation in solubility depending on their ionic solution environments. These frequently complex effects may involve either specific interactions between charged side chains and ions in solution or, particularly at high salt concentration, reflect more comprehensive changes in the solvent properties. The effects of salts on increasing the solubility of organic substance in water is often referred to as salting-in. Opposite behavior found on decreasing solubility is called salting-out.

a) Salting-out

Often the polyoxyethylenated surfactant will still have a certain affinity to water. In order to decrease that affinity, an ionic salt like a NaCl solution is added to the water layer. This will increase the ionic character of the water layer. The increase in the ionic strength of the water layer will drive the non-polar hydrophobic species into the organic layer away from the ionic water layer. The ions from the added salt solution will attract the water molecules in an effort to solvate the ions. This releases the water molecules from any solvation with the ether oxygens atoms.This results in a decrease of head size of the surfactant and subsequently in a change in micellar shape as stated above. When the monomeric form of surfactant is salted out by the presence of an electrolyte, micellization is favoured and the CP is decreased.

b) Salting-in

At very low ionic strength, a phenomenon known as “salting-in” occurs. When some species are added into the surfactant solution and accompanied with the reduction in an ionic strength of the solution due to the interactions between hydrophilic part of the surfactant and added species, this results an increase of head size of the surfactant and the disordering of the water molecules in the solution. Thus, micellization are not favorable, consequently, the CP is increased. Hence, if the monomeric surfactant is salted in, CP of the solution is risen up.

The effects of anion and cation in the electrolyte are additive and appear to depend on the radius of the hydrated ion, that is, the lyotropic number; the smaller the radius of the hydrated ion, the greater the effect [11].

1.2.4 Cloud Point Extraction (CPE)

The unique phenomenon, CP, permits the design of simple schemes for extraction, preconcentration and purification. Any analyte which being soluble in water is able to interact with and bind to micelles after raise the temperature over CP, can be concentrated in the surfactant rich phase. This criterion has been developed and claimed as a novel technique called Cloud Point Extraction (CPE). Its application participates on separation and recovers some substances such as polyaromatic hydrocarbon and metals which have interaction with the nonionic surfactant. This method is used in water-base system, therefore it saves the environment.

Distinct features of CPE are solute-surfactant interaction occurring in the homogeneous phase before separation. Thus, this method can be applied to separate a specific solute, which has interacted with surfactant, from the others that do not bind to the surfactant molecules.

1.2.4.1 Parameters Influence on CPE

The extraction efficiency using CPE methodology is influenced by many parameters as following:

1) pH of the solution
2) Settling temperature
3) Equilibration time
4) The ratio of surfactant to analyte

a) pH of the solution

Solution pH is an important factor in those cloud point extractions involving analytes that possess an acidic or basic moiety. At low pH, nonionic surfactants that having polyoxyethylene chains can be protonated, yielding positively charged

groupings called oxonium ion that may adsorb onto negative analysts [10]. At high pH, hydroxyl ion binds with polyoxyethylene chains with hydrogen-bonding give a negatively charged grouping [11]. However, solution pH also affects to the target analytes. Therefore, the optimization for solution pH is a requirement for a CPE system.

b) Settling temperature

The equilibration temperature is one of the most influencial factors on to the effectiveness of the extraction. Too low or too high settling temperature may induce the poor phase separation yielding low extraction efficiency. It was reported that the equilibration temperature providing good percentage of extraction should be 15-20 ^{o}C higher than CP of the initial solution [1]. The optimum settling temperature for extraction apparatus should be one of the experimental parameters.

c) Equilibration time

The time of equilibration at elevated temperature above CP is of interest according to the shortest time period required for complete separation of phases. The kinetic rate for the separation would suggest the equilibrium on phase partition.

d) Ratio of PONPE-9 to gold ion

It is known that the extraction efficiency is induced with an affinity binding between the nonionic surfactant and the target analyte. The binding ratio between surfactant and analyte is one of the effective parameter to provide the maximum efficiency. It is possible that the optimum ratio for extraction study would not equal to the conformation ratio. That is attributable to the purity of both surfactant and analyte.

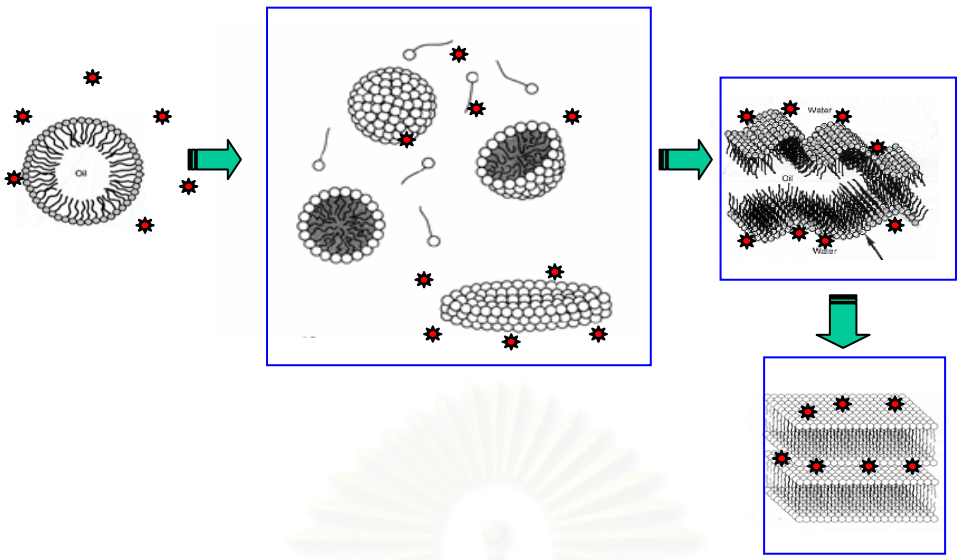

Figure 1.8 Schematic diagram representation of cloud point extraction [8].

1.2.5 Thermodynamic Equation for Surfactant System

Thermodynamic method is constructed to study the phenomena of surfactant in mixture and interpret the thermodynamic analysis to explain the interaction between components in the surfactant solution. According to this approach, the composition of surfactant and ion at the interface and that in micelle can be evaluated by the surface tension measurement. Therefore, the interaction phenomenon in the mixture can be investigated.

Gibbs (1878) treated the interfacial layer as a two–dimensional surface phase that has zero volume but nonzero values of other thermodynamic properties. This method is widely used for studying interfacial phenomena of surfactant [3,9,10].

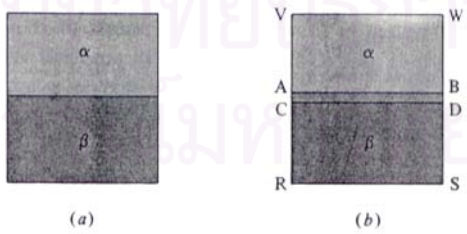

Figure 1.9 Schematic diagram representation of interfacial layer between two phases [3].

In Gibbs approach, the actual system of Figure 1.9b (which consists of bulk phase α and β plus the interphase region) is replaced by the hypothetical model

system of Figure 1.9a. In the model system, phase α and β are separated by a surface of zero thickness, the Gibbs dividing surface. Phase α and β on either side of this dividing surface are defined to have the same intensive properties as bulk phase α and β, respectively, in the actual system. The location of the dividing surface in the model system is somewhat arbitrary but generally corresponds to a location within or very close to the interphase region of the actual system. Experimentally measurable quantities must be independent of the choice of location of dividing surface, which is just a mental construct. The Gibbs model ascribes the thermodynamic quantities inherent in the interface to the one dividing surface whatever values of thermodynamic properties are necessary to make the model system having the same total volume, internal energy, entropy, and amount of components that the actual system has.

Let σ denote a thermodynamic property of the dividing surface. From the assumption, the dividing surface has zero thickness and zero volume

$$V^{\sigma} = 0 \tag{1.1}$$

We put V to be the volume of the actual system and V^{α} and V^{β} are the volumes of phase α and β in the model system. Then, from

$$V = V^{\alpha} + V^{\beta} + V^{\sigma} \tag{1.2}$$

So,
$$V = V^{\alpha} + V^{\beta} \tag{1.3}$$

If n_i is the total amount of component i in the system, n^{α}, n^{β} and n^{β} are the amount of component i in α, β, and σ, respectively.

$$n_i^{\alpha} = c_i^{\alpha} V^{\alpha}, \; n_i^{\beta} = c_i^{\beta} V^{\beta} \tag{1.4}$$

where c_i^{α} is the molar concentration of component i in the bulk phase α

c_i^{β} is the molar concentration of component i in the bulk phase β

We have
$$n_i = n_i^{\alpha} + n_i^{\beta} + n_i^{\sigma} \tag{1.5}$$

and
$$n_i^{\sigma} = n_i - n_i^{\alpha} - n_i^{\beta} = n_i - (c_i^{\alpha} V^{\alpha} + c_i^{\beta} V^{\beta}) \tag{1.6}$$

where n_i^{σ} is the surface excess amount of component i and can be either positive, negative, or even zero. The definition states that the surface excess amount of n_i^{σ} is the difference between the amount of i in the actual system and that in the system if

the homogeneity of the bulk phases α and β is persisted right up to the dividing surface.

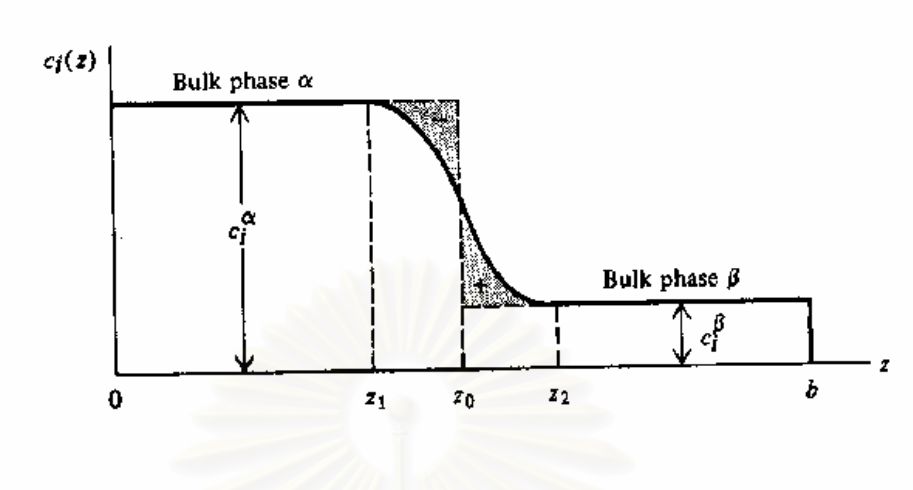

Figure 1.10 Schematic illustration of surface excess [3].

The value of n_i^{σ} depends on the location of the dividing surface. From the Figure 1.10, C_i of the component *i* in an actual system varies with z coordinate as shown by $c_i(z)$ curve. The interfacial region is between z_1 and z_2 and the dividing surface is placed at z_0.

a) Gibbs Adsorption Isotherm

Surface excess amount of i is defined as $n_i^{\sigma} = n_i - (C_i^{\alpha}V^{\alpha} + C_i^{\beta}V^{\beta})$ (1.7)

The quantity results from the presence of the interface and is dependent on the shape of the concentration profile of i in the transition region between α and β. From a practical standpoint, the surface excess can also be considered to be amount of i adsorbed at the surface.

Surface excess concentration, $\Gamma_i^{(\sigma)} = \frac{n_i^{\sigma}}{A^{\sigma}}$ (1.8)

b) The Gibbs Adsorption Equation

The first law of thermodynamics for a close system ; $du = dq + dw$

For a reversible process ; $dq = Tds$

In a two-phase system ; $dw_{rev} = -pdV + \gamma dA^{\sigma}$

Therefore, for a close system $du = Tds - pdV + \gamma dA^{\sigma}$ (1.9)

For an open system ; $du = Tds - pdV + \gamma dA + \sum_i \mu_i dn_i$ (1.10)

For the phase α ; $du^{\alpha} = Tds^{\alpha} - pdV^{\alpha} + \sum_i \mu_i dn_i^{\alpha}$ (1.10a)

For the phase β ; $du^{\beta} = Tds^{\beta} - pdV^{\beta} + \sum_i \mu_i dn_i^{\beta}$ (1.10b)

From the definition of the surface excess quantities,

$$du^{\sigma} = du - du^{\alpha} - du^{\beta},$$

$$ds^{\sigma} = ds - ds^{\alpha} - ds^{\beta},$$

$$dV = dV^{\alpha} + dV^{\beta},\ dn_i^{\sigma} = dn_i - dn_i^{\alpha} - dn_i^{\beta}$$

Then we have $du^{\sigma} = Tds^{\sigma} + \gamma dA^{\sigma} + \sum_i \mu_i dn_i^{\sigma}$ (1.11)

Integrating Eq. 1.11 for a process in which the size of the model system is increased at constant temperature, T, and pressure, p, and concentration in the phase, starting from state 1 and ending at state 2, we have

$$u^{\sigma} = Ts^{\sigma} - \gamma A^{\sigma} + \sum_i \mu_i n_i^{\sigma} \quad (1.12)$$

because the intensive variables T , γ, and chemical potential, μ_i, are constant and can be taken outside the integral sign.

Therefore

$$du^{\sigma} = Tds^{\sigma} + s^{\sigma}dT + A^{\sigma}d\gamma + \gamma dA^{\sigma} + \sum_i \mu_i dn_i^{\sigma} + \sum_i n_i^{\sigma} d\mu_i \quad (1.13)$$

The sign of the γdA^{σ} is positive rather than negative because γ is conceived of as a tension (pulling) rather than a pressure (pushing).

Finally, the Gibbs adsorption isotherm at the interface has been given by subtracting Eq. 1.5 as ;

$$s^{\sigma}dT + A^{\sigma}d\gamma + \sum n_i^{\sigma} d\mu_i = 0 \quad (1.14)$$

This equation is the analog of Gibbs-Duham equation of a bulk phase.

At constant temperature, Eq. 1.14 is reduced to

$$-d\gamma = \frac{\sum n_i^{\sigma} d\mu_i}{A^{\sigma}} = \sum \Gamma_i^{\sigma} d\mu_i \quad (1.15)$$

For the two component liquid-vapor system where the Gibbs dividing surface is defined so that the surface excess concentration of the solvent is zero $\left(\Gamma^{\sigma}=0\right)$, the Gibbs adsorption equation for solute is

$$d\gamma = -\Gamma_2^{(1)}\, d\mu_2, \tag{1.16}$$

where 2 designates a solute dissolved in bulk phase 1. At equilibrium, the chemical potential of each component is equal in all phases, so that μ_i at the interface can be taken as that value in either of adjacent bulk phases. The chemical potential of 2, then, can be related to its concentration in either of the bulk phases by

$$d\mu_2 = RT\, d\, ln a_2^{(1)} = RT\, d\, ln X_2\theta_2 \tag{1.17}$$

where $a_2^{(1)}$ is the activity of 2 in (1) bulk phase, X_2 is its mole fraction, and θ its activity coefficient which can be approximated as unity in dilute solution and the last term in Eq. 1.17 can be substituted by the molar concentration, c_2.

Thus, in a dilute solution, this leads to the relationship

$$\Gamma_2^{(1)} = -\frac{1}{RT}\left[\frac{d\gamma}{d\, lnc_2}\right] \tag{1.18}$$

This equation is called Gibbs adsorption equation.

c) Mixed surfactant system

The mixture often exhibits new phenomena which are not found in their respective pure surfactant systems. There are many approaches to study the behavior of surfactant mixture provided useful information. The surface excesses of two surfactants are estimated by use of Gibbs adsorption equation. It is remarked that the mixed adsorbed films of homologous surfactants behave like an ideal mixture. Some researchers point out that those thermodynamics were incomplete because of no accounting of solvent behavior and ignoring the dissociation of ionic surfactants. Other models for mixed micellization have been developed by several researchers. Motomura et al. showed that the composition of surfactants in a mixed adsorbed film can be estimated directly from surface tension measurements without introducing such assumption [4]. They also treated micelles as a macroscopic bulk phase and assumed that intramicellar thermodynamic quantities can be given by the excess thermodynamic functions similar to those used for the adsorbed film. From their

studies, they could evaluate the composition of the mixed micelles. This method made it possible to compare the composition in the adsorbed film with that in the micelle at the cmc.

For the system consisting of air and the aqueous solution of nonionic surfactant 1 and 2, the Gibbs-Duham equation of the system is given by

$$sdT - Vdp + Ad\gamma + n_w d\mu_w + n_1 d\mu_1 + n_2 d\mu_2 + n_a d\mu_a = 0 \qquad (1.19)$$

Here the subscripts w, 1, 2, and *a* designate water, surfactant 1, surfactant 2, and air, respectively. Air is assumed to be a pure component. For the homogeneous regions in the water and air phases at a great distance from the surface, the corresponding equations can be applied

$$s^w dT - dp + c_w^W d\mu_w + c_1^W d\mu_1 + c_2^W d\mu_2 + c_a^W d\mu_a = 0 \qquad (1.20)$$

and

$$s^a dT - dp + c_w^a d\mu_w + c_1^a d\mu_1 + c_2^a d\mu_2 + c_a^a d\mu_a = 0, \qquad (1.21)$$

where s and c_i are the entropy and number of moles of component *i* per unit volume, respectively.

The definition of Γ_i^H is

$$\Gamma_i^H = \frac{n_i - (V^w c_i^w + V^a c_i^a)}{A}, \qquad (1.22)$$

which is the excess number of moles of surfactant *i* per unit area at the interface with reference to the two dividing planes that are parallel to the surface and satisfy the relations.

$$\Gamma_w^H = \frac{n_w - (V^w c_w^w + V^a c_w^a)}{A} = 0 \qquad (1.23)$$

and

$$\Gamma_a^H = \frac{n_a - (V^w c_a^w + V^a c_a^a)}{A} = 0 \qquad (1.24)$$

Further, the corresponding thermodynamic quantity y^H is defined by

$$y^H = \frac{Y - (V^w y^w + V^a y^a)}{A} \qquad (1.25)$$

Subtracting Eqs. 1.20 and 1.21 multiplied by V^W and V^a, respectively, from Eq. 1.19 and then substituting Eqs. 1.22- 1.25 into the result equation, it is obtained as

$$d\gamma = -s^{H}dT + v^{H}dp - \Gamma_1^{H}d\mu_1 - \Gamma_2^{H}d\mu_2 \quad (1.26)$$

This is fundamental equation which describes the adsorption behavior of the nonionic surfactant mixture.

To study the miscibility of surfactants, it is convenient to employ the total molality of mixture defined by

$$m = m_1 + m_2 \quad (1.27)$$

and the mole fraction of surfactant *i* in the total surfactant by

$$X_i = \frac{m_i}{m_1 + m_2} \quad (1.28)$$

where m_i is the molality of surfactant *i*. Assuming that the solution is ideally dilute solution, the total differentials of the chemical potentials of the surfactants are expressed as

$$d\mu_1 = -s_1 dT + v_1 dp - \frac{RT}{m}dm - \frac{RT}{X_1}dX_1 \quad (1.29)$$

and

$$d\mu_2 = -s_2 dT + v_2 dp - \frac{RT}{m}dm + \frac{RT}{X_2}dX_2 , \quad (1.30)$$

where y_i is a dummy variables to represent the partial molar thermodynamic quantity of surfactant *i* in the solution. Substitution of Eqs 1.29 and 1.30 into Eq. 1.26 and rearrangement of the resulting equation yields

$$d\gamma = -\Delta s\, dT + \Delta v\, dp - \frac{RT\ \Gamma^{H}}{m}dm - \frac{RT\ \Gamma^{H}}{X_1 X_2}(X_2^{H} - X_2)\, dX_2 \quad (1.31)$$

where Γ^{H} is the total excess number of moles of mixture defined by

$$\Gamma^{H} = \Gamma_1^{H} + \Gamma_2^{H} \quad (1.32)$$

and X_2^{H} is the mole fraction of surfactant 2 in the adsorbed film defined by

$$X_2^{H} = \frac{\Gamma_2^{H}}{\Gamma_1^{H} + \Gamma_2^{H}} \quad (1.33)$$

Further, Δy is the thermodynamic quantity of the interface formation defined by

$$\Delta y = y^{H} - (\Gamma_1^{H} y_1 + \Gamma_2^{H} y_2) \quad (1.34)$$

Therefore, if the γ valve is measured experimentally as a function of m and X_2 at constant T and p, the value of Γ^{H} and X_2^{H} are found to be evaluated by the use of the relations

$$\Gamma^{H} = -\frac{m}{RT}\left(\frac{\partial\gamma}{\partial m}\right)_{T,p,X} \tag{1.35}$$

$$X_2^{H} = X_2 - \frac{X_1 X_2}{RT\Gamma^{H}}\left(\frac{\partial\gamma}{\partial X_2}\right)_{T,p,m} \tag{1.36}$$

and

$$X_2^{H} = X_2 - \frac{X_1 X_2}{m}\left(\frac{\partial m}{\partial X_2}\right)_{T,p,\gamma} \tag{1.37}$$

where the subscript X stands for X_2. This approach provides useful information regarding the miscibility of surfactants in the adsorbed film.

On the other hand, the thermodynamic behavior of surfactants in the mixed micelle is described by the analogue of Eq. 1.26

$$s^{M}dT - v^{M}dp + N_1^{M}d\mu_1 + N_2^{M}d\mu_2 = 0 \tag{1.38}$$

where y^{M} is a dummy variables to represent the excess molar thermodynamic quantity of mixed micelle with reference to the dividing spherical interface which makes the excess number of moles of water zero and N_i^{M} is the corresponding number of molecules of surfactant i in one micelle particle. Taking into account that the micelle formation is treated thermodynamically like the appearance of macroscopic bulk phase and m on the right sides of Eqs.1.29 and 1.30 is replaced by the cmc, C, in a limited concentration range near the cmc, Eq. 1.38 is rewritten as

$$\frac{RT}{C}dC = -\Delta_w^{M}s\,dT + \Delta_w^{M}v\,dp - \frac{RT}{X_1 X_2}(X_2^{M} - X_2)\,dX_2 \tag{1.39}$$

where we have introduced the quantities

$$\Delta_w^{M}y = \frac{y^{M} - (N_1^{M}y_1 + N_2^{M}y_2)}{N_1^{M} + N_2^{M}} \tag{1.40}$$

and

$$X_2^{M} = \frac{N_2^{M}}{N_1^{M} + N_2^{M}} \tag{1.41}$$

The above equation yields the following relation at constant T and p.

$$X_2^{M} = X_2 - \frac{X_1 X_2}{C}\left(\frac{\partial C}{\partial X_2}\right)_{T,p} \tag{1.42}$$

Since the value of C is estimated concomitantly as a function of X_2 , if γ is measured through a wide range of m as function of X_2 at constant T and p , the composition of mixture in the micelle can be evaluated by experimentally.

From those, it is possible to consider the equilibrium between the mixed adsorbed film and mixed micelle at the cmc. Since Eq. 1.31 is appliciable to the adsorbed film even at the cmc, then

$$d\gamma^{C} = -\Delta s^{C} dT + \Delta v^{C} dp - \frac{RT\,\Gamma^{H,C}}{C} dC - \frac{RT\Gamma^{H,C}}{X_1 X_2}(X_2^{H,C} - X_2)\, dX_2 \tag{1.43}$$

Therefore, the following equation is derived at constant T and p:

$$X_2^{H,C} = X_2^{M} - \frac{X_1 X_2}{RT\,\Gamma^{H,C}}\left(\frac{\partial \gamma^{C}}{\partial X_2}\right)_{T,p} \tag{1.44}$$

From these equations, it is provided that the plot γ^{C} versus X_2 curve gives information on the relationship between $X_2^{H,C}$ and X_2^{M}, whereas the m versus X_2 curve provides information about the dependence of X_2^{H} on X_2. In this connection, it should be emphasized that the C versus X_2 curve is closely associated with the dependence of X_2^{M} on X_2.

1.3 Literature Review

The cloud point methodology has been used in different analytical applications: preconcentration of several metal ions has been originally reported by Watanabe et al. using PONPE-7.5. PAN (1-(2-pyridylazo)-2-naphthol) was used as a chelating agent for CPE of nickel in soil and zinc in tap water [12]. The function of the chelating agent is to form an insoluble or sparingly water soluble complex with the metal ion and introduce some selectivity into the process. The cloud point of the dilute micellar solution of PONPE-7.5 is about 1 ^{o}C and hence the solution is turbid at room temperature. The two phases were separated by centrifuging. The recovery

percentage of zinc reached to about 93 % at pH 10 while that of nickel was about 91%.

In 1981, the scope of cloud point extraction was extended by Bordier to include protein separation [13]. Hydrophilic proteins were found exclusively in the aqueous phase, and integral membrane proteins with an amphiphilic nature were recovered in the surfactant-rich phase. The poly(oxyethylene)-7.5-(p-tert-octylphenyl) ether (Triton X-114) was used to solubilize membranes and whole cells, and the soluble material was submitted to phase separation. Integral protein can thus be separated from hydrophilic proteins and identified as such in crude membrane or cellular detergent extracts. Thermal phase partitioning has been employed as an analytical procedure in cellular and molecular biology.

Alcaraz et al. studied the phase separation of the receptor for immunoglobulin E and its subunits in Triron X-114 [14]. Immunoglobulin E (IgE) and IgE complexed either with intact receptors or with the α-chains of the receptor alone were principally partitioned into the upper phase of surfactant-depletion phase, whereas the unliganded receptor as well as the isolated α, and especially the β and γ chains of the receptor, preferentially are partitioned into the surfactant-rich phase.

Ganong and Delmore investigated the phase separation temperature of mixtures of Triton X-114 and Triton X-45 and then applied to separate protein (Bovine) [15]. Bovine brain particulate fraction at 5 mg/mL protein was solubilized with either Triton X-114 or Triton X-114/Triton X-45 (9:1 w/w) at a final concentration of 5%. On phase separation and centrifugation, 84% of recovered activity was found in the surfactant-rich phase using Triton X-114, and 79% using the mixtures of Triton X-114 and Triton X-45.

Recently, CPE has been extended in the design of the preconcentration of some organic compounds and some metal ions as a step prior to the concentration measurement by high-performance liquid chromatography (HPLC) and atomic absorption (AA). Ahel and Giger studied the preconcentration of alkylphenols and alkylphenol mono-and diethoxylates in environmental sample using Triton X-100 as a separation media [16]. Garcia Pinto et al. preconcentrated polycyclic aromatic

hydrocarbons and organophosphorus pesticides in the surfactant rich phase of Triton X-114 before the measurement by HPLC [17,18]. Preconcentration of as little as 15 mL of sample with a Triton X-114 concentration of 1.0% permits the detection of amounts lower than 0.4 ppb. Sirimanne et al. determined a small amount of polycyclic aromatic hydrocarbons and polychlorinated dibenzo-p-dioxins in human serum after the preconcentration by CPE using Triton X-100 [19]. The highest average extraction recovery of 98% was obtained at 12% (w/v) Triton X-100, 4.5 M NaCl, and 50^{o}C.

Furthermore, Akita et al. studied the extraction of phenol and aromatic compound with PONPE-10 using CPE method [20]. It was found that phenol was partitioned into surfactant-rich phase over a wide pH range from acid to neutral solution. Thus it was considered that the neutral species of phenol is more liable to be extracted than ionic species. In the pH region below 8, [PONPE-10] = 0.1 M, [phenol] = 0.05 M, [NaCl] = 2 M, the percent extraction of phenol was about 90%. Akita et al. also investigated the extraction of pyridine derivatives, pyridine, picoline, and lutidine [21]. It was found that in the pH region higher than 8, the percent extraction of pyridine, picoline, and lutidine were 70%, 50% , and 40%, respectively. It was also found that organics which lower the cloud point to larger extent can attain higher extraction.

Many works have applied CPE for the preconcentration of trace amounts of metal ion into the surfactant-rich phase to increase the precision of the instrumental analysis. In these studies, chelating agent were employed to form an insoluble or sparingly water soluble complex to introduce some selectivity to the target metal ion which was then separated to the surfactant-rich phase.

Garcia Pinto et al. had been successfully used CPE for the preconcentration of trace amounts of cadmium as a prior step to its determination by flame atomic absorption spectrometry [22]. The procedure based on the formation of a complex of cadmium ion with 1-(2-pyridylazo)-2-naphthol (PAN) was used for preconcentration step of cadmium in a surfactant-rich phase of Triton X-114. Under the optimum condition, 0.25% Triton X-114 and PAN concentration of 4.8 x 10^{-5} mol L^{-1}, a

precision of 3.0% was achieved. The preconcentration of only 15 mL of sample with 0.05% Triton X-114 permits the detection of < 0.4 ppb of cadmium with a concentration factor of 120. Fernandez Laespada et al. determined a small amount of uranium using the complexant system of PAN and Triton X-114 [23]. The optimum extraction recovery was close to 98% for [Triton X-114] = 0.25%, [PAN] = 1.0 x 10^{-4} mol L^{-1}, and pH = 9.2. Moreover, the preconcentration of trace amounts of nickel and zinc using PAN and Triton X-114 were reported by Oliveros et al. [24]. Detection limit of 8 ppb of zinc and 6 ppb of nickel were obtained.

It is clear that PAN is not a specific complexant for metal ion. Therefore appropriate masking reagent must be employed for practical determination of target metal ion [12]. Recently, other complexants have been reported to support the determination of some metal ions. Silva et al. used the complex form of Erbium (III)–2-(3,5-dichloro-2-pyridylazo)-5-dimethylaminophenol to analyze the trace amount of urbium with PONPE-7.5 by CPE [25]. An extraction percentage higher than 99.9% was achieved when the procedure was carried out under the optimal experimental conditions, [PONPE-7.5 = 1 % (w/v), equilibration time = 10 minutes, equilibration temperature = 313 K and working pH = 8.5.

Vaidya and Porter determined a small amount of cadmium in water using a chromogenic crown ether in a mixed micellar solution [26]. Moreover, Mesquita de Silva et al. developed the preconcentration method for low concentration of silver and gold ion in geological samples using Triton X-114 as phase separation mediated [27]. Ammonium o,o-diethyldithiophosphate was added as a complexant. After phase separation, the surfactant-rich phase was diluted with methanol. The enriched silver and gold were determined by flame atomic absorption spectrometry. The detection limited of 0.53 ng mL^{-1} for gold and 0.46 ng mL^{-1} for silver were obtained

Despite many successful applications of CPE, relatively little work has been devoted to investigate the extraction process scheme for extracting target analytes. Akita et al. studied the factors affecting the percent extraction of gold and then proposed the scheme of gold ion recovery from printed substrate by CPE using PONPE-7.5 without complexant [28]. The schematic diagram process proposed by

Akita et al. is shown in Figure 1.11. The percent recovery of gold was reported to be 78.0% with 99.8% purity. However, it seems to have a difficulty in the separation of gold from PONPE-7.5 to obtain the purified metallic gold. The organic solvent like chloroform which was used for stripping gold from PONPE-7.5 was the disadvantage in the view point of harmful inhalation for human. Moreover, the process is rather complex regarding to the three times of the stripping step that stripped out gold ion from organic solvent with 0.1 M HCl.

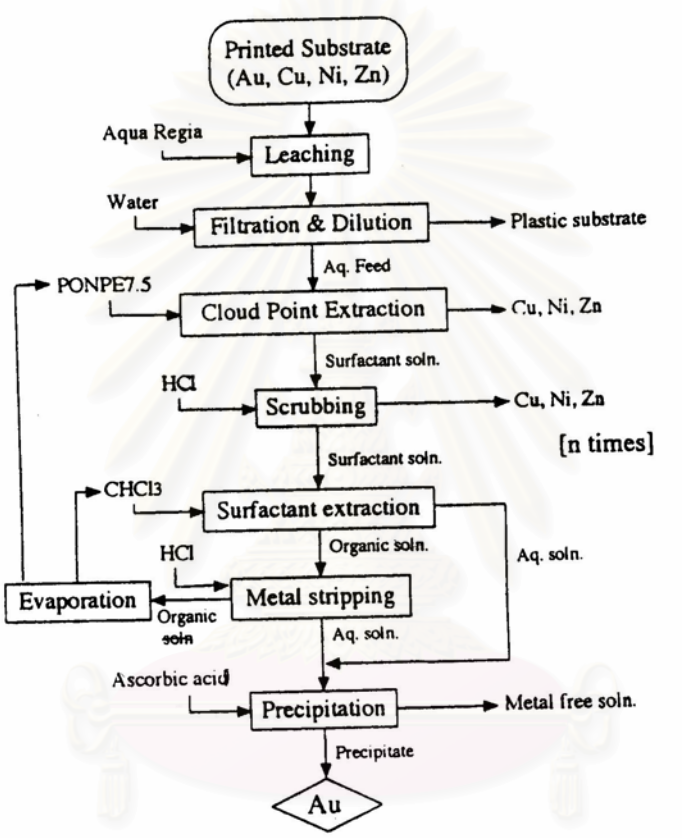

Figure 1.11 Process scheme proposed by Akita et al. [28].

1.4 Scope of Thesis

The aim of this research work is to study the factors affecting the cloud point extraction efficiency of gold (III) using PONPE-9 as a separation media. A process scheme for recovering gold (III) ion is proposed based on the optimum experimental results obtained. The study of thermodynamics properties of the surfactant solution is included to obtain the relationship of surface tension data and the interaction between gold (III) ion and nonionic surfactant at different conditions. Moreover, the

experimental studies of parameters affecting the cloud point temperature of PONPE-9 are also carried out.

This thesis reveals the advantage of CPE methodology to extract gold (III) ion from multimetals solution using PONPE-9. The proposed process scheme aims to be an alternative process regarding to the simple procedure. Chapter 1 of this thesis presents a review of relevant literature and some basic concept to understand the cloud point phenomena of nonionic surfactant and affected parameters. Cloud point extraction methodology is included and a variety of its application is stated. Moreover, thermodynamics of interface is included: the excess thermodynamic quantity changes were derived and obtained from the experimental data and give useful information to understand the phenomena of surfactant mixtures.

Chapter 2 proposes the developed thermodynamic equations in term of thermodynamic quantities changes for a surfactant in solution. Those equations are applied to study the temperature effect on the adsorption and micelle formation of the nonionic surfactant namely pentaethylene glycol monoalkyl ethers.

Chapter 3 presents the distribution of polyoxyethylene oligomers in a commercial PONPE-9 using high performance liquid chromatographic study. The direct measurement of PONPE-9 using UV-spectrophotometric method is performed. The experimental studies on cloud point temperature and phase diagram of PONPE-9 are illustrated and a various effects influence on cloud point of PONPE-9 is shown.

Chapter 4 informs the appropriate condition obtained from the evaluation of factors affecting the cloud point extraction of gold (III) ion in hydrochloric solution. The process scheme for extracting gold (III) ion from mixed metal ions is proposed. The results of the 1-lit experiment are presented and the feasibility and efficiency of the process are projected.

Chapter 5 proposes the developed thermodynamic equations for mixed surfactant system. Those equations are used for the study on the interaction between polyoxyethylene nonyl phenyl ether and gold (III) ion in the adsorbed film and micelle. This interaction was noted during systematic investigations that were based on very accurate surface tension measurements and on the thermodynamic treatments.

Chapter 6 restates the important conclusion of the thesis and recommends directions for future work.

CHAPTER 2

TEMPERTAURE EFFECT ON THE ADSORPTION AND MICELLE FORMATION OF PENTAETHYLENE GLYCOL MONOALKYL ETHERS

2.1 Introduction

This work is for the study of entropy and enthalpy changes of nonionic surfactant by using the equation derived by means of excess thermodynamic quantities changes [4]. The measurement of extremely small heat flow in surfactant system has a limitation according to the instrumental precision. It is probably due to the fact that the total number of surfactant molecules participating in the adsorption is so small that the total enthalpy change to be detected is extremely small, in the order of μJ for 1 cm^2 interface. Therefore, the indirect method given in this chapter, that is, the measurement of surface tension as a function of temperature and surfactant concentration and the thermodynamic analysis of them, is highly useful to estimate the enthalpy of adsorption and micelle formation [29]. Some investigators studied the measurement of the critical micelle concentration, cmc, and related them to the change of standard Gibbs's energy of micellization [10,30]. However, it has been shown to be more useful to discuss the adsorption at the interface and micelle formation by the use of the excess thermodynamic quantities [4,29,31].

According to the results on ionic surfactants, the values of entropy and enthalpy of adsorption from monomeric state decrease with increasing the adsorption at the interface. It is attributed to the oriented structure of surfactant molecule at the interface. However, the behavior observed for some nonionic surfactant systems such as alkyl sulfinylethanol and alkylsulfoxide has shown the striking contrasts in the concentration dependence; the entropy goes up when adsorption increases [29,32]. For the temperature dependence, however, it shows the same behavior as the ionic surfactant systems by having a lower surface density at higher temperature. Those

phenomena have been discussed under two effects occurring in adsorption process. First, the orientation at the interface gives a decrease in entropy value. Second, the dehydration around the surfactant molecules provides an increase in entropy value. It was intensively required to understand why such a difference between ionic and nonionic surfactants was brought about. Therefore, polyethylene glycol monoalkyl ether C_iE_j nonionic surfactants have been employed to investigate the dehydration that affects the size of the dehydrated molecule and then the surface density and the entropy state. C_iE_j is one of good choices because it is possible to control both orientation and dehydration effects by tuning the lengths i and j.

According to the results of C_iE_j systems, it was proved with confidence that the behavior of nonionic surfactants has the trend on increasing entropy and enthalpy toward the increasing adsorption. However, the temperature effect on surface density of C_iE_j is opposite to the others [33-36]. Then, one of the main purposes here is to make a conclusion on the temperature dependency of the surface density and entropy.

Pentaethylene glycol monodecyl ether, $C_{10}E_5$ is a polyoxyethylenated nonionic surfactant in which possesses five series of polyoxyethylene as hydrophilic part and decyl hydrocarbon as hydrophobic part as shown in Figure 2.1. It has been employed to study the mentioned purposes. The surface tension of its aqueous solution has been measured as a function of temperature at various concentrations around the critical micelle concentration cmc under atmospheric pressure. The data have been analyzed by applying the thermodynamic relations reported previously [37-39].

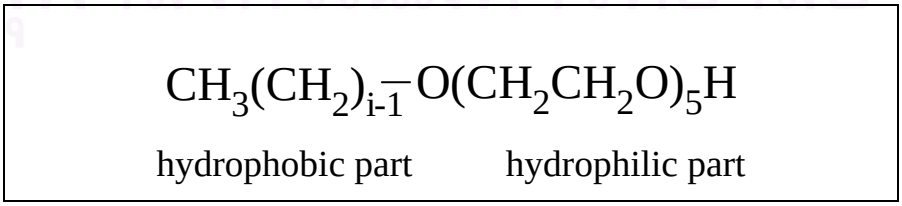

Figure 2.1 Pentaethylene glycol monodecyl ether, C_iE_j.

Moreover, the effect of hydrophobic chain length i on the surface density of C_iE_j has not been always obvious compared to that of hydrophilic chain length j. Therefore, three different hydrophobic chain length of C_iE_j namely, C_8E_5, $C_{10}E_5$ and $C_{12}E_5$ were also employed in this study. It has been demonstrated that there are appreciable effects of the hydrophobic chain length on the adsorption and micelle formation in several aspects of thermodynamic properties.

2.2 Experimental

2.2.1 Materials

Pentaethylene glycol monodecyl ether ($C_{10}E_5$) and pentaethylene glycol monododecyl ether ($C_{12}E_5$) were purchased from NIKKO CHEMICALS CO.,LTD., and pentaethylene glycol monooctyl ether (C_8E_5) from BACHEM Feinchemikalien AG.. Both C_8E_5 and $C_{10}E_5$ were purified by recrystallizing them from hexane solutions [39]. $C_{12}E_5$ was used without further purification. The purity of the surfactants was confirmed by gas-liquid chromatography and the absence of a minimum on the surface tension versus concentration curves in the vicinity of cmc. The purified surfactants were dried by silica gel and stored in the frozen state in a dark bottle. Water used in surface tension measurement was distilled three times from alkaline permanganate solution.

2.2.2 Surface Tension Measurement

The surface tension of the surfactant aqueous solution was measured by drop volume technique. The experiment consists of measuring the mass of a drop which has just detached itself under the influence of gravity alone from the horizontal tip of a sharply cut and polished capillary of accurately known radius. Surfactant solution was carefully filled in a known radius micro-syringe whereas its tip was sharply cut and polished. Air bubbles entering the inlet side were discarded. The syringe was

mounted vertically in clamp holder which was then placed in constant temperature bath. A drop at capillary tip was made by plunging the movable needle into the solution. The plunged distance was accurately measured by micrometer. The drop volume, V , was calculated by $\ell\pi r^2$, where ℓ is the plunged distance, r is capillary radius. The surface tension was calculated by Harkins and Brown equation [40].

$$\gamma = \frac{V(\Delta\rho)g}{r}F \qquad (2.1)$$

where γ = surface tension ($N.m^{-2}$);

$\Delta\rho$ = density difference between fluid and surrounding

= $\rho_{H_2O} - \rho_{air} = 0.997047 - 0.001177$ ($g.cm^{-1}$) ;

g = gravity = 980.665 ($cm\ s^{-2}$);

V = drop volume = $\ell\pi r^2$ (cm^3);

ℓ = plunged distance of needle (cm);

r = radius of capillary (cm);

F = correction factor which was calculated by

$$= 0.14782 + 0.27896\left(\frac{r}{V^{\frac{1}{3}}}\right) - 0.166\left(\frac{r}{V^{\frac{1}{3}}}\right)^2$$

The surface tension of the surfactant aqueous solution was measured as a function of temperature at various concentrations around the cmc under atmospheric pressure [41,42]. The surfactant concentration was varied over the range 0 to 1.90 $mmol.kg^{-1}$. The measurement was carried out in the controlled temperature water bath at a various temperature from 15 to 35 ^oC. The temperature was controlled within 0.01 K. The experimental error was ± 0.05 $mN\ m^{-1}$.

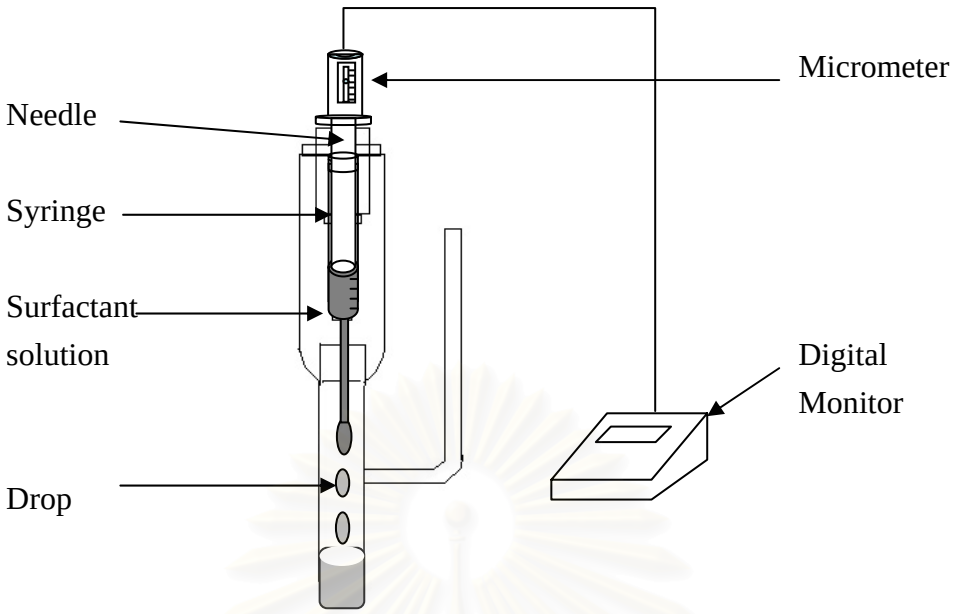

Figure 2.2 Equipment for surface tension measurement by drop weight volume method.

2.3 Results and Discussion

2.3.1 Temperature Effect on Surface Tension of $C_{10}E_5$

The surface tension γ of the aqueous solution of $C_{10}E_5$ was plotted against temperature T at constant surfactant concentration m_1 and pressure from a low concentration to a high concentration in Figures 2.3a to 2.3c. Those reveal that γ decreases with increasing T at all concentrations. These results are similar to those of other nonionic surfactants [29,32] and ionic surfactants [37,43-45] in a rough appearance. However, there exist some significant differences among them as mentioned later. Looking more closely at the experimental results, the curve is slightly concave upward at low m_1, linear at high m_1, and has a break point at the cmc, respectively. Figure 2.3b shows an apparent declination of the temperature effect on γ

at the temperature above the break point. Taking into account that the physical quantities inherent in the interfacial region do not change appreciably at the cmc, the declination is responsible for the change in the bulk solution, that is, the micelle formation. It should be noted that at the concentration above cmc, the curves have rather the same magnitude of slope and parallel to the curves at a high molality. So do the curves below the break point.

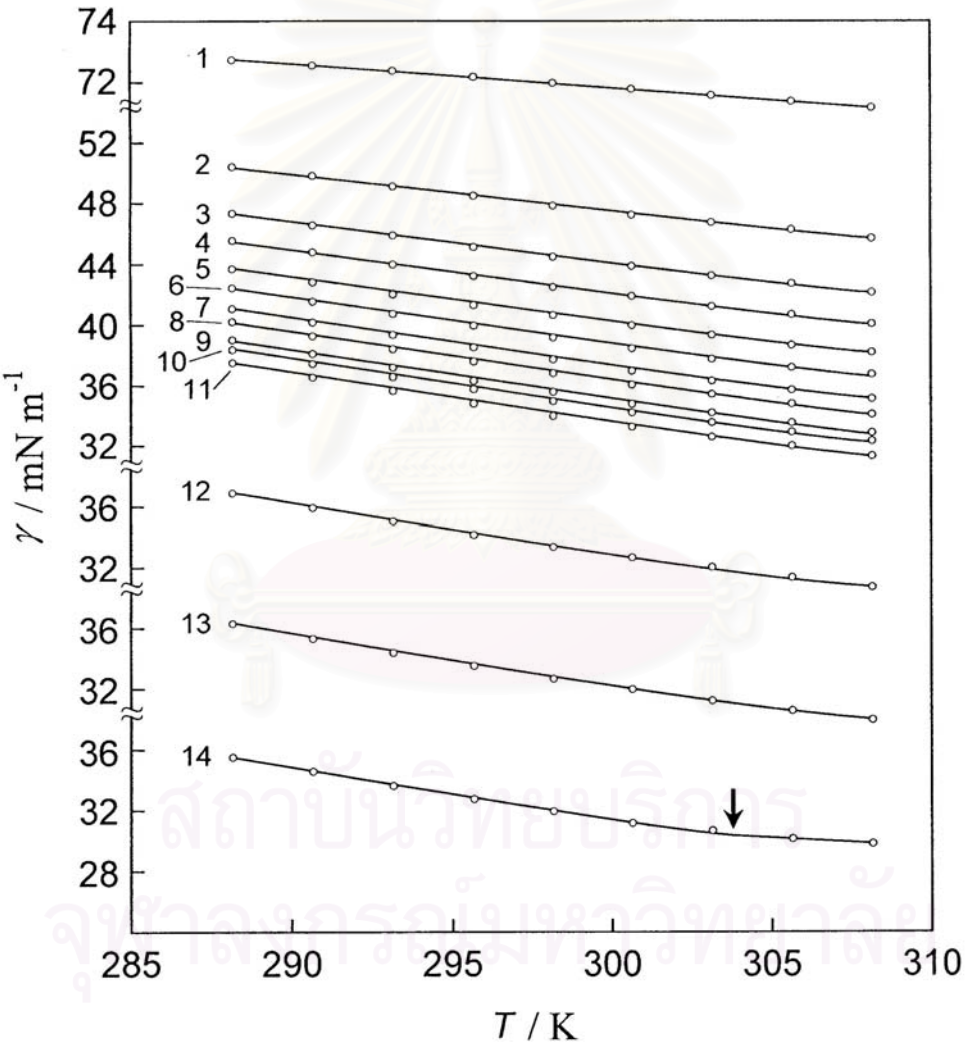

Figure 2.3a Surface tension versus temperature curves of $C_{10}E_5$. (1) m_1 = 0 mmol kg^{-1}, (2) 0.10, (3) 0.15, (4) 0.20, (5) 0.25, (6) 0.30, (7) 0.35, (8) 0.40, (9) 0.45, (10) 0.50, (11) 0.55, (12) 0.60, (13) 0.65, and (14) 0.70.

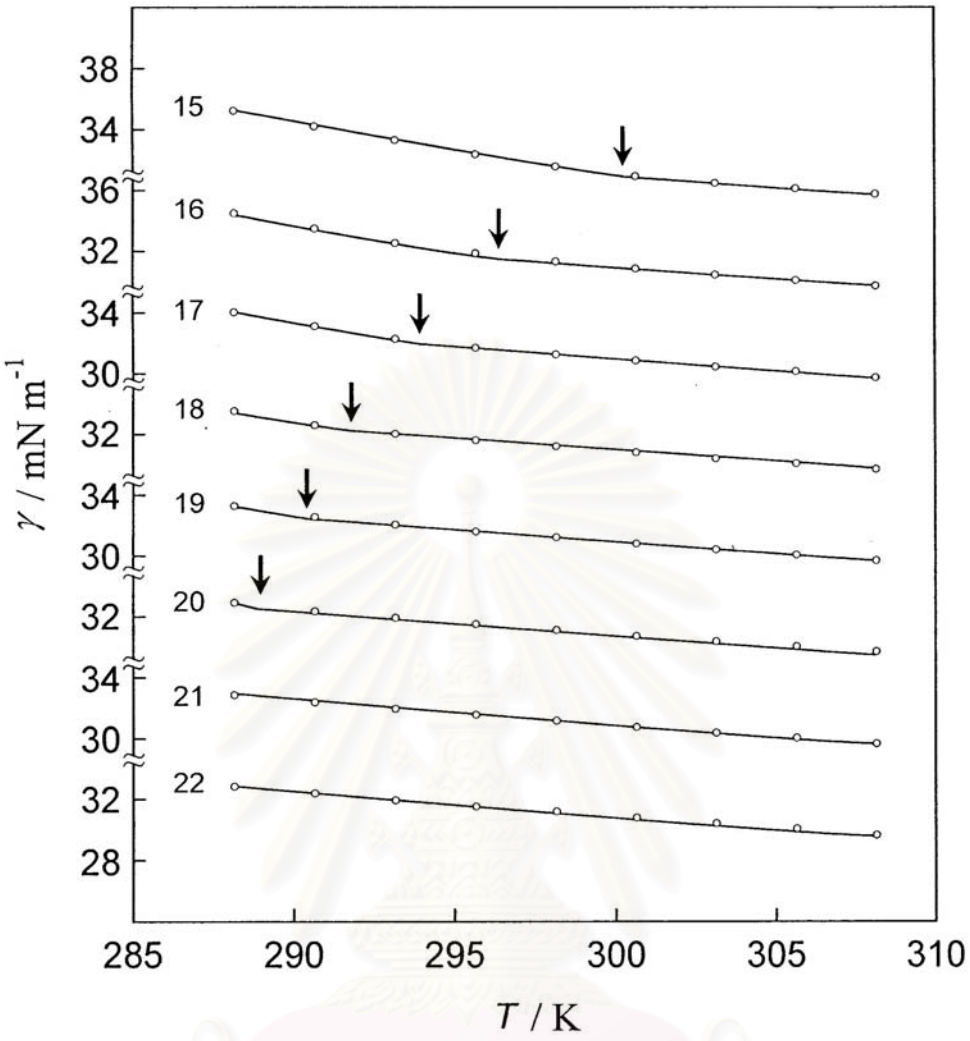

Figure 2.3b Surface tension versus temperature curves of $C_{10}E_5$. (15) m_1 = 0.75 mmol kg^{-1}, (16) 0.80, (17) 0.85, (18) 0.90, (19) 0.95, (20) 1.00, (21) 1.05, (22) 1.10.

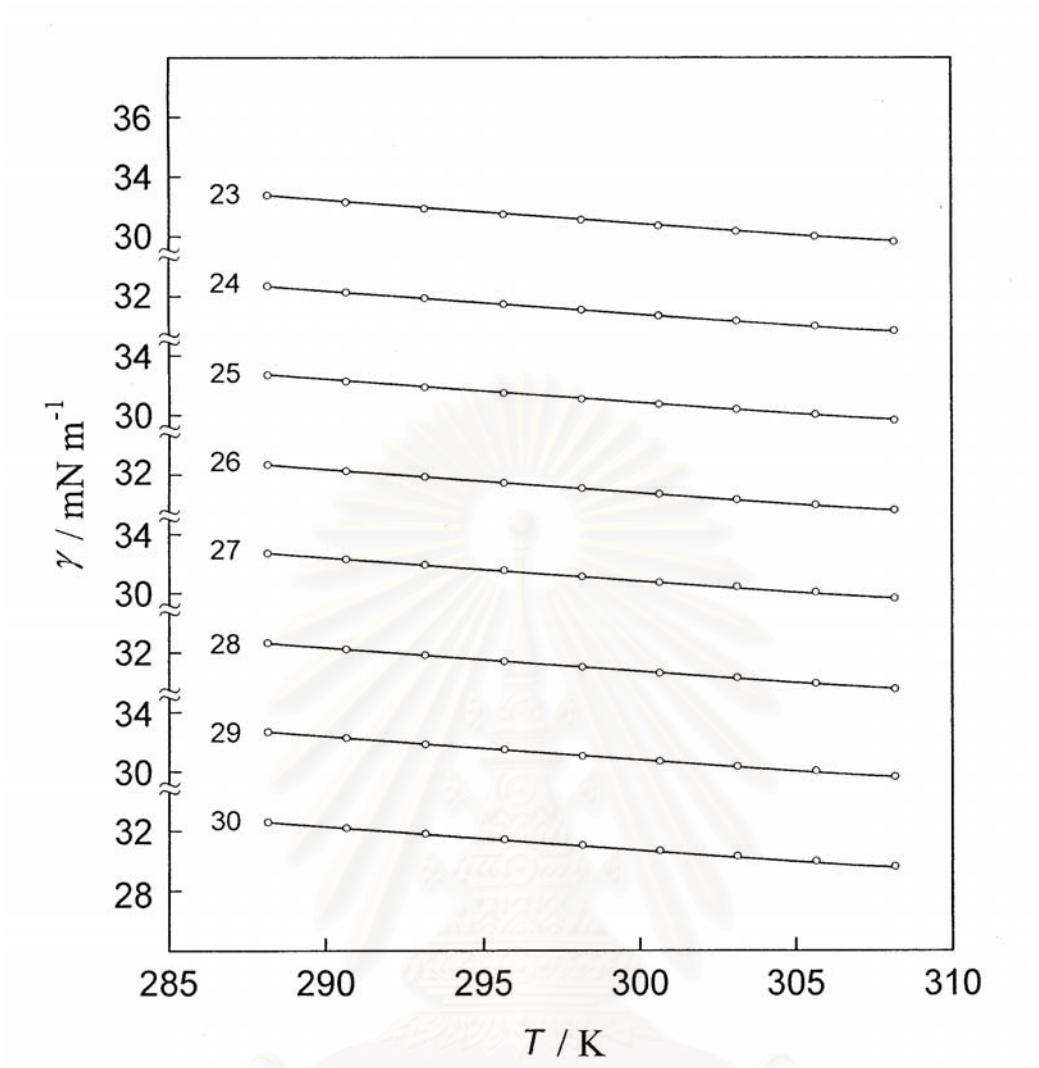

Figure 2.3c Surface tension versus temperature curves of $C_{10}E_5$. (23) m_1 = 1.20 mmol kg^{-1}, (24) 1.30, (25) 1.40, (26) 1.50, (27) 1.60, (28) 1.70, (29) 1.80, (30) 1.90.

2.3.2 Temperature Effect on cmc

The results are also shown as a plot of γ versus m_1 at constant T in Figure 2.4. The γ decrease with increasing m_1 and the curves have a distinct break point at the cmc. Figure 2.5 depicts the cmc versus T curve. It shows the gradual decrease of cmc upon the increasing temperature. This is caused by high temperature inducing the dehydration around hydrophilic part. It provides the surfactant molecules to form micelle conveniently. The concave upward of the curve shows that cmc is more strongly dependent on T at a low temperature than at a high temperature.

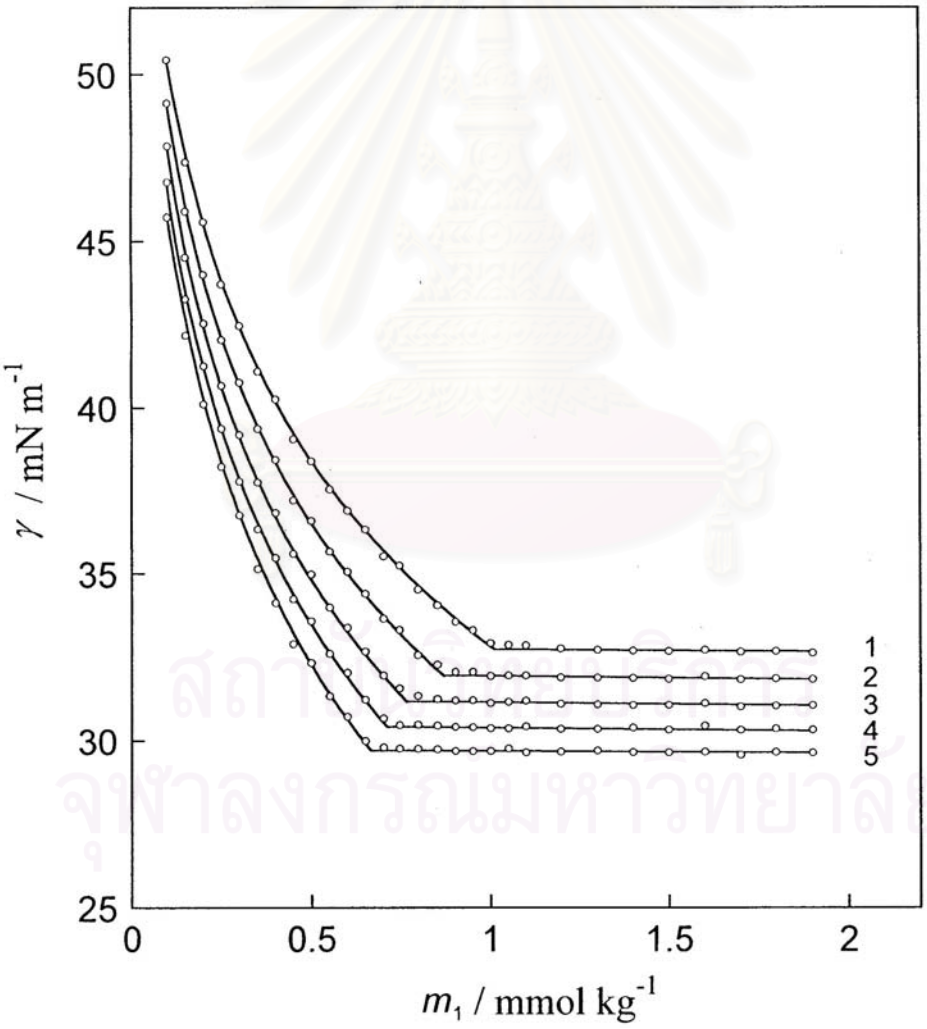

Figure 2.4 Surface tension versus molality curves of $C_{10}E_5$. (1) T = 288.15 K, (2) 293.15 K, (3) 298.15 K, (4) 303.15 K, and (5) 308.15 K.

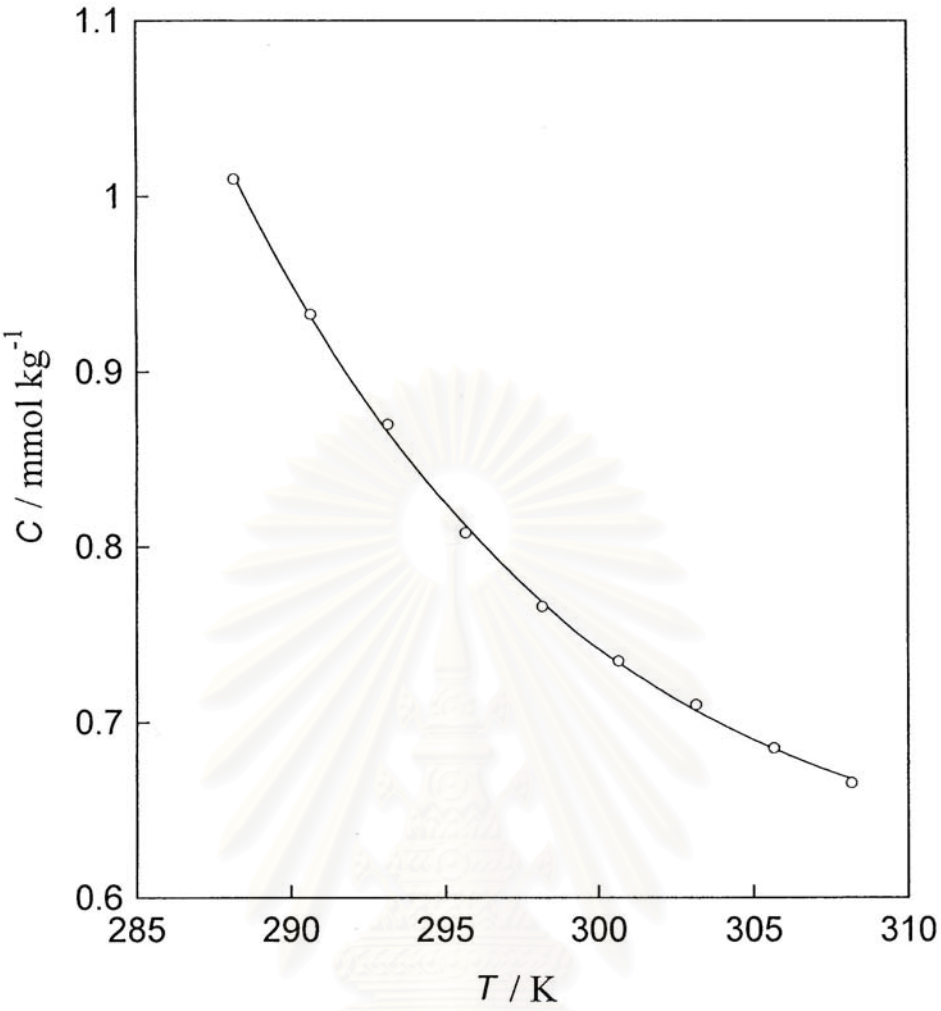

Figure 2.5 Critical micelle concentration versus temperature curve of $C_{10}E_5$.

2.3.3 Temperature Effect on Surface Density

The thermodynamic equations developed and proved previously were applied to examine the thermodynamic properties of nonionic surfactant adsorption and micelle formation [32,37,43]. The thermodynamic quantities of the air/water interface are defined with respect to the two diving planes, making the excess numbers of moles of water and air zero [38]. By assuming the aqueous solution to be ideally dilute and the molality of the surfactant in the aqueous solution to be equal to the total molality of the surfactant at the concentration below the cmc because the quantity of adsorbed surfactant molecules are negligibly small, the surface excess density

Γ_1^{H} can be calculated by applying the equation

$$\Gamma_1^{\mathrm{H}} = -(m_1 / RT)(\partial\gamma / \partial m_1)_{T,p} \qquad (2.2)$$

The calculated Γ_1^{H} of the $C_{10}E_5$ is drawn as a function of m_1 at the different temperatures under atmospheric pressure in Figure 2.6. The curves show the increase of Γ_1^{H} with increasing m_1 and Γ_1^{H} reach the maximum at a concentration near the cmc. The dependence of the Γ_1^{H} on T has been clearly shown: the raising temperature increases appreciably the value of surface density. That means the dehydration effect, caused by raising temperature, diminishes the head size of the surfactant molecules and then provides the closer packing. Therefore, at the concentration below the cmc, the higher temperature is, the higher Γ_1^{H} becomes at the interface.

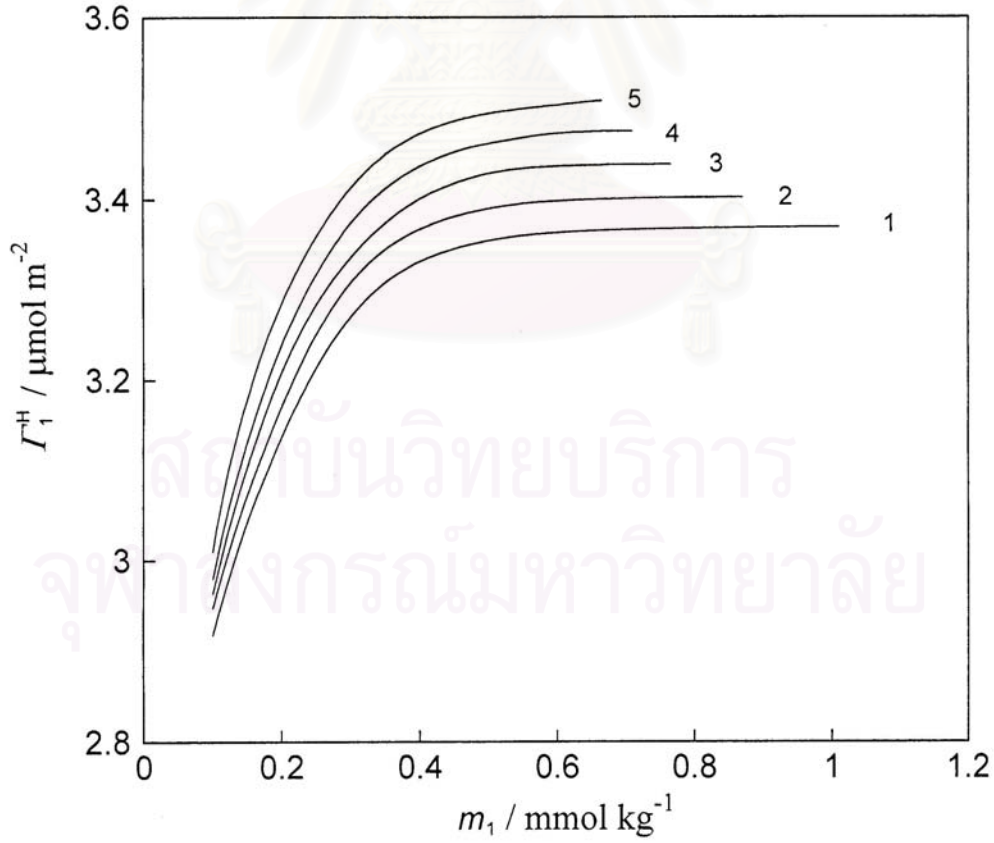

Figure 2.6 Surface density versus molality curves of $C_{10}E_5$. (1) T = 288.15 K, (2) 293.15 K, (3) 298.15 K, (4) 303.15 K, and (5) 308.15 K.

This result is very important from two points of view; first, it is usually found that the surface density decreases with increasing temperature due to the increase in thermal motion of molecules for ionic surfactants and some nonionic surfactants, for example, alkylsulfinyl ethanol OSE [32] and alkylmethylsulfoxide OMS [29] and second, the temperature dependence of Γ_1^{H} for C_iE_j systems is still controversial [33-36]. On the other hand, this result gives curiosity to understand the reason supporting that phenomenon. A concept describing it by using the difference in the amount of dehydration was then proposed. Because of long head of C_iE_j, it is bounded by large amount of hydration in the solution. Upon heating, large amount of dehydration provides a closer packing and then a higher Γ_1^{H}. Comparing to other surfactants with a small nonionic and an ionic head group which are bounded by a small hydration in the solution, the dehydration reduces the head size rather small compared to the thermal motion effect, then gives lower Γ_1^{H} at a high temperature.

2.3.4 Entropy Associated with Adsorption

From the previous paper, the entropy associated with the adsorption from the monomeric state in the aqueous solution $\Delta s(1)$ is defined by

$$\Delta s(1) = s^{\mathrm{H}} - \Gamma_1^{\mathrm{H}} s_1 \qquad (2.3)$$

where s^{H} and s_1 are the surface excess entropy per unit surface area and the partial molar entropy of the monomeric surfactant in the aqueous solution, respectively [41].

At the concentration below the cmc C, the $\Delta s(1)$ can be evaluated by

$$(\partial\gamma / \partial T)_{p,m_1} = -\Delta s(1) \qquad m_1 < C \qquad (2.4)$$

at the given total molality. At the concentration above the cmc, the concentration of monomeric surfactant in the bulk phase is close to C and the relation that describes the entropy change is given as below (see derivation of equation in Appendix B)

$$(\partial\gamma/\partial T)_{p,m_1} = -\Delta s(1) - (RT/C)\Gamma_1^{H}(\partial C/\partial T)_p \qquad m_1 \geq C \tag{2.5}$$

This equation informs the entropy of adsorption at the interface that is in equilibrium with the micelle in the bulk solution. For the micellar solution, $\Delta s(\mathrm{M})$ is the entropy change of the adsorption of surfactant from the micellar state per unit surface area and defined by

$$\Delta s(\mathrm{M}) = s^{H} - \Gamma_1^{H}(s^{M}/N_1^{M}) \tag{2.6}$$

where N_1^{M} and s^{M} are the excess number of surfactant molecules in a micelle particle and excess molar entropy of micelle particle, respectively. It should be noted that the micelle formation is treated as if a macroscopic bulk phase appears in the solution by introducing the concept of the excess thermodynamic quantities with respect to a spherical dividing surface [37]. Here $\Delta s(\mathrm{M})$ can be evaluated by

$$(\partial\gamma/\partial T)_{p,m_1} = -\Delta s(\mathrm{M}) \qquad m_1 > C \tag{2.7}$$

The entropies of adsorption are estimated by applying eqs. 2.4 and 2.7 to the γ versus T curve in Figure 2.3 and plotted against m_1 at constant temperature in Figure 2.7. It should be noticed that at the concentration below the cmc, the shown values are the entropy of adsorption at the air/water interface from monomeric surfactant $\Delta s(1)$. It is seen from Figures 2.6 and 2.7 that the value of $\Delta s(1)$ increases with increasing the molality, that is, with increasing the Γ_1^{H}. Even though, it is usually perceived that the surfactant orientation at the interface provides the decrease of the entropy and this concept has been proved for ionic surfactants [31,37,43-45]. Therefore, it is opposite to the nonionic surfactant both C_iE_j system and sulfoxide system, OSE and OMS [29,32]. This suggests a different phenomenon which accompanies an increase in entropy. This is attributed to the adsorption at the interface accompanied with the

dehydration around surfactant molecules and provides an increase in the value of entropy. Therefore, the change in entropy is responsible for, at least, two competitive factors; orientation and dehydration. For nonionic surfactant, the dehydration effect has a priority over the orientation effect.

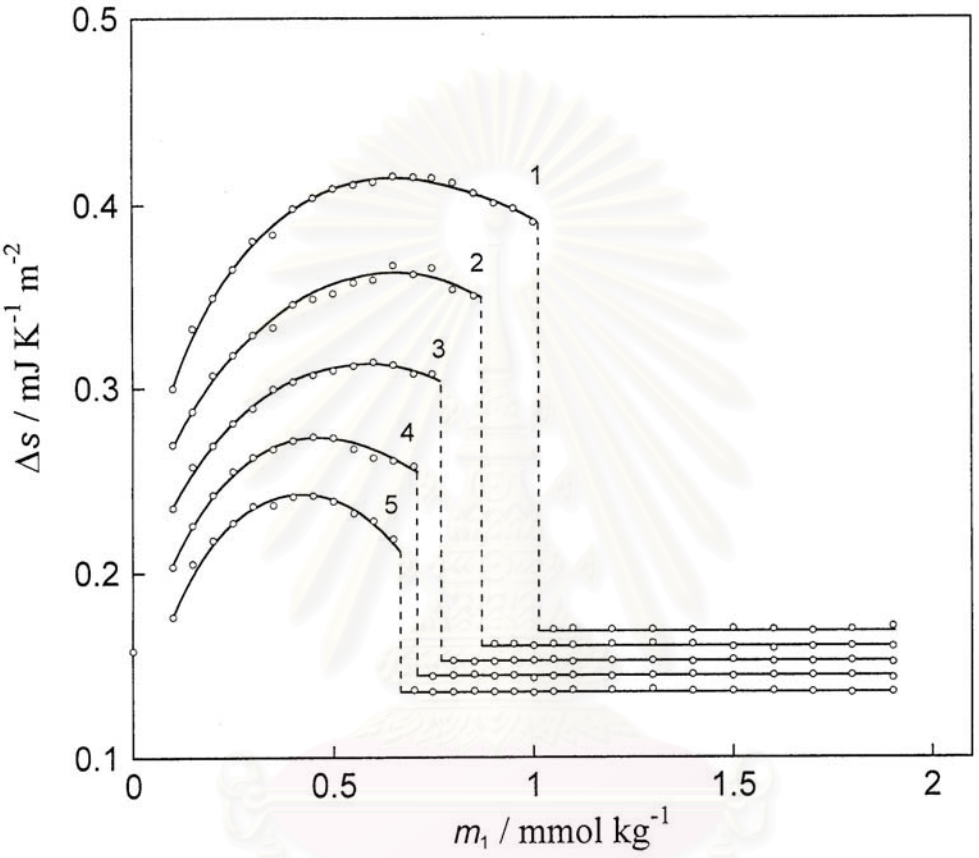

Figure 2.7 Entropy of adsorption vs. molality curves of $C_{10}E_5$. (1) T = 288.15 K, (2) 293.15 K, (3) 298.15 K, (4) 303.15 K, and (5) 308.15 K.

The progression of the entropy change with the increasing molality at a given T was observed. The entropy change $\Delta s(1)$ defined by Eq. 2.3 is expressed also in terms of the partial molar entropy changes, $s_i^{\mathrm{I}} - s_i$, and the interfacial densities of component molecules as [38]

$$\Delta s(1)/\Gamma_1^{\mathrm{H}} = (\Gamma_{\mathrm{W}}^{\mathrm{I}}/\Gamma_1^{\mathrm{H}})(s_{\mathrm{W}}^{\mathrm{I}} - s_{\mathrm{W}}) + (\Gamma_{\mathrm{a}}^{\mathrm{I}}/\Gamma_1^{\mathrm{H}})(s_{\mathrm{a}}^{\mathrm{I}} - s_{\mathrm{a}}) + (s_1^{\mathrm{H}} - s_1) \qquad (2.8)$$

where the subscripts w and a refer to water and air and the superscript I shows that the

quantities are inherent in the interfacial region. The interfacial density of air molecules is negligible small that the second term can be neglected. Now, as demonstrated in Figure 2.8, the value $\Delta s(1)$ is positive, increases with increasing surface density Γ_1^{H} until Γ_1^{H} reaches an almost saturation value, and then followed by a decrease with further small increase in Γ_1^{H}. The positive value of $\Delta s(1)$ at $\Gamma_1^{\mathrm{H}} = 0$ shows $s_{\mathrm{w}}^{\mathrm{I}} > s_{\mathrm{w}}$. Furthermore, since the surface density of water goes down with increasing Γ_1^{H}, the contribution of the first term to $\Delta s(1)$ is diminished with increasing Γ_1^{H}. Therefore, the positive value of $\Delta s(1)$ even at a high Γ_1^{H} suggests the inequality $s_1^{\mathrm{H}} > s_1$; the partial molar entropy of surfactant is increased by the adsorption from the solution irrespective of the orientation of surfactant molecule at the interface. This is of cause attributable to the increase in entropy due to the dehydration.

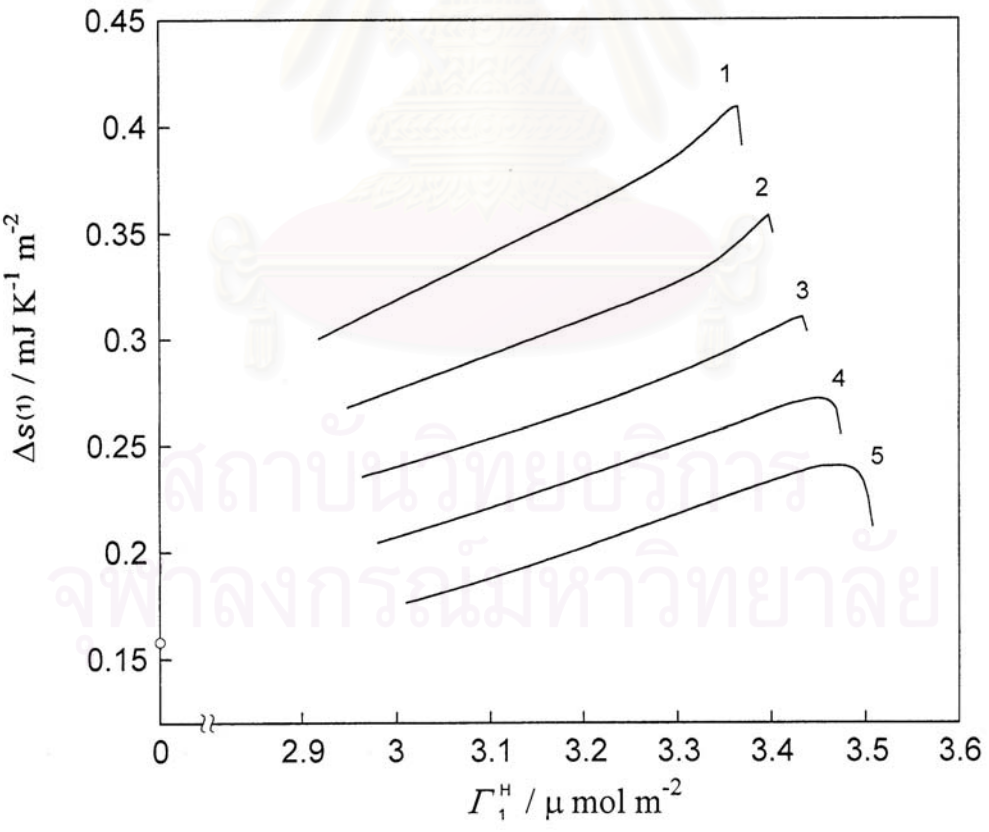

Figure 2.8 Entropy of adsorption vs. surface density of $C_{10}E_5$. (1) T = 288.15 K, (2) 293.15 K, (3) 298.15 K, (4) 303.15 K and (5) 308.15 K.

Taking account of these situations, it is said that the increase in $\Delta s(1)$ with increasing Γ_1^{H} probably corresponds to the increase in the amount of dehydration. In the region of almost saturation value of Γ_1^{H}, even a small increase in Γ_1^{H} is expected to bring about further oriented structure, and this leads a decrease in s_1^{H} and then in $\Delta s(1)$.

In the presence of micelle particles, Eq. 2.5 shows that $(\partial\gamma/\partial T)_{p,m}$ is composed of not only $\Delta s(1)$ but also the second term. Therefore the abrupt change of $(\partial\gamma/\partial T)_{p,m}$ from the peak to the ground is attributable to micelle formation.

In the viewpoint of the temperature effect, both surface density and entropy change depend but conversely on the temperature as Figures 2.6 and 2.7 demonstrate; the surface density of the $C_{10}E_5$ increases while the value of $\Delta s(1)$ decreases at the elevated temperature. The analysis focused on the significance of the dehydration in the bulk solution and that at the interfacial region as follows [39].

The thermal agitation at a higher temperature enhances the dehydration of surfactant molecules in the interfacial region and also in bulk phase. This brings about the increase in both s^{H} and s_1 values at a higher temperature. However, Figure 2.7 performs a lower value of entropy at a higher temperature, which informs that the increasing rate of s_1 is larger than that of s^{H}. The explanation may be more substantiated by interpreting the results in Figure 2.8 at a given surface density. Since the entropy s^{H} is expected to be not so different at the fixed Γ_1^{H} while the value of s_1 grows up at higher temperature, then, the value of Δs decreases along the increasing temperature. The assumption on higher value of s_1 at higher temperature has been proved by the titration calorimetry, it showed that the water-surfactant interaction decreases remarkably with increasing temperature [40]. This means high

dehydration at higher temperature bringing a higher s_1.

The contrary phenomenon between the ionic surfactant and nonionic surfactant in the viewpoint of entropy has been elaborated. We have proposed the main criteria to explain the contrast. That is the difference in charge density of hydrophilic groups between two types of the surfactants. Ionic surfactant bears a strong interaction between water and charged head in the solution. Then, small amount of the dehydration can occur in the adsorption process and then decrease the entropy accompanied by the adsorption. In the case of nonionic surfactants, a comparatively small attraction between water and the non-charged head causes a significant dehydration at elevated temperature and provides the increase in the entropy of the adsorption by overcoming the decrease of the entropy accompanied by the orientation during the adsorption.

At concentrations above the cmc, the value is the entropy of adsorption at the air/water interface from micellar state of surfactant $\Delta s(\mathrm{M})$. It is shown that $\Delta s(\mathrm{M})$ is independent of T and m_1. This means that the microcircumstances in adsorbed film and in micelle are rather similar to each other.

2.3.5 Entropy of Micelle Formation

The entropy of micelle formation per mole of surfactant from the monomeric state in aqueous solution was evaluated by

$$\Delta_{\mathrm{W}}^{\mathrm{M}} s = s^{\mathrm{M}} / N_1^{\mathrm{M}} - s_1 \qquad (2.9)$$

This term describes the entropy changes per mole of surfactant in micelle and that of monomeric surfactant in the aqueous phase. By using Eqs. 2.4 to 2.7, the $\Delta_{\mathrm{W}}^{\mathrm{M}} s$ can be calculated by two methods of the following equations [37]

$$\Delta_{\mathrm{W}}^{\mathrm{M}}s = [\Delta s(1) - \Delta s(\mathrm{M})]/\Gamma_1^{\mathrm{H}} \quad (2.10)$$

and $$\Delta_{\mathrm{W}}^{\mathrm{M}}s = -(RT/C)(\partial C/\partial T)_p \quad (2.11)$$

The $\Delta_{\mathrm{W}}^{\mathrm{M}}s$ can be determined by both of Eqs. 2.10 and 2.11 ($\Delta s(\mathrm{M})$ from Eq. 2.7) and the deviation of those results justify the validity of the thermodynamic treatment. The calculated results obtained by the two independent ways are shown in Figure 2.9. The solid line represents the calculated results from Eq. 2.11 and Figure 2.5 and the circles represent the results from Eq. 2.10 and Figure 2.7. The result shows the considerably different at low temperatures and gets closer in value as the temperature increases.

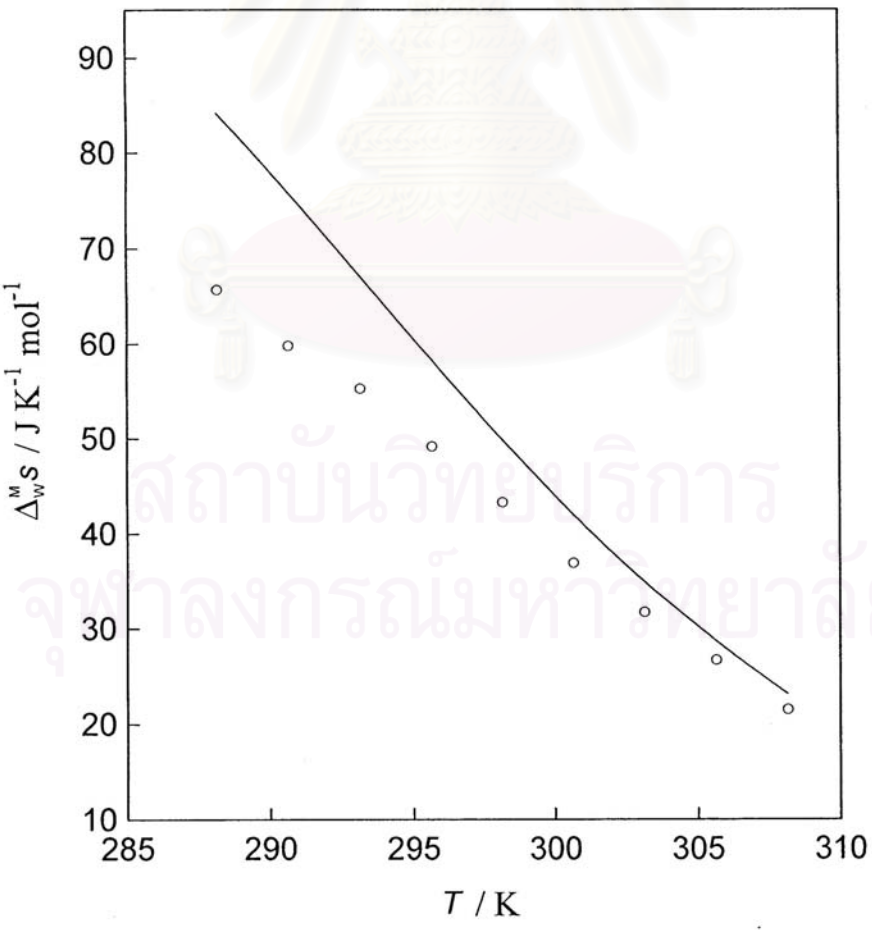

Figure 2.9 Entropy of micelle formation vs. temperature curve of $C_{10}E_5$.

(o) $\Delta_{\mathrm{W}}^{\mathrm{M}}s = [\Delta s(1) - \Delta s(\mathrm{M})]/\Gamma_1^{\mathrm{H}}$, (–) $\Delta_{\mathrm{W}}^{\mathrm{M}}s = -(RT/C)(\partial C/\partial T)_p$.

This means that the treatment of micelle behavior as an appearance of macroscopic bulk phase by introducing the concept of the excess thermodynamic quantities inherent in the micelle becomes more reasonable at high temperatures. Although there exists such a difference, it is sure that the $\Delta_{\mathrm{W}}^{\mathrm{M}}s$ is positive and decreases with increasing temperature. Regarding to the dependence of $\Delta_{\mathrm{W}}^{\mathrm{M}}s$ on temperature, it obviously shows that the increasing temperature provides the decrease of $\Delta_{\mathrm{W}}^{\mathrm{M}}s$. That is also upon the dehydration effect.

2.3.6 Comparison among the C_iE_5

In the followings, the effect of hydrocarbon chain length on the adsorption and micelle behavior of C_iE_5 are illustrated by comparing the thermodynamic properties among C_8E_5, $C_{10}E_5$ and $C_{12}E_5$.

First, a comparison of the surface tension γ versus $\ln[m_1/\mathrm{mmol\ kg^{-1}}]$ was examined. From Figure 2.10, it is certainly proved that C_iE_5 with longer hydrocarbon chain can decrease the γ value and cmc of the solution more than those having shorter hydrocarbon. This is based on that a long hydrocarbon chain functions as an oil-like part of the molecule and then has more tendency to participate in micelle that has an oil-like core.

Second, the surface density at the cmc $\Gamma_1^{\mathrm{H},C}$ of all C_iE_5, are plotted against T in Figure 2.11. We found that at constant T, the $\Gamma_1^{\mathrm{H},C}$ is in the order of

$C_8E_5 < C_{10}E_5 < C_{12}E_5$.

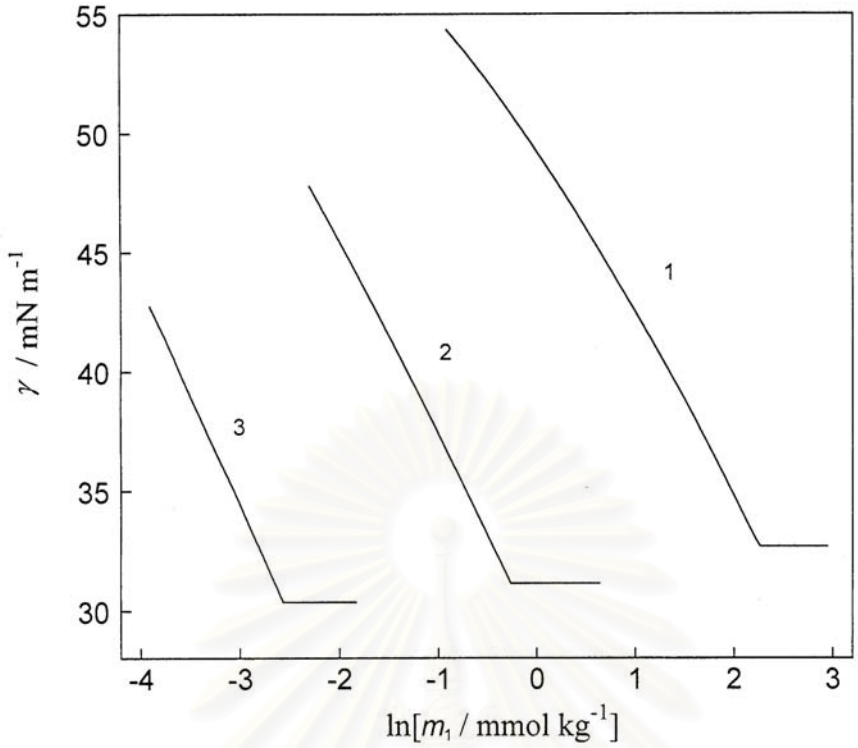

Figure 2.10 Surface tension vs. natural logarithm of molality curves at 298.15 K. (1) C_8E_5, (2) $C_{10}E_5$, (3) $C_{12}E_5$.

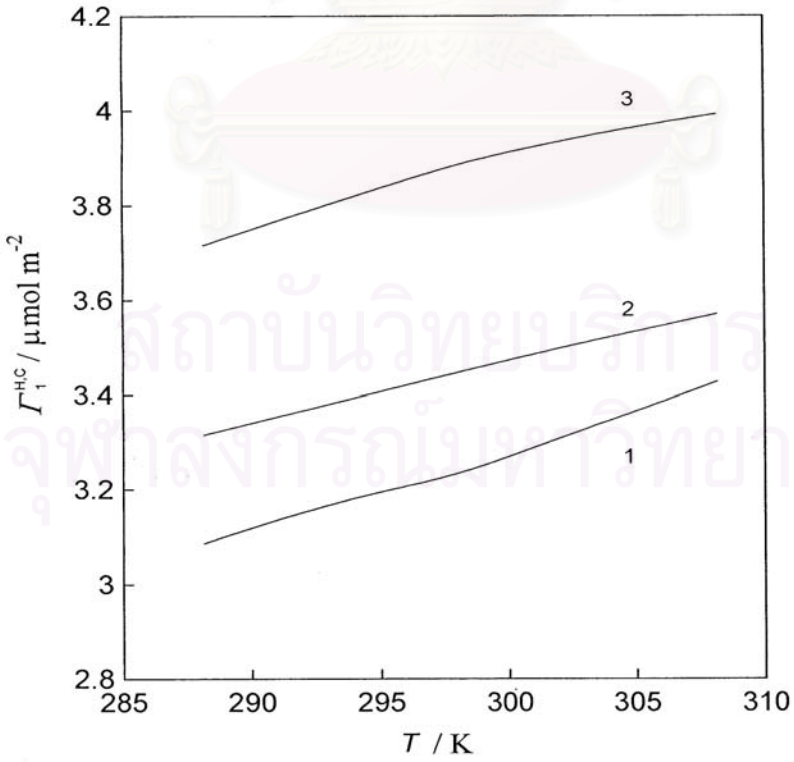

Figure 2.11 Surface density at cmc versus temperature curves. (1) C_8E_5, (2) $C_{10}E_5$, (3) $C_{12}E_5$.

It shows that the longer the hydrocarbon chain is, the more attractive force between the hydrocarbon chains is induced and packed to each other. The curves also emphasize the dependence of the Γ_1^{H} on the temperature. It is noted that the dehydration effect adds up the attractiveness effect and then provides the higher Γ_1^{H} at higher temperature. Hence, the value of $\Gamma_1^{H,C}$ for all C_iE_5 increase with increasing the temperature.

The interesting results on the comparison of the entropy change per mole at the cmc Δs^C of C_iE_5 are demonstrated by the $\frac{\Delta s^C}{\Gamma_1^{H,C}}$ versus T plots in Figure 2.12. The curves elucidate that the increase of $\frac{\Delta s^C}{\Gamma_1^{H,C}}$ with decreasing hydrocarbon chain length is in the order as;

$C_8E_5 > C_{10}E_5 > C_{12}E_5$

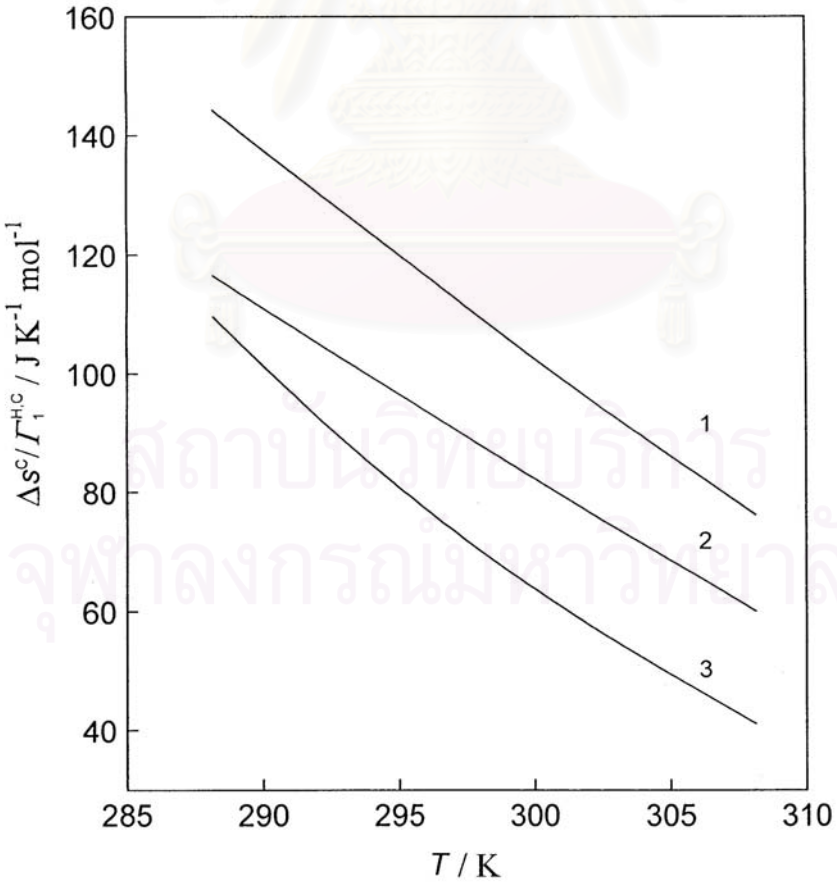

Figure 2.12 $\frac{\Delta s^C}{\Gamma_1^{H,C}}$ versus temperature curves. (1) C_8E_5, (2) $C_{10}E_5$, (3) $C_{12}E_5$.

This means that the longer hydrocarbon chain make the surfactant molecules at the interface more ordered and reduce the entropy s_1^H. Therefore, it is again justified on two competitive factors, the orientation and the dehydration. In this case, the orientation takes more effects on entropy for the longer hydrocarbon chain.

The micelle formation among three C_iE_5 are compared. Figure 2.13 shows the ln[C/mmol kg^{-1}] versus T curves. The effects of the chain length and temperature on the cmc are essentially the same that C_iE_j molecules tend to be more accumulated at the interface with increasing chain length and temperature.

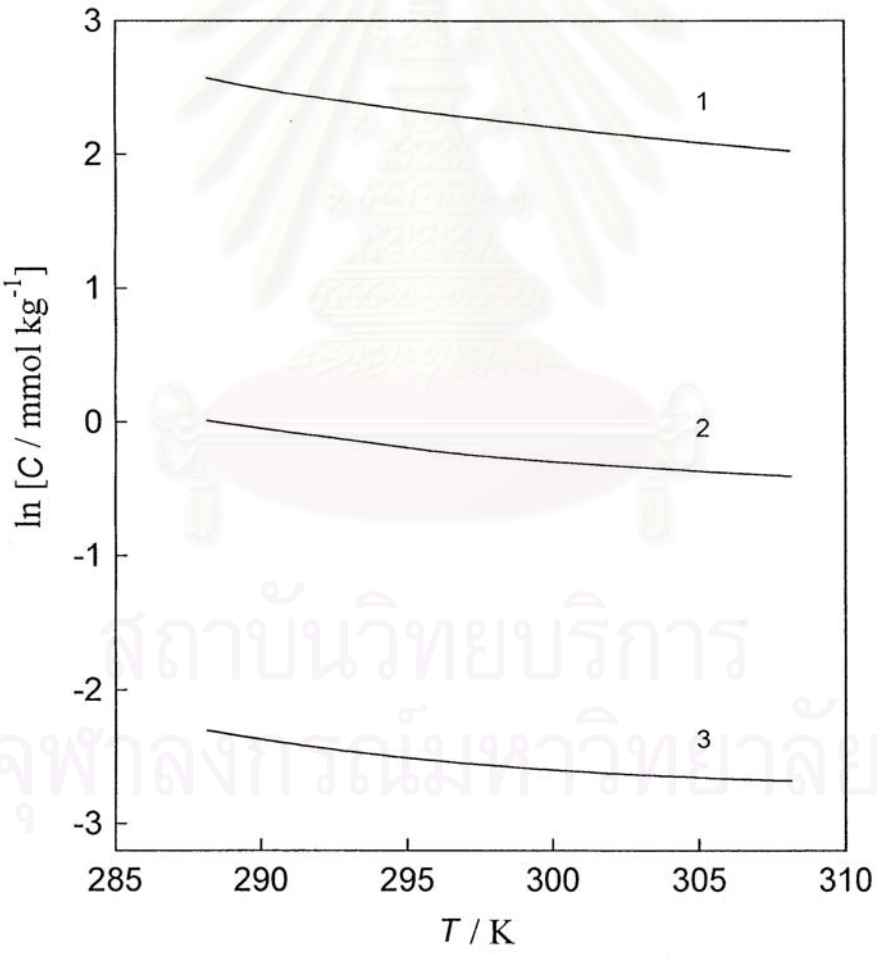

Figure 2.13 Natural logarithm of critical micelle concentration vs. temperature curves. (1) C_8E_5, (2) $C_{10}E_5$, (3) $C_{12}E_5$.

2.3.7 Enthalpy of Micelle Formation

Regarding to the enthalpy change associated with the micelle formation $\Delta_{\mathrm{W}}^{\mathrm{M}}h$, it is defined and can be calculated from the entropy values because the chemical potentials of the components are uniform throughout the system by the following equation

$$\Delta_{\mathrm{W}}^{\mathrm{M}}h = [\Delta h(1) - \Delta h(\mathrm{M})]/\Gamma_1^{\mathrm{H}} = T[\Delta s(1) - \Delta s(\mathrm{M})]/\Gamma_1^{\mathrm{H}} \quad (2.12)$$

With the reference to Eqs. 2.10 and 2.11, $\Delta_{\mathrm{W}}^{\mathrm{M}}h$ is also calculated by

$$\Delta_{\mathrm{W}}^{\mathrm{M}}h = -(RT^2/C)(\partial C/\partial T)_p \quad (2.13)$$

Figure 2.14 shows the plots between $\Delta_{\mathrm{W}}^{\mathrm{M}}h$ versus *T*. Each curve shows positive value of $\Delta_{\mathrm{W}}^{\mathrm{M}}h$ that implies the endothermic process in micelle formation.

Since the slope is negative, it is said that at the higher temperature, where surfactant molecule has a smaller head size, the consumption energy to form micelle is lower than that when the surfactant has a big head size at the lower temperature. The results can be explained clearly in term of the heat capacity associated with the micelle formation defined by

$$\partial\Delta_{\mathrm{W}}^{\mathrm{M}}h/\partial T = \Delta_{\mathrm{W}}^{\mathrm{M}}C_p$$

$$= C_p^{mic} - C_p^{mono} \quad (2.14)$$

where C_p^{mic} and C_p^{mono} are the heat capacity of micellar state and that of monomeric state, respectively. Owing to the negative slope, the heat capacity of monomer is larger than that of micelle. This suggests the difference in contact area with water between monomer and micellar states, that is, the former is larger than the latter. At the higher temperature, C_p^{mono} decreases because of the dehydration and gives a decrease of $\Delta_{\mathrm{W}}^{\mathrm{M}}h$. The comparison among surfactants shows the magnitude of decreasing rate of $\Delta_{\mathrm{W}}^{\mathrm{M}}h$ at elevated temperature in the order of

$C_8E_5 > C_{10}E_5 > C_{12}E_5$

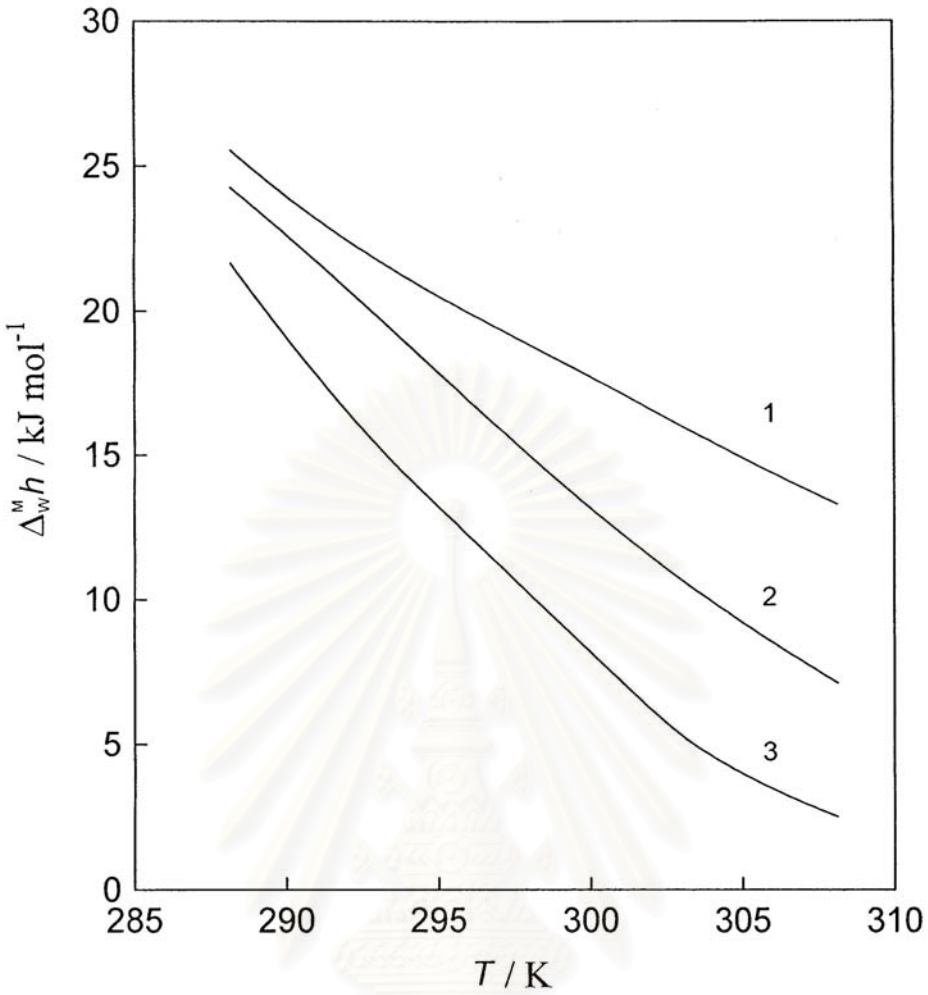

Figure 2.14 Enthalpy of micelle formation versus temperature curves. (1) C_8E_5, (2) $C_{10}E_5$, (3) $C_{12}E_5$.

The decreasing rate appears to be increased with increasing the alkyl chain length. Since the core of micelle particle is akin to liquid paraffin and then the difference in the magnitude of the heat capacity of micelle core among C_iE_5 is negligible compared with the difference in $\Delta_W^M C_p$. The difference in $\Delta_W^M C_p$ may arise from the difference in the C_p^{mono} value; the increase of the hydration around the hydrophobic part with increasing chain length increase the value of C_p^{mono}. Therefore, C_iE_5 with long chain has low $\Delta_W^M h$.

2.4 Conclusion

In the surfactant solution, there are two competing effects on the thermodynamic quantity changes. One is the orientation effect that diminishes the entropy of the system and the other is the dehydration effect that increases the entropy. For C_iE_j nonionic surfactant that has a long head group, the increasing temperature strongly influences amount of the dehydration and then results in the increasing surface density at the interface. The increase of entropy changes along the increase of adsorption is acquired by the priority of dehydration over orientation effect, which is opposite to an ionic surfactant. The higher temperature attenuates both the entropy of adsorption and micelle formation, however, with the positive in entropy value for all changes. Studies undertaken for the hydrocarbon chain length effect can reveal the trend that the longer hydrocarbon chain aids in packing closer of surfactant molecules and increases the surface density but decreases the surface tension, cmc, entropy and enthalpy changes. That demonstrated the importance of the effect of hydrophobic part to the behavior of nonionic surfactant solution besides that of hydrophilic part.

CHAPTER 3

EFFECT OF PARAMETERS ON CLOUD POINT OF POLYOXYETHYLENE NONYL PHENYL ETHER

3.1 Introduction

Polyoxyethylene nonyl phenyl ether surfactant series (PONPE) is presently the most extensive line of available products due to its stability in working condition. The excellent stability of this surfactant in general is demonstrated by their use in acid-cleaning formulation for metals, in highly alkali detergent systems, and in the high-temperature application found in oil-drilling needs [11]. During the last decade, PONPE have been used in virtually all fields of analytical chemistry in order to improve existing methods and to develop new analytical procedures [16-19]. Moreover, many separation processes mediated by PONPE have been developed, particularly, applications including high-performance liquid chromatography (HPLC), extraction, gel filtration, ultracentrifugation, and electrokinetic capillary chromatography have open new possibilities for the separation of molecules in certain research areas such as analytical biotechnology, public health or the study of environmental pollutant [46].

Aqueous micellar solution of polyoxyethylenated nonionic surfactant is completely soluble in water at normal room temperature. However, it displays an inverse solubility-temperature relationship in water [10,11]. As the solution temperature increases, the solubility of polyoxyethyleneated surfactant decreases. It is in contrast to the solubility of other substances that the solubility increases with increasing temperature. In water, the long hydrophilic part of polyoxyethylene is bounded with a large amount of water in order to be soluble in water. The rise in solution temperature yields large amount of dehydration which provides a closer packing of surfactant in micelle and a larger in size and more hydrophobic of micelle. Then, micellar growth and increased intermicellar attraction cause the formation of particles that are so large that the solution becomes visibly turbid. The temperature at which the solution turns turbid is called the cloud point (CP).

There are many parameters that can alter the cloud point temperature of polyoxyethylenated aqueous solution such as electrolyte concentration, surfactant concentration, and pH of the solution. Salting-in and salting-out effects are applied to explain the alteration of cloud point as described in Chapter 1. Salting–out effect reflects in a collapsing of cloud point temperature of surfactant solution while as salting-in reflects the controversial in an opposite effect.

Surfactant in most cases, industrial products, is prepared via series of polymerization reactions and it is a mixture of a variety of components. Thus, PONPE-9 is a mixture of polyoxyethylene nonyl phenyl ether that the average number of oxyethylene is 9. This type of surfactant can be separated according to the length of the alkyl chain by reversed-phase chromatography or according to the length of the ethoxy chains usually by normal-phase chromatography.

Since one molecule of PONPE surfactant has an aromatic nuclei, phenyl group, which could absorb an ultraviolet spectrum at 277 nm, thus, the assay of PONPE surfactant can be achieved by using UV-spectrophotometric method.

Presented are the preliminary studies on the properties of PONPE-9 used as the separation media of this work. First, an analysis of ethoxyoligomer distribution of PONPE-9 using normal-phase HPLC was conducted. Second, quantitative determination of PONPE-9 using UV-spectrophotometric method was performed. Then, various effects on PONPE-9 concentration in water-rich phase after CPE were illustrated. Finally, the cloud point as the upper temperature limit of solubility and phase diagram of PONPE-9 were determined. Moreover, a various parameters which affect cloud point of PONPE-9 were also investigated.

3.2 Experimental

3.2.1 Materials

Polyoxyethylene nonyl phenyl ether ($HO(CH_2CH_2O)nC_6H_4C_9H_{19,}$ PONPE-9) provided by Rhodia (Thailand), Co. Ltd. was used as received. Reagent grade gold (III) chloride solution was purchased from Fluka (Thailand) Co. Ltd., HPLC grade

isopropyl alcohol and n-hexane (Marlinkquot) was purchased from Lab System Co. Ltd. Nitrogen gas was obtained from Thai Industrial Gas Public Company Limited (TIG). All materials and reagent were of analytical-reagent grade unless specified otherwise. A metal solution was prepared by dissolving an appropriate amount of $HAuCl_4.4H_2O$ in dilute hydrochloric solution. De-ionized water was used throughout. A solution of PONPE-9 was prepared by dissolving PONPE-9 in water. Solution pH was adjusted with hydrochloric solution and sodium hydroxide solution.

3.2.2 Determination of Ethoxylate Oigomer Distribution

PONPE-9 was diluted by isopropyl alcohol and filtered through 0.20-μm Millipore filters. All solvents were thoroughly degassed with nitrogen gas before use. The high-performance liquid chromotograph setup consists of a single-piston pump (Shimadsu HPLC Model SIL-10A) and a single-wavelength UV/visible detector (Model SPD-10A). The sample was injected into the chromatographic system by using the automatic sampler. Separations were performed on a sodium type of Shim-pack ISC-30 (gel type), sulfonic acid ion exchange resin of a styrene-divinyl benzene copolymer, 6 mmϕ x 100 mm, 5 μm particle size column, protected by a guard column of the same phase and particle size. Eluent A was isopropyl alcohol and eluent B was n-hexane. Gradient flow of isopropyl alcohol and n-hexane with the increase of isopropyl alcohol at 5% per minute was used. The UV-Detector was set at 277 nm. Data processing and quantification were performed by using the computer software.

3.2.3 Spectrophotometric Determination of PONPE-9

0.1 g of PONPE-9, weighed to the nearest milligram, was introduced into a 100-mL volumetric flask. Some distilled water was added and swirled to give clear solution. Solution pH was adjusted by adding NaOH or HCl. A Mettler Toledo pH/ion analyzer Model MA 235 was used for pH measurements. Then, the mixture was diluted with distilled water and solution pH was measured for a precision data. This solution was diluted if necessary to obtain an absorbance at 277 nm between 0.2 and 1.2. The adsorption spectrum was recorded on Unicam UV-visible Heλios which is a

double beam spectrophotometer with 1.0 cm quartz cells. The solution was scanned against water as a blank from 190 nm to 320 nm.

3.2.4 Cloud Point Determination and Electrolyte Effect

Cloud point of a series of PONPE-9 aqueous solution was determined by observing the temperature required for the onset of turbidity upon heating a 4.0-mL aqueous solution of the surfactant in a small test tube that had been placed in a controlled temperature water bath. The temperature was raised in small increment until the clear solution began to be cloudy. The cloud point temperature reported is the average of duplicate measurements. For the study of the electrolyte effect on cloud point of PONPE-9, PONPE-9 concentration was fixed at 1% (w/v) and a series of electrolytes and organic substance was separately added to obtain a stipulated concentration. The electrolytes and organic substances used in this work were listed in table 3.1. The solution was mixed thoroughly and left in the room temperature at least 10 minutes. Cloud point temperature was measured according to the procedure described above.

3.2.5 Cloud Point Extraction Procedure

Aliquots of aqueous solution containing the PONPE-9 in the range of 1-2.5 % (w/v) and gold (III) ion 10 ppm were well mixed in 25-mL cylindrical tubes at room temperature. The mixed solution was then placed in the constant temperature water bath and allowed to separate into two phases at a stipulated temperature for a certain time. The volume of both the surfactant-rich phase and water-rich phase were read on the volumetric cylinder. The PONPE-9 and metal contents in the aqueous phase were determined by UV-spectrophotometer (Unicam UV-visible Heλios) and atomic absorption spectrophotometer (Varian Spectra 300/400), respectively. The PONPE-9 and metal concentrations of surfactant-rich phase were then calculated on the basis of mass balance.

Table 3.1 Lists of inorganic salts and organic substance used in the study of electrolyte effect.

Chemicals	Formula
1. Ammonium carbonate	$(NH_4)_2CO_3$
2. Ammonium chloride	NH_4Cl
3. Ammonium hydroxide (NH_4OH)	NH_4OH
4. Ammonium oxalate	$(NH_4)_2C_2O_4$
5. Sodium chloride	$NaCl$
6. Lithium chloride	$LiCl$
7. Sodium carbonate	Na_2CO_3
8. Sodium hydrogen carbonate	$NaHCO_3$
9. Sodium sulfate	Na_2SO_4
10. Sodium phosphate	Na_3PO_4
11. Sodiumacetate	$NaC_2H_3O_2$
12. Sodium oxalate	$Na_2C_2O_4$
13. Sodium citrate	$Na_3C_6H_6O_5$
14. Dimethyl Glyoxime (DMG)	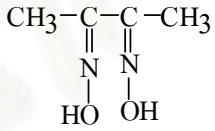
15. Butanol	$CH_3CH_2CH_2CH_2OH$
16. Sodium Lauryl Sulfate (SLS)	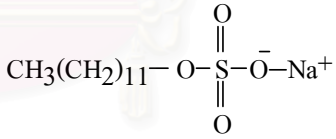
17. Poly Vinyl Alcohol (PVA)	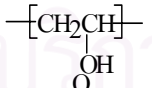
18. Di-Sodium Ethylene Diamine Tetraacetic Acid (di-sodium EDTA)	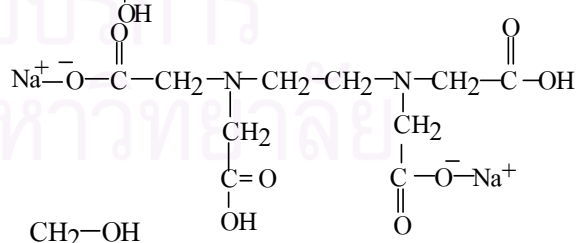
19. Ethylene Glycol (EG)	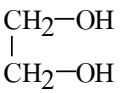
20. Glycerol	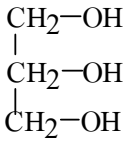
21. Polyethylene glycol (PEG)	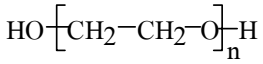

3.3 Results and Discussion

3.3.1 Polyoxyethylene Oligomer Distribution

PONPE-9 solution was injected into HPLC system, the separation was obtained. Figure 3.1 shows a chromatogram of such separation. Gradient elution high performance liquid chromatography was found to be a good method for the analysis of PONPE-9. The shorter ethylene oxide units are eluted at relatively shorter retention times than the longer ethylene oxide ones. The peak areas obtained from HPLC chromatogram, and the percentage of each ethoxylated component can be calculated using computer analysis program. The polyoxyethylene oligomer distribution of PONPE-9 is presented in Table 3.2. The highest peak, percentage of peak area is 21%, responses the polyoxyethylene oligomer which possesses nine series of oxyethylene. Therefore, percent of PONPE-9 in commercial PONPE-9 is about 21%.

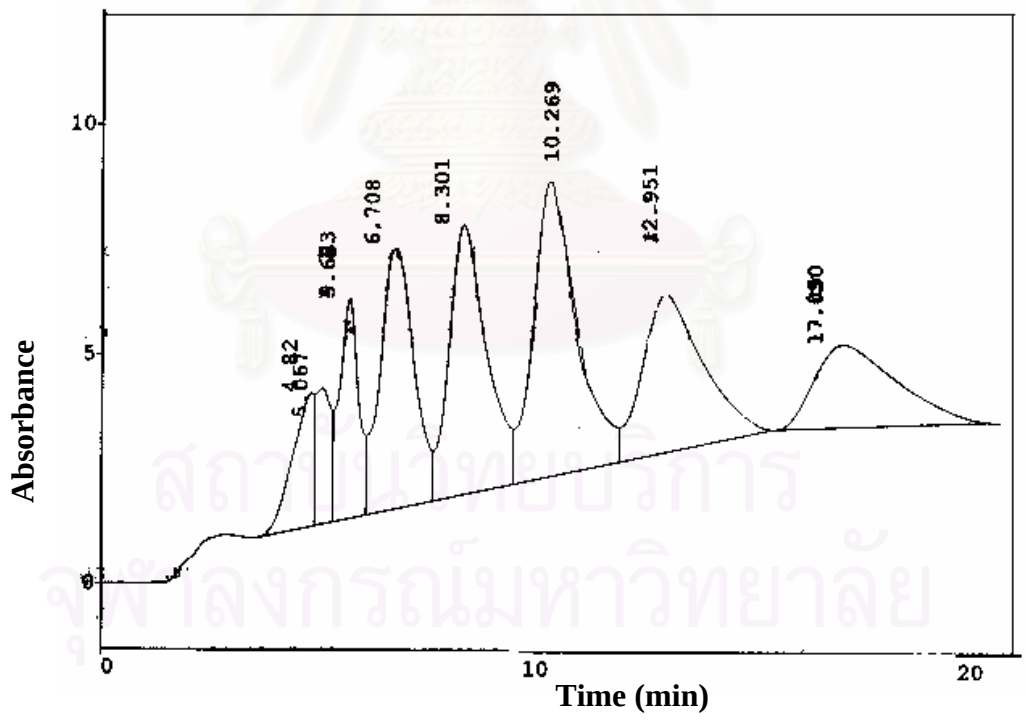

Figure 3.1 HPLC chromatogram of PONPE-9. Solvent gradient from isopropyl alcohol 5 % to 100 % with convergence –2 in 20 minutes, flow rate = 1.0 mL/min, detection wavelength = 277 nm.

Table 3.2 Polyoxyethylene oligomer distribution of PONPE-9 solution

Peak number	Time (min)	Area	Height	%Concentration	EO number
1	4.822	98018	2904	5.01	≤4
2	5.067	70928	2966	3.63	5
3	5.683	145046	4799	7.42	6
4	6.708	307612	5745	15.73	7
5	8.301	355267	5871	18.16	8
6	10.269	410101	6005	20.97	9
7	12.951	332790	3440	17.01	10
8	17.050	236202	1804	12.08	≥11

3.3.2 Spectrophotometric Determination of PONPE-9

An aqueous solution of 0.01% (w/v) PONPE-9 was prepared and its pH was then measured. The absorption spectra measured between 190 and 320 nm against water is shown in Figure 3.2. Absorption peaks are at 199, 223, and 276 nm, respectively. The absorption at 276 nm performs the absorption of phenyl group in PONPE-9 molecule and similar observations were reported by some investigators [17,18,47-48]. A wavelength of 276 nm was used in the subsequent measurement for calibration curve study.

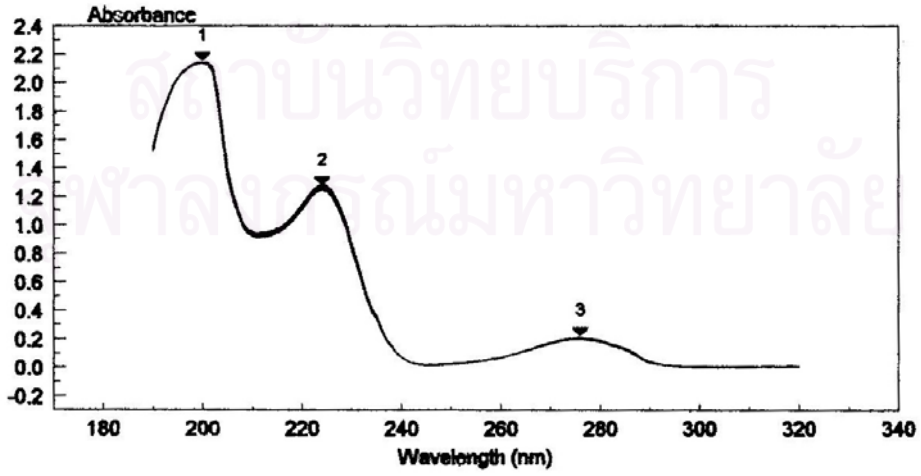

Figure 3.2 Absorption spectra of PONPE-9 in absence of HCl. [PONPE-9] = 0.01% (w/v), pH = 6.28.

Since the extraction of gold (III) with PONPE-9 via CPE was carried out in HCl solution, the examined solution consisted of HCl, gold (III) ion, and PONPE-9. The direct measurement of PONPE-9 can be achieved only if other species have no interference at determined wavelength. Then, the followings are the studies of effects on PONPE-9 adsorption.

a) Effect of pH on Spectrum of PONPE-9

A series of 0.1% (w/v) PONPE-9 at various pH (0.61 – 6.28) was prepared and the solution pH was adjusted with HCl solution. A solution of PONPE-9 in the absence of HCl was used as reference (pH = 6.28). The solutions were subjected to measure its absorption against water and the results are shown in Figure 3.3. It is shown that the absorption spectra of PONPE-9 are identical for the solution in the stipulated pH range from 0.60 to 6.28 (pH = 0.60, 0.86, 0.98, 1.36, 1.90, 2.85, 3.71, 4.38, 6.28). This suggests that HCl has negligible absorption at 276 nm.

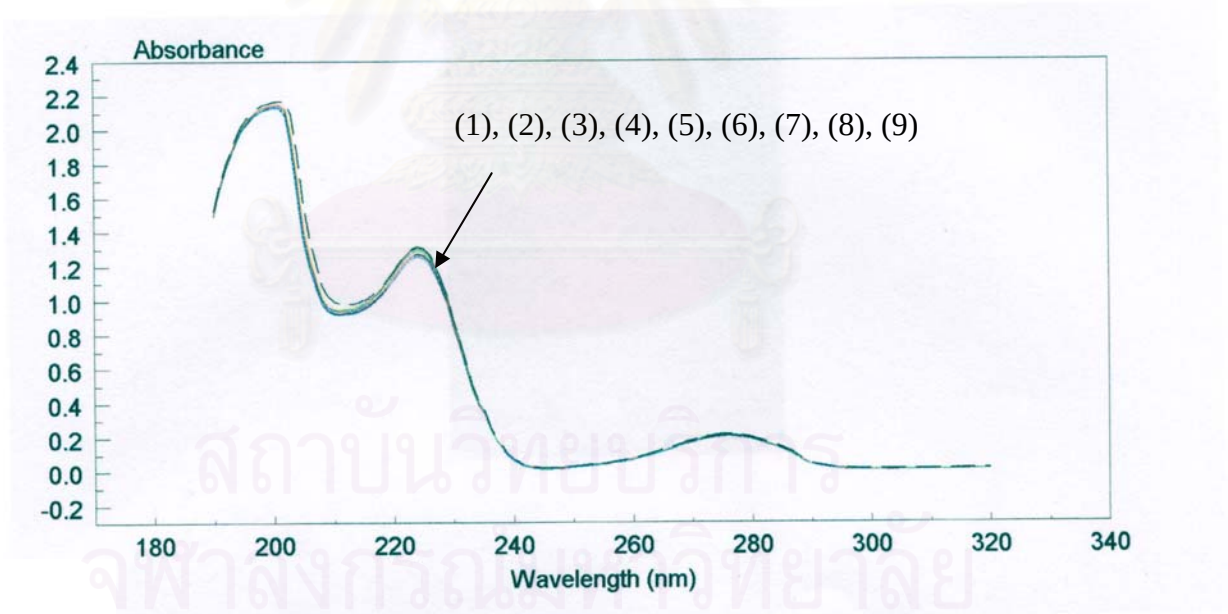

Figure 3.3 Absorption spectra of PONPE-9 solution in presence of HCl at various pH (1) pH = 0.60, (2) 0.86, (3) 0.98, (4) 1.36, (5) 1.90, (6) 2.85, (7) 3.71, (8) 4.38, (9) 6.28, [PONPE-9] = 0.01% (w/v).

The negligible effect of HCl on PONPE-9 adsorption was ensured by the measurement of the adsorption of HCl aqueous solution. Figure 3.4 shows the adsorption spectra of an aqueous solution of 0.01 M HCl and 0.01 M NaOH in the absence of surfactant. The spectrum (1) shows that HCl has no adsorption while spectrum (2) exhibits a high adsorption of NaOH in the range of 240 – 280 nm. This substantiates that HCl does not interfere the quantitative measurement of PONPE-9 at 276 nm whereas NaOH does.

Therefore the determination of PONPE-9 concentration in HCl solution can be achieved by direct adsorption at 276 nm.

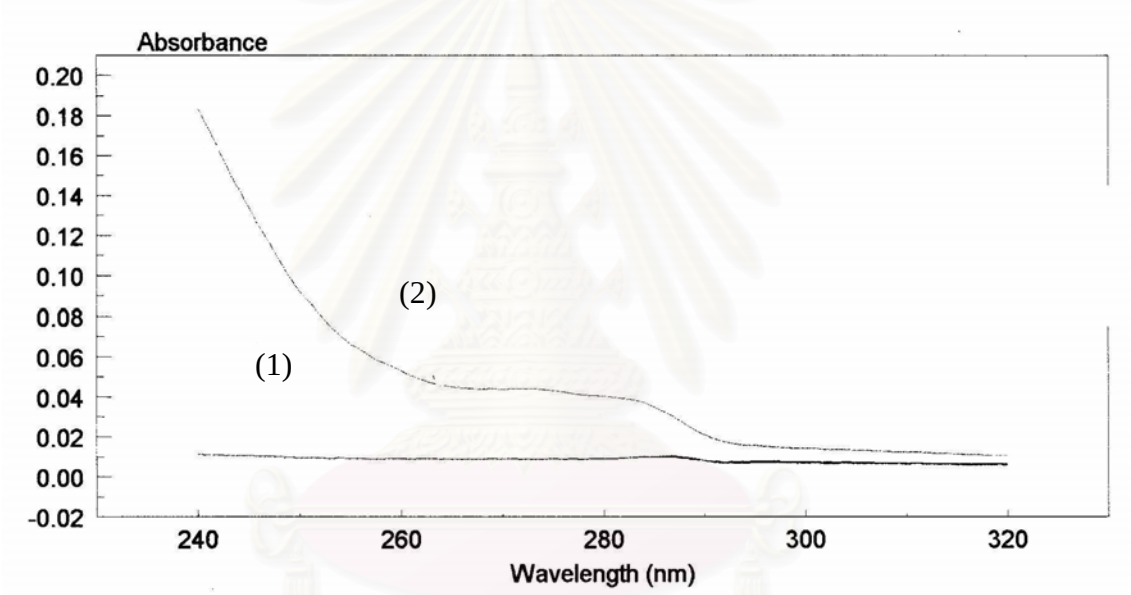

Figure 3.4 Absorption spectra of aqueous solution in the absence of PONPE9 (1) 0.01 M HCl at pH = 2, (2) 0.01 M NaOH at pH = 13.

b) Effect of Gold Ion on Spectrum of PONPE-9

In order to investigate the absorption of PONPE-9 in the presence of gold (III) ion, a series of solution was prepared. The concentration of PONPE-9 and gold (III) ion was 0.03% (w/v) and 333 ng/mL, respectively. Figure 3.5 illustrates the absorption spectra of 0.03 % (w/v) PONPE-9 (1), 0.03 % (w/v) PONPE-9 and 333 ng/mL Au^{3+} (2), 0.02 % (w/v) PONPE-9 and 333 ng/mL Au^{3+} (3), and 333 ng/mL Au^{3+} (4). Regarding to the spectra of (1) and (2), the presence of gold ion in PONPE-9

solution has negligible effect on the absorption spectra of PONPE-9. From Figure 3.5, the solution of gold (III) ion in the absence of PONPE-9 (4) exhibits no absorption at the 276 nm.

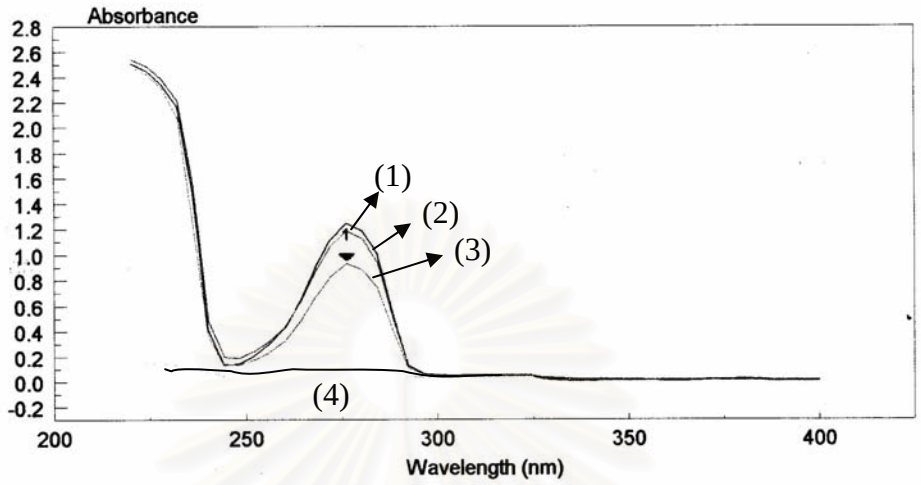

Figure 3.5 Absorption spectra of PONPE-9 solution in absence and presence of Au^{3+} ion. (1) 0.03 % (w/v) PONPE-9, (2) 0.03 % (w/v) PONPE-9 in 333 ng/mL Au^{3+}in 0.03 % (w/v) PONPE-9, (3) 333 ng/mL Au^{3+} in 0.02 % (w/v) PONPE-9, (4) 333 ng/mL Au^{3+}.

From the above observation, there is the negligible effect of HCl concentration and gold (II) ion on the absorption of PONPE solution. Thus, a wavelength of 276 nm is used in the direct quantitative determination of PONPE-9 concentration in the presence of gold ion and HCl. The limitation range of PONPE-9 concentration for this purpose was studied for linear adsorption on PONPE-9 concentration according to Beer's Law [48].

The absorbance at 276 nm for a series of PONPE-9 solutions at various concentration in the range of 0 to 0.10% (w/v) was measured. The data was plotted against concentration as depicted in Figure 3.6. The calibration curve is linear in the range of 0-0.04 % (w/v) PONPE-9. Then, the quantitative measurement of PONPE-9 was achieved by direct measurement of the UV absorbance in the concentration range of 0-0.04 % (w/v) according to Beer's law.

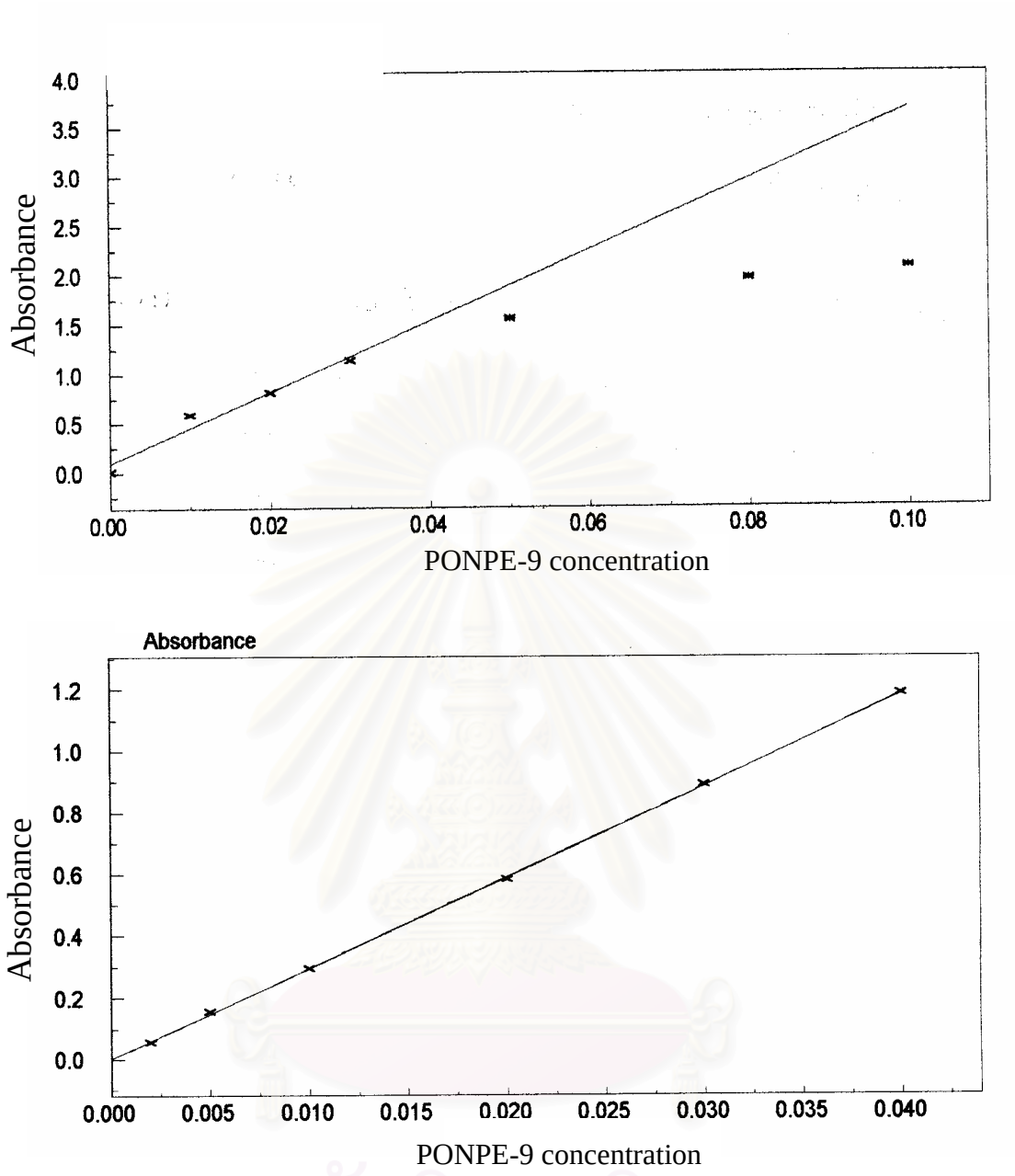

Figure 3.6 Calibration curves for spectrophotometric determination of PONPE-9 at 276 nm. [PONPE-9] = 0 – 0.04% (w/v), pH = 6.28.

3.3.3 Effects of Initial PONPE-9 Concentration and Temperature on PONPE-9 Concentration in Water-Rich Phase

A series of cloud point extraction experiments with fixed gold (III) ion concentration of 10 ppm and initial PONPE-9 concentration, $[PONPE\text{-}9]_o$, in the range of 0.5 – 3.0% (w/v) was conducted at a settling temperature between 55 and 80^oC. After the separation into two phases reached equilibrium, the PONPE-9 concentration in the aqueous solution of water-rich phase, $[PONPE\text{-}9]_w$, was measured by using the spectrophotometric method as described above. The concentration of PONPE-9 in surfactant-rich phase, $[PONPE\text{-}9]_s$, was then calculated based on mass balance (see Appendix C). The results of $[PONPE\text{-}9]_w$ and $[PONPE\text{-}9]_s$ after CPE at 60^oC were plotted against $[PONPE\text{-}9]_o$ as shown in Figure 3.7. It can be seen that PONPE-9 in water-rich phase is slightly dependent of the initial concentration of PONPE-9 and that in the surfactant-rich phase is in linear proportion to the initial concentration of PONPE-9.

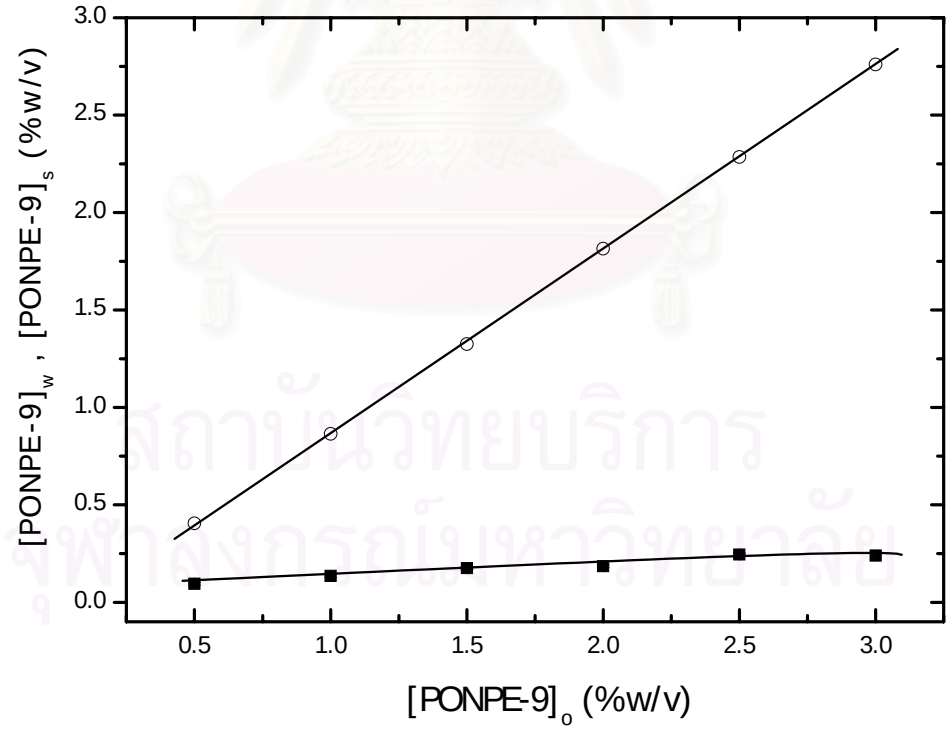

Figure 3.7 PONPE-9 concentration in the water-rich (■) and surfactant-rich phases (○) versus initial concentration of PONPE-9. $[PONPE\text{-}9]_o$ = 0.5 – 3.0% (w/v), $[Au^{3+}]_o$ = 10 ppm, T = 60 ^oC.

The effect of settling temperature on $[PONPE\text{-}9]_w$ was investigated. In this series of experiments, $[PONPE\text{-}9]_o$ and gold (III) ion was fixed at 2.5% (w/v) and 10 ppm, respectively. CPE was conducted at the temperature range of 55 to 80^oC. The results are shown in Figure 3.8. The lowest $[PONPE\text{-}9]_w$ is found for the CPE conducted between 65 to 75 ^oC. This suggests that the settling temperature affects the concentration of PONPE-9 in both phases of CPE. The concentration of PONPE-9 in water-rich phase at various settling temperature are shown in Table 3.3. It should be mentioned that a solution in which PONPE-9 concentration correspond to the table list was prepared and used as the reference the determination of gold (III) ion concentration in water-rich phase by atomic absorption at a given temperature, so the effect of viscosity on the analytical signal was minimized.

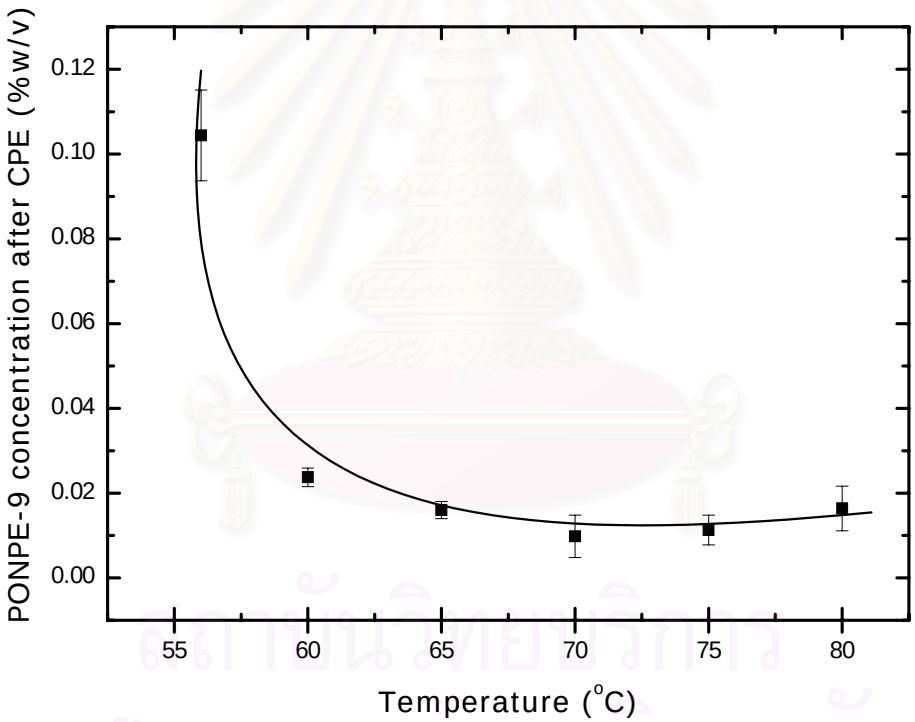

Figure 3.8 Effect of temperature on concentration of PONPE-9 in water-rich after CPE. $[PONPE\text{-}9]_o$ = 2.5% (w/v), $[Au^{3+}]_o$ = 10 ppm, T = 55 - 80 ^oC.

Table 3.3 The concentration of PONPE-9 in water-rich phase after CPE for various pH

Settling Temperature (^{o}C)	$[PONPE\text{-}9]_w$ (%w/v)
56	0.10
60	0.03
65	0.02
70	0.01
75	0.01
80	0.02

3.3.4 Cloud Point of PONPE-9 and Phase Diagram

A series of cloud point determination experiments was undertaken using a various concentrations of PONPE-9 in the absence and presence of gold (III) ion. Mole ratio of gold (III) ion to PONPE-9 was fixed at 7.4 : 1. Figure 3.9 shows the phase diagram, i.e. plots of the temperature at which the single isotropic solution converts to the two coexisting isotropic phases, as a function of surfactant concentration of the solution for the aqueous solution of PONPE-9 in the absence and presence of gold (III) ion. Both coexistence curves are concave-upward bell shape. The critical temperature, T_c, and the critical surfactant concentration, X_c, for aqueous solution of PONPE-9 in the absence of gold are 53.3±0.5 ^{o}C and 2.5-4.0% (w/w), respectively. Across the concentration range studied, the presence of gold (III) ion decreases the CP of PONPE-9. The decrease is marked for the surfactant concentration below 2% (w/w). At the concentration of PONPE-9, 2.5 to 10.0% (w/w), the different between cloud point temperatures is approximately the same. However, the effect of gold is diminished toward the higher concentration of the surfactant above 13% (w/w). Specifically, the critical temperature T_c and the critical surfactant concentration , X_c, for aqueous solution of PONPE-9 in the presence of gold (III) ion, at mole ratio of gold ion to PONPE-9 is 7.4 : 1, are 52.4 ^{o}C and 2.0-4.4% (w/w).

Theoretically for the separation between two phases of surfactant at a given temperature higher than the cloud point temperature, the surfactant concentrations in the two coexistence phases, surfactant-rich and water-rich phases, can be determined from Figure 3.9 by locating the intersections of the horizontal tie line corresponding to that temperature with the coexistence curve. The concentrations of surfactants read from the coexistence curve present the ones in the water-rich phase and the surfactant-rich phase, consequently. From Figure 3.9, as $(T - T_c)$ increases, the difference in the surfactant concentrations in each phase increases. This scenario will be investigated in detail in chapter 4.

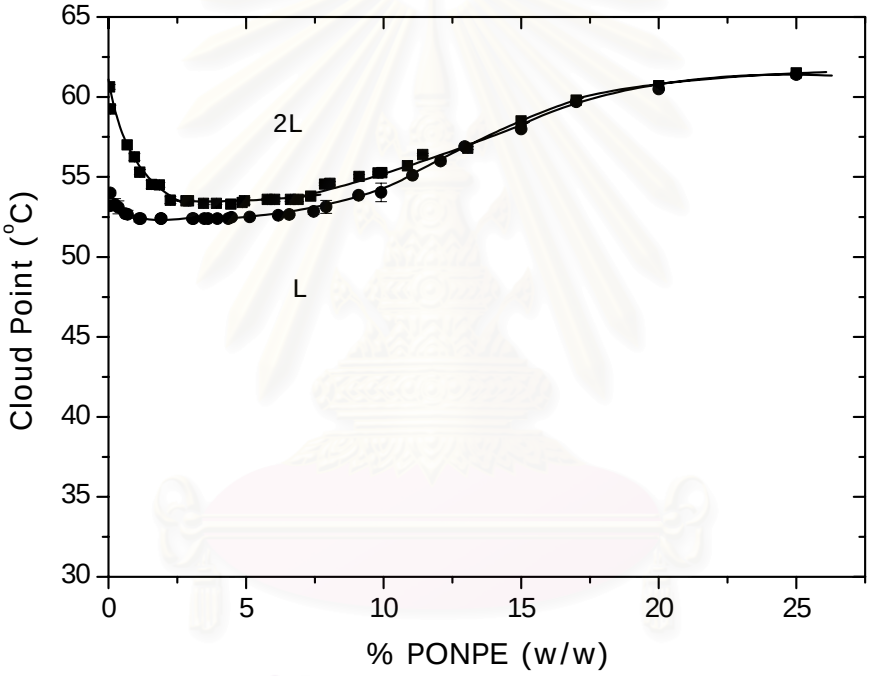

Figure 3.9 Phase diagram of surfactant PONPE-9 in aqueous solution in absence (●) and presence of gold (III) ion (■). L = single isotropic phase region, and 2L = two isotropic phase region, [PONPE-9] = 0.04 – 25% (w/v), pH = 6.58, $[Au^{3+}/$ PONPE-9] = 7.4 : 1.

a) Effect of pH

In order to recover gold (III) ion in the hydrochloric solution with PONPE-9 using CPE, the effect of pH on the cloud point of PONPE-9 was investigated.

Therefore, a series of cloud point determination experiments in which the concentration of PONPE-9 was 2.5% (w/v) and pH of the solution was varied in the range of 1 to 12 was carried out. The effect of pH on the cloud point temperature of PONPE-9 solution in the absence and presence of gold (III) ion is shown in Figure 3.10. Cloud point of PONPE-9 does not change in the pH range of 2 to12. However, at high hydrogen ion concentration, pH = 1-2, the cloud point temperature rises. It is attributed to the oxonium ions which are formed at the ether oxygens in the very low pH solution. This imposes the salting-in effect according to the repulsive force among surfactant head group and results in increasing CP of PONPE-9 [11].

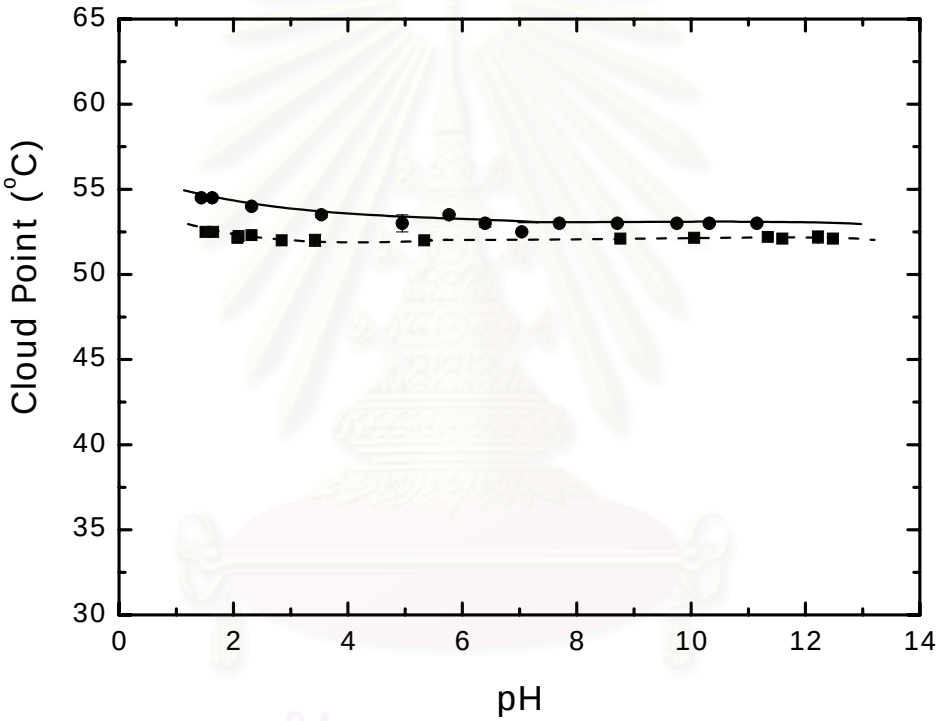

Figure 3.10 Effect of pH on cloud point of PONPE-9 in absence (●) and in presence (■) of gold (III) ion, 5 ppm. [PONPE-9] = 2.5 %(w/v), pH =1.44 – 12.48.

b) Effect of PONPE-9 to Au^{3+} Ratio

Since one important parameter influenced the extraction efficiency of gold (III) ion using CPE method is the ratio of PONPE-9 to gold (III) ion, the effect of that ratio to cloud point temperature of PONPE-9 was investigated. A series of cloud point determination experiments with a PONPE-9 concentration of 2.5% (w/v) and

concentration of gold (III) ion in the range of 1 to 18 ppm, was carried out. In Figure 3.11, curve (1) shows that cloud point of PONPE-9 is roughly constant in the range of ratio of PONPE-9 to Au^{3+} of 700 to 3200 and slightly increase in a high gold concentration solution. It is noteworthy that stock gold (III) ion was dissolved in hydrochloric acid. The addition of gold ion in the solution increases HCl concentration. Then, the higher amount of gold ion in the solution, the lower the pH of the solution as shown in curve (2). As the concentration of gold ion increases and the ratio of PONPE-9 to Au^{3+} is lower than 700, the cloud point slightly raises in the same manner of pH effect (see Figure 3.10).

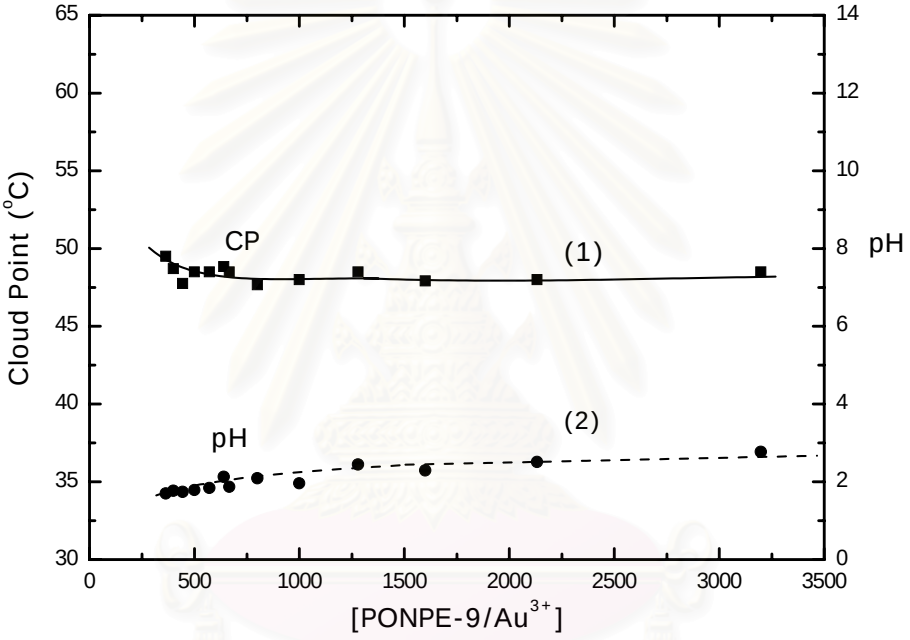

Figure 3.11 Effect of ratio of PONPE-9 to gold (III) ion on cloud point temperature (1) and pH (2). [PONPE-9] = 2.5 %(w/v), [Au^{3+}] = 1 – 20 ppm, pH = 1.44 – 12.48.

c) Effect of Electrolyte

In this series of cloud point determination experiments, the concentration of PONPE-9 was fixed at 1% (w/v) and various types of salts and organic substances were individually added and mixed thoroughly. Inorganic salts and organic substances used in this study were listed in Table 3.1. The results of the study of inorganic salt effects are shown in Figures 3.12 and 3.13. Figure 3.12 shows the effect of a number of inorganic salts (LiCl, NH_4Cl, NaCl, Na_2CO_3, Na_2SO_4, and Na_3PO_4) on cloud point

of PONPE-9. It can be seen that the inorganic salts presented in the PONPE-9 aqueous solution decrease the cloud point temperature. It is attributed to the salting-out effect that ions from salt solution promotes the dehydration of surfactant molecule. This lowers the temperature required for the coacervation of surfactant and decreases CP of surfactant. Figure 3.12 also shows the effectiveness of ion type that the anion causes the lowering of cloud point temperature. This is clearly shown by the small difference of salting-out power of LiCl, NH_4Cl, and NaCl and the marked differences in salting-out power of sodium salt, NaCl, Na_2CO_3, Na_2SO_4, and Na_3PO_4. For comparison, the order of effectiveness of ions is shown in table 3.4 and similar results were reported by Saito [10], and Schick [11].

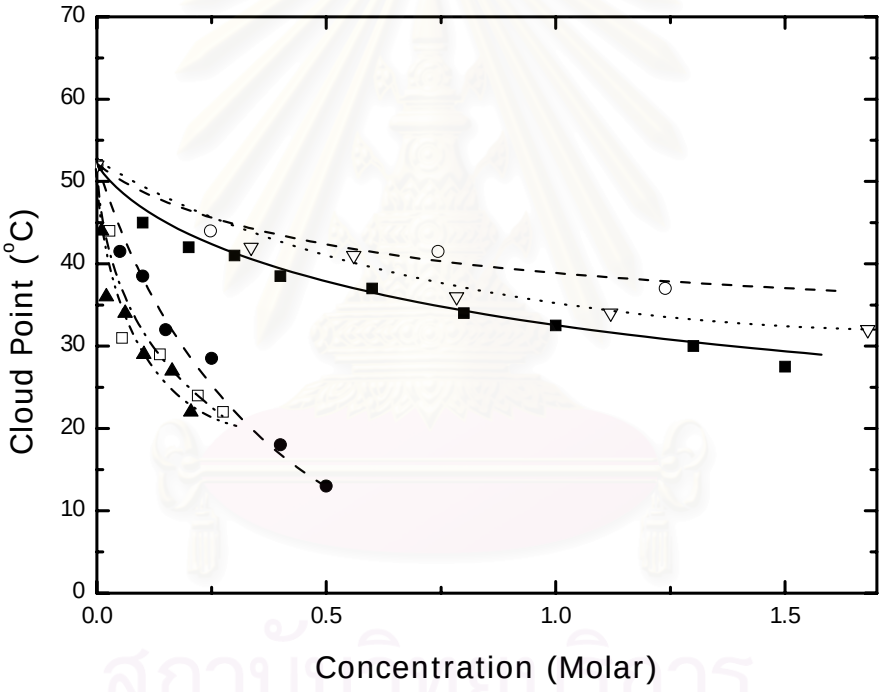

Figure 3.12 Effect of inorganic electrolyte on the cloud point temperature of PONPE-9. [PONPE-9] = 1%(w/v), [LiCl] (○), [NH_4Cl] (▽), [NaCl] (■), [Na_2CO_3] (●), [Na_2SO_4] (□), [Na_3PO_4] (▲).

From Figure 3.13, the effect of ammonium compound and ammonium salts (NH_4OH, NH_4Cl, $(NH_4)_2CO_3$, and $(NH_4)_2C_2O_4$) on cloud point are illustrated. It is suggested that the salting-out power of anions is in the order of $C_2O_4^{2-}$> CO_3^{2-} > Cl^- >

OH^-. It is described that high hydrated ions affect on high dehydration of surfactant molecules.

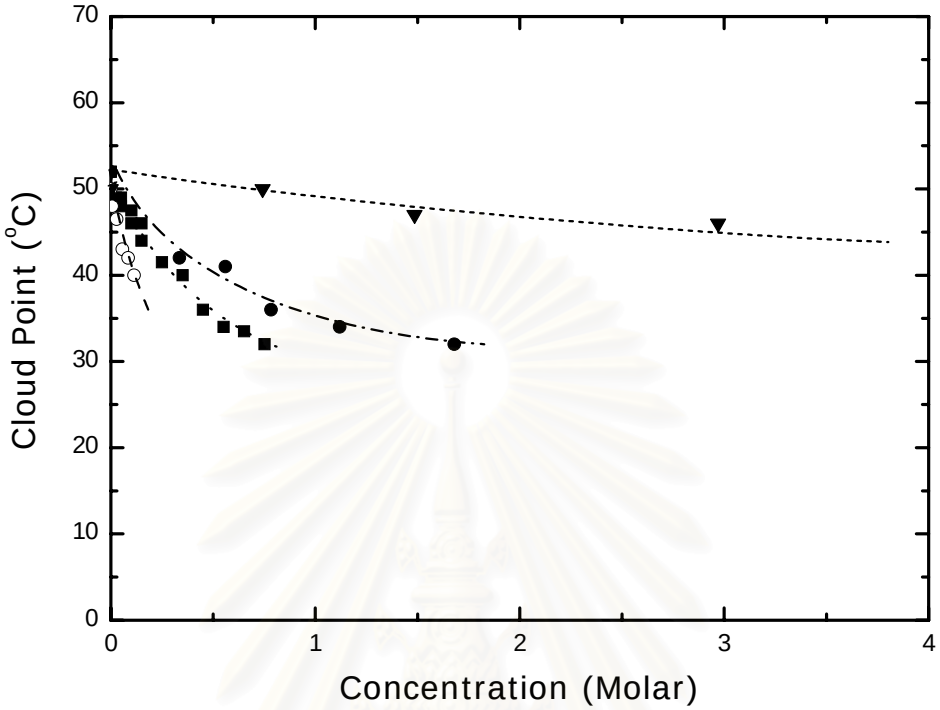

Figure 3.13 Effect of ammonium salts concentration on cloud point temperature of PONPE-9. [PONPE-9] = 1%(w/v), [NH_4OH] (▼), [NH_4Cl] (●), [$(NH_4)_2CO_3$] (■), [$(NH_4)_2C_2O_4$] (○).

Table 3.4 Approximately salting-out effectiveness of ions on cloud point temperature of PONPE-9 [a]

Anions	Cations	Carboxylate ions
OH^-	Li^+	$C_2H_3O_2^-$
Cl^-	NH_4^+	$C_2O_4^{2-} \cong C_6H_6O_5^{3-}$
CO_3^{2-}	Na^+	
$C_2H_3O_2^-$		
$PO_4^{3-} \cong SO_4^{2-}$		

[a]Effectiveness increase with lower position in table

The declining of cloud point with the increasing organic sodium salts concentration is shown in Figure 3.14. It should be noted here that sodium acetate, sodium oxalate and sodium citrate posses 1, 2, and 3 carboxylic groups respectively. Then, the effectiveness of carboxylate ions on the cloud point of PONPE-9 is in the order of $C_2O_4^{2-} \cong C_6H_6O_5^{3-} > C_2H_3O_2^-$. It suggests the little effect of carboxylic group on cloud point of PONPE-9. This may be due to the interaction between the poly-carboxylic group and the ether oxygens of PONPE-9 and then micellization is not favored.

From this work, the results are in accordance with Debye-McAulay equation that the upper temperature limit of solubility of polyoxyethylene in water is lowed in a manner proportional to the salt concentration and the valencies of the salt ions [11]. Also, the small hydrated ion should be more effective than the large hydrated ions in salting out the polymer.

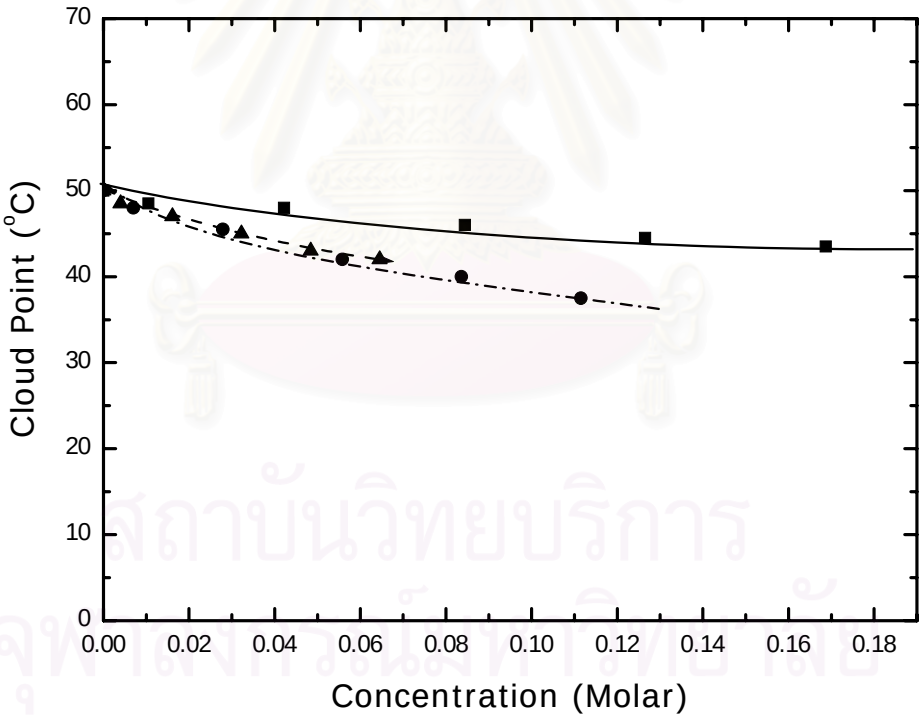

Figure 3.14 Effects of organic sodium salts concentration on cloud point temperature of PONPE-9. [PONPE-9] = 1%(w/v), [$NaC_2H_3O_2$] (■), [$Na_2C_2O_4$] (▲), [$Na_3C_6H_6O_5$] (●).

For the addition of organic substance to aqueous solution of PONPE-9, the changes in cloud point temperature are shown in Figure 3.15. For the presence of SLS (sodium lauryl sulfate; anionic detergent), PEG (polyethylene glycol), EDTA (ethylenediaminetetraacetic acid), and glycerol, the cloud point of PONPE-9 is lowered according to the salting-out effect. In contrast, ethylene glycol, polyvinyl alcohol, and dimethyl glyoxime raise the cloud point of PONPE-9 solution due to salting-in effect. The strong hydrogen-bonding affinity of ether oxygens of the polyoxyethylene chains can be attracted with the hydroxyl groups of additive molecules and gives more hydrophilic surfactant molecules. Therefore, the cloud point of the solution is increased.

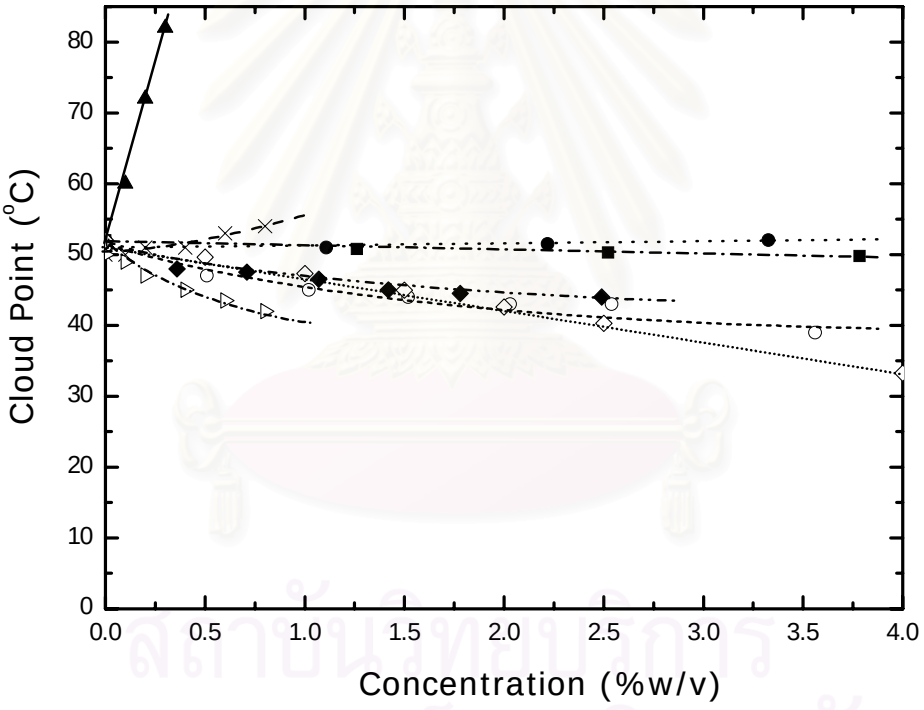

Figure 3.15 Effects of organic substance on cloud point temperature of PONPE-9. [PONPE-9] = 1% (w/v), DMG (▲), PVA (×), EG (●), Glycerol (■), SLS (◆), EDTA (○), Butanol (◇), PEG (▽).

3.4 Conclusion

Commercial PONPE-9 used in this work has 21% polyoxyethylene of 9 separated by normal phase HPLC using gradient flow of isopropyl alcohol and hexane. PONPE-9 absorbs an ultraviolet spectrum via the phenolic group in its molecule at 277 nm and the concentration of HCl and gold (III) ion do not interfere the adsorption. Thus, direct quantitative determination of PONPE-9 using UV-spectrophotometric measurement can be achieved. The settling temperature has insignificant influence on the concentration of PONPE-9 in water-rich phase after applying CPE. Cloud point of PONPE-9 solution depends on not only its concentration but also electrolyte concentration. It was found that many inorganic salts and some organic substance decrease cloud point temperature of PONPE-9. The declining of CP was also observed in the mixture of PONPE-9 and gold (III) ion.

CHAPTER 4

CLOUD POINT EXTRACTION OF GOLD (III) ION USING POLYOXYETHYLENE NONYL PHENYL ETHER

4.1 Introduction

Aqueous solutions of polyoxyethylenated nonionic surfactants heated above a certain temperature, become turbid like cloud phenomena. The temperature at which clouding occurs is called Cloud Point (CP). Above the cloud point, the solution separates into two phases: one, the surfactant-rich phase which is very small in volume; and the other, the water-rich phase, in which the surfactant concentration is approximately equal to its critical micelle concentration (cmc) [8]. Any analytes that can interact with and bind the micellar entity will become concentrated in the surfactant-rich phase upon heating the solution above CP. This phenomenon has been utilized in the design of some extraction and preconcentration schemes. The methodology applied for separating some analytes to the surfactant-rich phase is known as Cloud Point Extraction (CPE). Almost all of nonionic surfactant used as the media in the CPE study are isooctyl phenoxy polyethoxy ethanol (TRITON X series), and polyoxyethylene-4-nonyl phenyl ether (PONPE series).

This general approach, originally introduced by Watanabe et al., has been utilized for the extraction of nickel in soil and zinc in tap water using PONPE-7.5 and an appropriate chelating agent namely 1-(2-pyridylazo)-2-naphthol (PAN) [12]. The function of the chelating agent is to form an insoluble or sparingly water soluble complex with the metal ion and introduce some selectivity into the process.

Many works have applied CPE to preconcentrate trace amounts of metal ion into the surfactant-rich phase to increase the precision of the instrumental analysis. In these studies, chelating agent were employed to form an insoluble or sparingly water soluble complex to introduce some selectivity to the target metal ion which was then separated to the surfactant-rich phase. Pinto et al. employed a complexant system of chelating agent, 1-(2-pyridylazo)-2-naphthol (PAN) and Triton X-114 to entrap chromium ion in the sample and the concentration was subsequently measured by

using flame atomic absorption spectrophometric method [22]. Fernandez Laespada et al. determined a small amount of uranium using the complexant system of PAN and Triton X-114 [23]. Moreover, the determination of nickel and zinc after preconcentration by CPE using PAN and Triton X-114 were reported by Oliveros et al. [24]. It is clear that PAN is not a specific complexant for metal ion. Therefore appropriate masking reagent must be employed for practical determination of target metal ion. Recently, other complexants have been reported to support the determination of some metal ions. Silva et al. used the complex form of Erbium (III)–2-(3,5-dichloro-2-pyridylazo)-5-dimethylaminophenol to analyze the trace amount of urbium by CPE methodology [25]. Vaidya and Porter determined a small amount of cadmium in water using a chromogenic crown ether in a mixed micellar solution [26]. Moreover, Mesquita de Silva et al. developed the method of determination of silver and gold ion in geological samples by flame atomic absorption spectrometry after the CPE using Triton X-114 mixed with ammonium o,o-diethyldithiophosphate [27].

Despite many successful applications of CPE, relatively little work has been devoted to investigate the extraction process scheme for extracting target analytes. Akita et al. proposed the scheme of gold ion recovery from printed substrate by CPE using PONPE-7.5 without complexant [28]. However, it seems to have a difficulty in the separation of gold from PONPE-7.5 to obtain the purified metallic gold and organic solvent like chloroform which was used for stripping gold from PONPE-7.5 was the disadvantage in the view point of harmful inhalation for human.

Although most works for gold recovery purpose have utilized PONPE-7.5, it is suspected that this type of surfactant with other chain length can be used for the same purpose with high efficiency obtained. Thus, PONPE-9 was selected because the cloud point of the solution is about 53±0.5 ^{o}C and the temperature for settling the solution is not too high. The aim of this work is to study the effect of variables for extracting gold (III) ion from hydrochloric acid solution using PONPE-9 as the extraction media. The effect of the variables including PONPE-9 to gold ion ratio, equilibration time and temperature, and pH of the solution on CPE efficiency were investigated. Moreover, a process scheme for recovering gold (III) ion from multimetals solution was proposed.

4.2 Experimental

4.2.1 Materials

Polyoxyethylene nonyl phenyl ether (n=9) ($HO(CH_2CH_2O)_nC_6H_4C_9H_{19,}$ PONPE-9) provided by Rhodia (Thailand), Co.Ltd. was used as received. Reagent grade gold (III) chloride solution, $ZnCl_2$, $NiCl_2$ and $CuCl_2.H_2O$ were purchased from Fluka (Thailand) Co.Ltd,. A metal solution was prepared by dissolving an appropriate amount of $HAuCl_4.4H_2O$ in dilute hydrochloric solution. Solution pH was adjusted with hydrochloric solution and sodium hydroxide solution. All chemicals used were of reagent grade.

4.2.2 Cloud Point Extraction Procedure

Typically, an aqueous solution containing the PONPE-9 in the range of 1 to 2.5 % (w/v) and gold (III) ion in the range of (6.3-25.3) x 10^{-5} M was well mixed in 25 cm^3 calibrated cylinder at room temperature. Solution pH was adjusted by HCl and NaOH solution. The mixed solution was then placed in the constant temperature water bath and allowed to separate into two phases at a prescribed temperature for a certain time. The volume of both the surfactant-rich phase and water-rich phase was read on the volumetric cylinder. The metal content in the aqueous phase was determined by atomic absorption spectrophotometer (Varian Spectra 300/400). The metal concentration of surfactant-rich phase was calculated on the basis of mass balance.

The percent extraction was calculated by the following equation:

$$\%E = 100[M_S/(M_S + M_W)] = 100[V_SC_S/(V_SC_S + V_WC_W)] \quad (4.1)$$

C_s = concentration of gold (III) ion in surfactant-rich phase

C_w = concentration of gold (III) ion in water-rich phase

M_s = mass of gold (III) ion in surfactant-rich phase

M_w = mass of gold (III) ion in water-rich phase

V_s = volume of surfactant-rich phase

V_w = volume of water-rich phase

It should be noted that the greater amount of gold in the surfactant-rich phase, the higher the extraction efficiency that could be obtained. The CPE of gold was carried out at various ratios of PONPE-9/gold, temperature, time, and pH to obtain the optimum condition.

4.2.3 Cloud Point Extraction from Multimetal Solution

The separation of gold from multimetal solution was also studied at various solution pH. Mixed metal ion solution of copper (II) ion, nickel (II) ion, Zinc (II) ion as well as gold (III) ion was prepared. The gold, copper, nickel, and zinc concentration is 5.0, 100.9, 8.25, and 0.8 ppm, respectively. This solution is the representative of printed substrate and dilute liquor. CPE was conducted in 25 cm^3 calibrated cylinder at the optimum condition. Metal content in both water-rich phase and surfactant-rich phase were determined by atomic absorption spectrometer. The percent extraction of each metal thus can be calculated according to the Eq. 4.1.

4.2.4 Gold Recovery Process by CPE in 1-liter Column

The CPE of gold was also performed in one liter settle column. The inner glass column with diameter of 12.0 cm have a valve for draining solution at the bottom and the outer acrylic column with 20.0 cm diameter was circulated with constant temperature water.

First, the mixed metal ion feed solution (see Table 4.1) was passed to the extraction column No.1. The CPE at the optimum condition (settling temperature = 65 ^oC, solution pH = 3, ratio of PONPE-9 to gold = 1500) was conducted in order to trap gold ion into the surfactant-rich phase. When the phase separation equilibrium was reached, the surfactant-rich phase was transferred to the extraction column No.2 and adjusted to pH 7. The CPE was conducted at the minimum separation efficiency condition obtained from the experimental result (settling temperature = 65 ^oC, pH = 7). It should be noted that the CPE conducted in the extraction column No.2 was to remove gold from the surfactant-rich phase. Thus, the chosen operating condition was the condition that yielded the lowest percent extraction of gold in the surfactant-rich

phase. The water-rich phase was then tranfered to a precipitation bath where metallic gold was precipitated. The gold-free surfactant solution was reused in the process.

Table 4.1 Metal contents of printed substrate and diluted liquor used as mixed metal solution feed.

	Gold ion	Copper ion	Nickel ion	Zinc ion
Aqueous feed for this work (ppm)	5	100.9	8.25	0.08
Substrate (mg/g-solid)*	5.9	119.8	9.8	0.09
Aqueous feed for gold recovery process* (ppm)	59	1183.6	98.8	0.9

*According to Akita et al. [28]

4.2.5 Metal Determination and Analysis

Gold contents in water-rich phase were determined by atomic absorption analysis method at wavelength 242.8 nm. Varian Spectra 300/400 equipped with a standard air-acetylene burner and hollow-cathode lamps (Varian) was employed. Blank was prepared by diluting PONPE-9 to 0.02 %. This was based on the result of the PONPE-9 determination in water-rich phase using UV-spectrophotometer (see Table 3.3). The standard solution of gold was prepared by diluting the standard solution of gold (1000 ppm) with distilled water and added with PONPE-9 to obtain the final gold concentration in the range of 1 to 10 ppm with 0.02 % PONPE-9.

Scanning electron microscope (SEM) mounted with Electron Dispersion X-ray (EDX) was used for investigating the surface and analyzing the percent purity of gold in precipitated gold. The gold powder was carefully mounted on SEM stub using double-sided tape and then examined under microscope Model JSM-6400, operated at 20 kV.

4.3 Results and Discussion

4.3.1 Cloud Point Extraction of Gold

Figure 4.1 shows a CPE experiment conducted in 25-cm^3 calibrated cylinder with aqueous solution of PONPE-9 2.5% (w/v) and 10 ppm gold (III) ion, and the solution pH is 1.86. The well-mixed solution of gold (III) ion and PONPE-9 is a homogeneous clear phase solution (see Figure 4.1a) which shows yellow color of gold (III) ion in hydrochloric acid. After the temperature of the solution was raised to CP (48.5 ^oC), the solution turns turbid as shown in Figure 4.1b. The two phases of the solution was obtained after leaving the solution at the temperature above CP for a specific time (see Figure 4.1c).

(a) **(b)** **(c)**

Figure 4.1 An experiments on cloud point extraction of gold using PONPE-9 as a separation media at pH = 1.87. [PONPE] = 2.5% (w/v), [Au^{3+}] = 10 ppm, T= 56 ^oC.

It can be seen that the surfactant-rich phase at the bottom is yellow, while the water-rich phase is a clear solution. This suggests that gold (III) ion is concentrated into the surfactant-rich phase due to the interaction between gold (III) ion and PONPE-9 which takes place at the polyoxyethylene chain in PONPE-9 molecules. It can be explained that polyoxyethylene nonionic surfactants are protonated at ether

oxygens to form oxonium ions, yielding positive charged groupings that can be adsorbed onto negative charge analytes [10]. It should also be noted that gold (III) ion presents in hydrochloric acid in form of tetrachloro auric ion [$AuCl_4^-$] which possess one negative charge [49]. Thus, it is possible that gold (III) ion is incorporated into the polyoxyethylene chains of micelle of PONPE-9 and provides good result on percent extraction.

Figure 4.2a, 4.2b, and 4.2c show the CPE experiments carried out with aqueous basic solution of PONPE-9 2.5% (w/v) and 10 ppm gold (III) ion. The pH of the solution was adjusted with NaOH. It can be seen that the well-mixed solution of PONPE-9 in the presence of gold ion and NaOH is purple in color (see Figure 4.2a). The turbid phenomena of the solution is illustrated in Figure 4.2b. The separation between phases is shown in Figure 4.2c, surfactant-rich phase is enriched with gold and shows purple color at the bottom phase.

Figure 4.2d, 4.2e, and 4.2f show the distinct phenomenon of CPE of gold in a solution of pH 7. The initial solution of gold (III) ion and PONPE-9 at pH 7 is purple likewise those at basic pH solution, then the solution is turbid after raising temperature to 52.5^{o}C. However, it is shown in Figure 4.2f that after reaching the equilibration time for partitioning between phases, surfactant-rich phase is clear thick solution, while the water-rich phase is purple color of gold in NaOH. This informs that at pH 7, gold ion prefers retaining in water-rich phase to retaining in surfactant-rich phase. It is attributed to the fact that the neutral form of polyoxyethylene chain cannot interact with gold-complex ion. This phenomenon is of interest and being the criteria for gold recovery process design as described in next section.

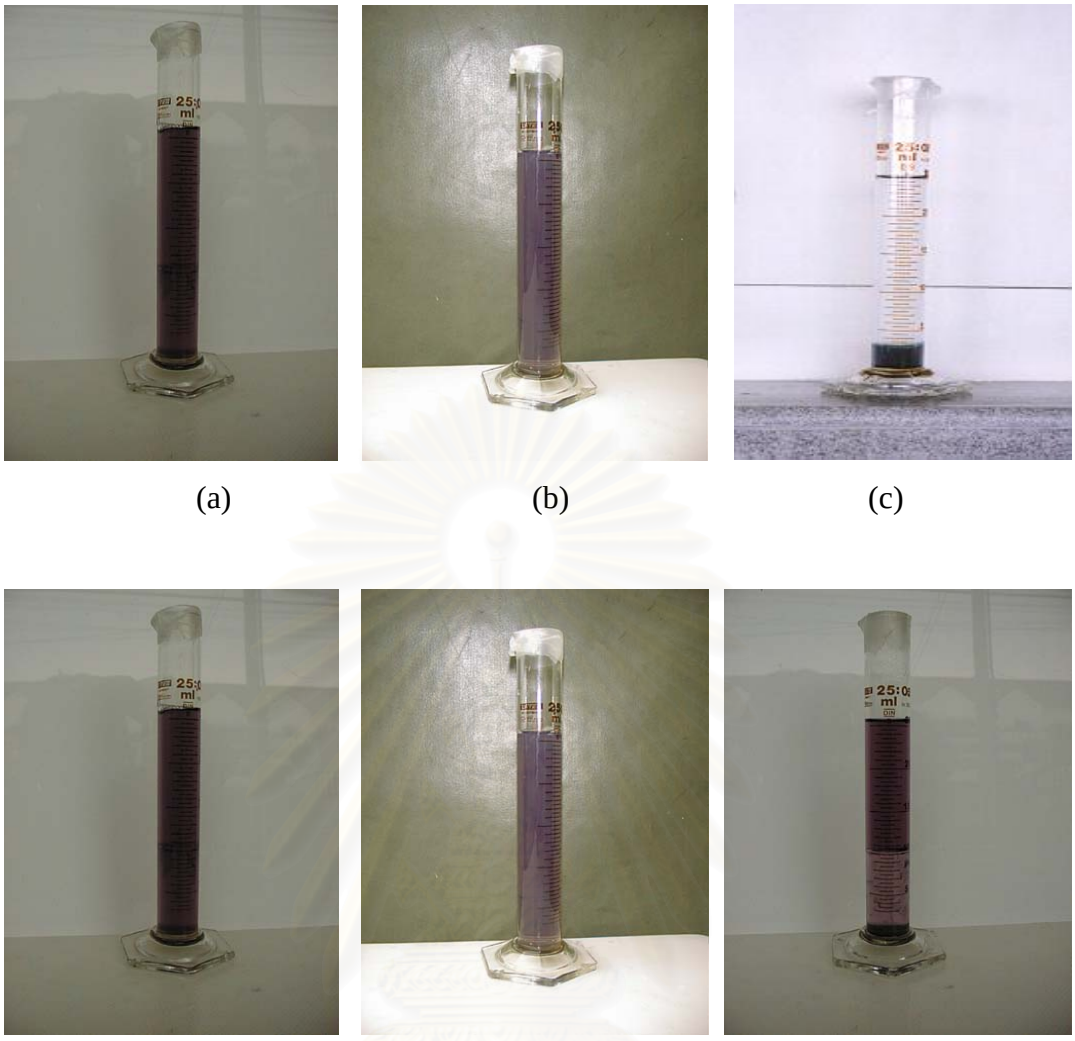

(a) (b) (c)

(d) (e) (f)

Figure 4.2 An experiment on cloud point extraction of gold using PONPE-9 as a separation media in a presence of NaOH in the basic pH range (a-c), in the solution pH of 7 (d-f). [PONPE] = 2.5% (w/v), [Au^{3+}] = 10 ppm, T = 56 ^{o}C.

4.3.2 Effect of Equilibration Time

It should be mentioned that many research works of CPE spent a long period of time such as overnight to make sure that the separation reached the equilibrium separation between phases. Therefore, the time required for allowing the equilibrium separation between phases was one of the important parameters that suggest the

feasibility of the process scheme. The time of equilibration was optimized by finding the shortest time period required for complete separation of the phases.

In this series of experiments, the concentration of PONPE-9 was kept constant at 2.5 % (w/v) and gold concentration was 5 and 10 ppm. The pH of the solution was in the range of 2.52 to 2.89. The temperature was controlled at 56, 60 and 65 ^{o}C. The results of these experiments are presented in Figure 4.3. $C_{Au,w}$ is the concentration of gold ion in the water-rich phase, and $C_{Au,o}$ is the initial concentration of gold ion in the solution. From Figure 4.3, the ratio of $C_{Au,w}/C_{Au,o}$ decreases rapidly with time and reach the equilibrium. At the settling temperature of 56, 60 and 65 ^{o}C, the results show the effect of temperature on the separation rate between phases. The higher the settling temperature, the shorter period of time required to reach separation equilibrium between phases. It is attributed to the dehydration rate upon the settling temperature. It is known that heat supplied to the surfactant solution causes dehydration from the surfactant moiety, surfactant aggregation, and consequently separation of surfactant from aqueous phase. Therefore, the dehydration rate depends on the amount of energy gained from supplied heat. Then, aggregation rate of the surfactant in surfactant-rich phase increases with increasing temperature. All curves suggest the required time of 6 h for the complete separation between phases

4.3.3 Effect of PONPE-9 to Gold Ion Ratio

In these experiments, the gold concentration was varied over the range of 1 to 18 ppm. The PONPE-9 was 1, 2.5% (w/v). The temperature was kept constant at 60 ^{o}C. The solution pH was in the range of 2.52 to 2.89. From Figure 4.4, the percent extraction of gold increases with increasing the ratio of PONPE-9 to gold ion from 400 to 1500. This result is based on the fact that the higher amount of surfactant, the more rooms available for gold ion to occupy. At the PONPE-9/gold ratio higher than 1500, the percent extraction shows insignificant change that suggests the excess of PONPE-9 required for binding with gold ion. The ratio of the surfactant PONPE-9 to gold (III) ion that provides the highest efficiency (98.78%) with a small amount of surfactant is about 1500.

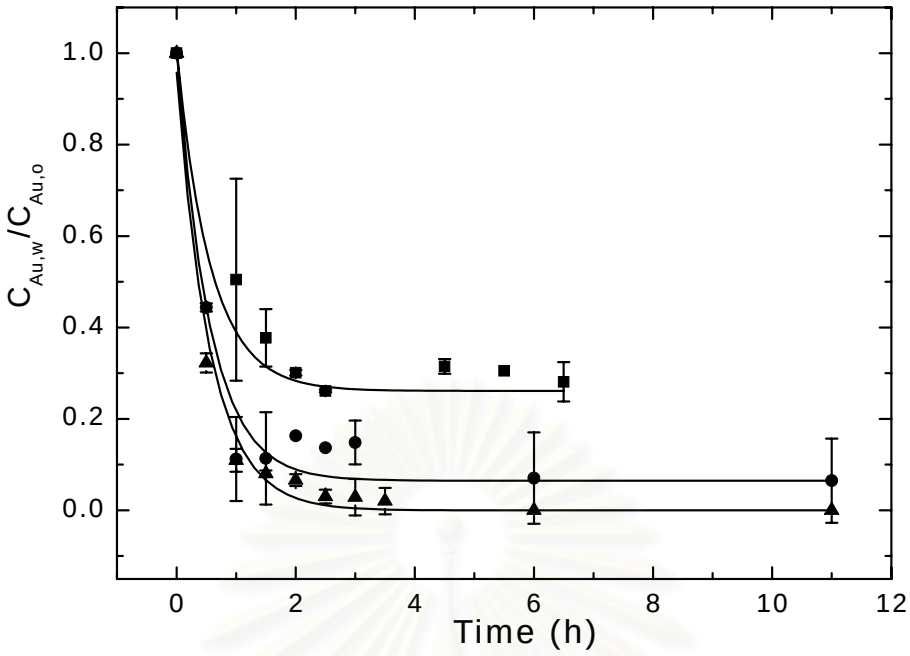

Figure 4.3 Effect of equilibration time on $C_{Au,w}/C_{Au,o}$ at T = 56 °C (■), T = 60 °C (●), T = 65 °C (▲). $C_{Au,o}$ is the initial concentration of gold ion in the mixed solution, $C_{Au,w}$ is the concentration of gold ion in the water-rich phase at any time, [PONPE-9] = 2.5% (w/v), [Au^{3+}]= 5,10 ppm, pH = 1.87.

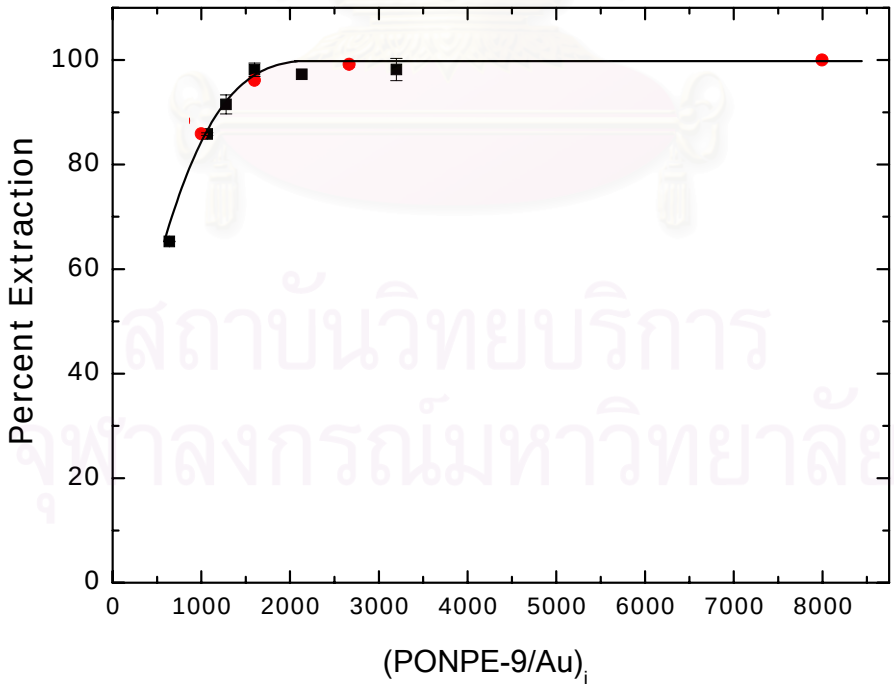

Figure 4.4 Effect of ratio of PONPE-9 and Au^{3+} on percent extraction. [PONPE-9] = 1% (w/v) (■), [PONPE-9] = 2.5 % (w/v) (●), [Au^{3+}] = 1 - 18 ppm, pH = 2.52 to 2.89, T = 60°C, t = 6 h.

4.3.4 Effect of Settling Temperature

The experiments were carried out in the temperature range 56 to 80 ^{o}C with PONPE-9 concentration of 2.5 % (w/v). The gold concentration was 5 and 10 ppm. The pH of the solution was adjusted to 1.97 and 2.98. The result of the dependence of the percent extraction of gold on the settling temperature is depicted in Figure 4.5. The percent extraction of gold initially increases, levels off, and then decreases as the settling temperature increased. The similar temperature effect result was observed for the extraction of 1-hexanol with Igepal CA-620 by Frankewich et al. [1] and for the extraction of gold in HCl with PONPE-7.5 by Akita et al.[28]. This behavior is ascribed to poor phase separation due to too small and too large temperature difference between the CP and settling temperature [28]. From Figure 4.5, the settling temperature in the range of 65 to 70 ^{o}C provides high percent extraction of gold. The range of the settling temperature could substantiate the conclusion published elsewhere that the greatest effect of equilibration temperature on the extent of extraction occurs when the equilibration temperature is less than 15-20 ^{o}C which is greater than that of the cloud point temperature [1]. Therefore, the settling temperature of 65 ^{o}C which gives the highest percent extraction (99.0%) with low energy consumption, is appropriate for the gold recovery scheme.

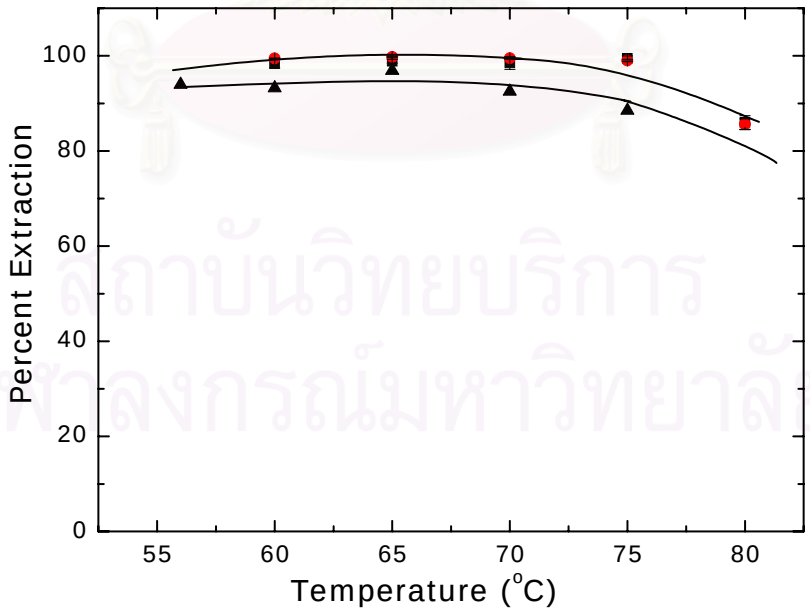

Figure 4.5 Effect of temperature on percent extraction. [PONPE-9/Au^{3+}] = 1599 at pH = 2.98 (■), [PONPE-9/Au^{3+}] = 1599 at pH = 1.97 (●), [PONPE-9 /Au^{3+}] = 799 at pH = 2.98(▲), t = 6 h.

4.3.5 Effect of pH

The interesting result was obtained in the study of effect of solution pH. In this series of experiments, the solution pH was varied over the range of 1 to 12. The PONPE-9 and gold concentration were kept constant at 2.5 % (w/v) and 5 ppm, respectively (the ratio of PONPE-9 to gold is 1599). The experiments were carried out at the settling temperature of 56, 65 and 80 ^{o}C. It is found that all experiments conducted at the pH of the solution in both of the acidic and basic solutions provide high percentage of extraction with maximum at pH 3, ca. 98-99 % of gold. It is in sharp contrast to gold extraction conducted at pH 7 that only 21-25 percent extraction can be achieved. This result suggests the pH influences on gold complex moiety involving the interaction between gold-complex ions and PONPE-9. At a low ionic strength condition, pH 7, a neutral form of surfactant does not interact with and bind the gold-complex. Therefore, a lesser amount of gold ion is extracted in surfactant-rich phase and the percentage of extracted gold decreases at pH 7.

Therefore, the solution pH affects the surfactant and the gold-complex ion structures. It is known that gold (III) ion exists in hydrochloric acid as tetrachloro gold (III) ion at low pH while gold (III) hydroxide is formed at high pH [49]. Both forms of the gold complex with ionic moiety can bind with PONPE-9 in micelle aggregation. It is controversial at pH 7, where the gold-complex ion and also surfactant exist in the neutral meioty. Thus, the interaction of PONPE nonionic surfactant and metal ion has been driven by both the dipole interaction between complex ion and polyoxyethylene of PONPE.

Though, the extraction of some target analytes from the surfactant-rich phase is not difficult, the removal of entrapped analytes from the mediated surfactant is encountered by the strong interaction between surfactant and analytes. From this experimental result, the CPE at pH 7 can be used as the method of separation of the gold-complex ion from PONPE-9.

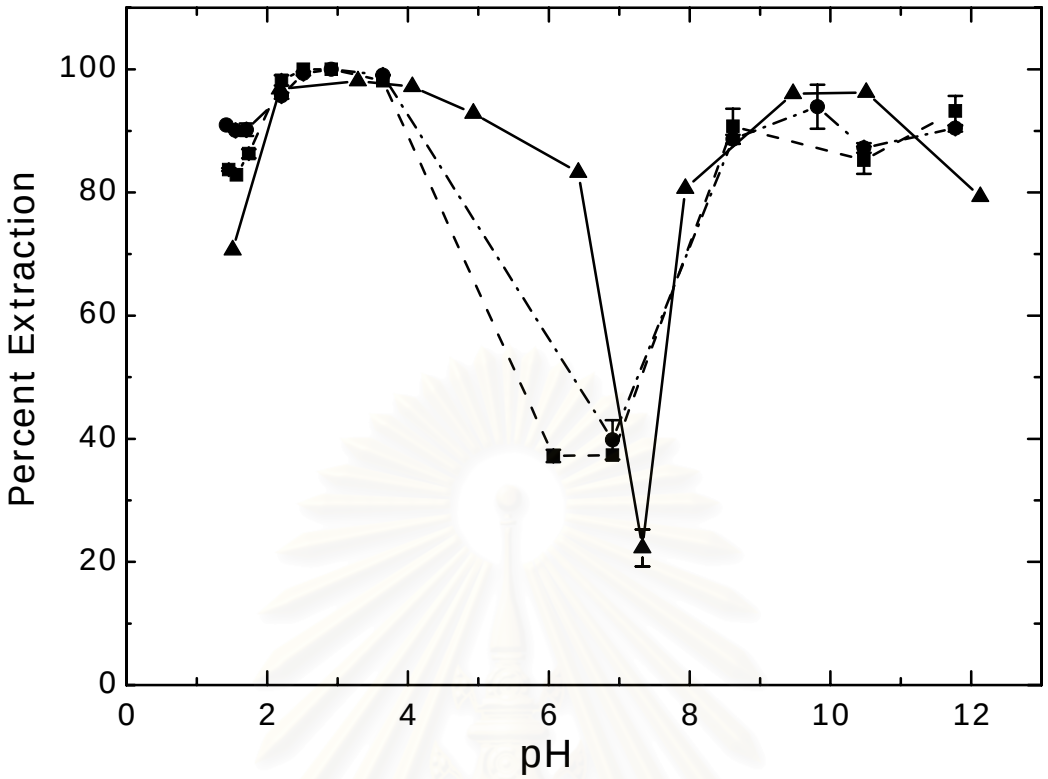

Figure 4.6 Effect of pH on percent extraction at T = 56 ^{o}C (■), T = 60 ^{o}C (●), T = 80 ^{o}C (▲). [PONPE-9] = 2.5% (w/v), [Au^{3+}] = 5 ppm, [PONPE-9 /Au^{3+}] = 1599, t = 6 h.

From this work, the appropriate conditions for the CPE of gold (III) ion are as follows:

1. The equilibration time for separation between phases is 6 hours.
2. The ratio of PONPE-9 to gold ion is 1500 : 1.
3. The settling temperature is 65 ^{o}C.
4. The maximum and minimum efficiency for recovering gold ion were at the solution pH of 3 and 7, respectively.

One of the aims of this work is to develop the process for recovering gold from mixed metal ions using a convenient method without using toxic organic solvent. The experiments for extracting gold from mixed metal ion solution were carried out at various pH. Mixed metal ion solution of copper (II) ion, nickel (II) ion, Zinc (II) ion as well as gold (III) (see Table 4.1) was used. This solution represents the solution etched from electronic printed substrate [28]. The extraction condition was at 65^{o}C and the ratio of PONPE-9 to gold ion of 1500. Figure 4.7 shows the

effect of pH on the percent extraction of each metal. It can be seen that the extraction of other metals is depressed and complete extraction of gold ion (98.8 %) is obtained in the same manner as that for the single metal system at the same pH region (see Figure 4.6). The percent extraction of gold ion (80- 95%) at lower pH (pH 1 to 2) is less than that at the pH 2 to 3.9 (98.8 %). Little change in the percent extraction of the undesirable metals is observed for the investigated pH range. Thus, the solution pH 3 was chosen to be the appropriate operating condition for the extraction of gold from multimetal solution. The obtained percent extraction of gold, copper, nickel and zinc are 98.8, 4.3, 10.0 and 0.0 %, respectively.

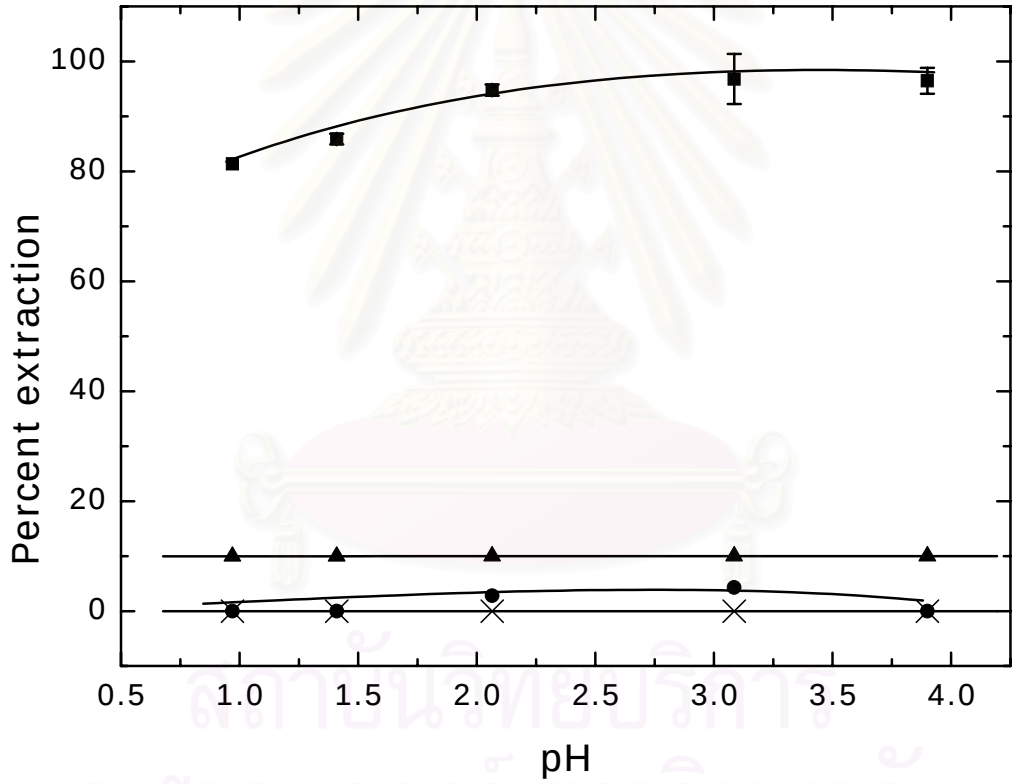

Figure 4.7 Effect of pH on percent extraction of metal ions. Au^{3+} (■), Ni^{2+} (▲), Cu^{2+} (●), Zn^{2+} (×), [PONPE-9] = 2.5 % (w/v), $[Au^{3+}]_o$ = 5 ppm, $[Cu^{2+}]_o$ = 100.9 ppm, $[Ni^{2+}]_o$ = 8.25 ppm, $[Zn^{2+}]_o$ = 0.08 ppm, pH = 1-3.8, T = 65 ^oC, t = 6 h.

The effect of NaCl concentration on percent extraction of gold of CPE was investigated. The concentration of PONPE-9 and metal ions (Au^{3+}, Cu^{2+},Ni^{2+}, Zn^{2+}) were the same as the previous experiment (see Table 4.1). The NaCl used as an electrolyte was varied in the range of 0 to 0.8 mol L^{-1} and the extraction condition was performed at 65^{o}C. The results are shown in Figure 4.8. It can be seen that NaCl added in the multimetal solution lowers the extraction efficiency of gold than that in the absence of NaCl. Even the CP of solution in the presence of NaCl is lowered than that in the absence of NaCl which should provides higher percent extraction according to the larger difference between settling temperature and cloud point. It is attributed to the poor phase separation caused by NaCl [28]. In particular, a solution with 1.0 M NaCl results in ambiguous phase separation, with the surfactant-rich phase being formed as an upper phase in the region of low pH. The effect of NaCl found in this work is in accordance with the result obtained from the CPE of gold using PONPE-7.5 reported by Akita et al. [28].

It should be noted that the high extraction efficiency of gold (III) ion is obtained without the addition of any complexing agents and NaCl. It may be an advantage from the viewpoint of process economics.

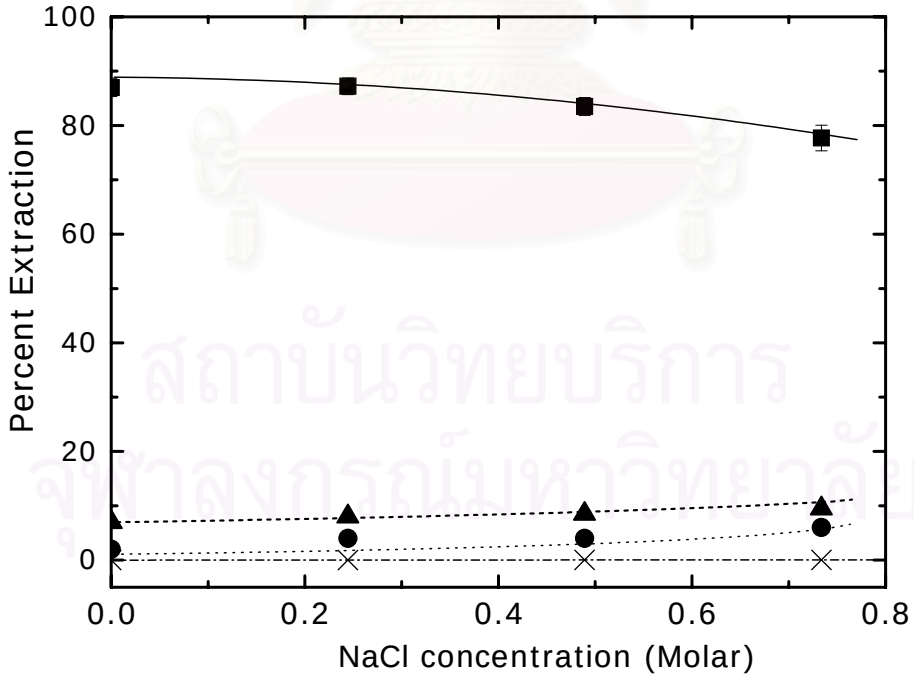

Figure 4.8 Effect of NaCl concentration on percent extraction of metal ions. Au^{3+} (■), Ni^{2+}(▲), Cu^{2+} (●), Zn^{2+} (×), [PONPE-9] = 2.5 % (w/v), $[Au^{3+}]_o$ = 5 ppm, $[Cu^{2+}]_o$= 100.9 ppm, $[Ni^{2+}]_o$ = 8.25 ppm, $[Zn^{2+}]_o$ = 0.08 ppm, pH = 3, T = 65 ^{o}C, t = 6 h.

4.3.6 Gold Recovery Process by CPE

The recovery of gold by CPE in a scale-up process was carried out in one liter extraction column. The time required for allowing the equilibrium separation between phases was determined. In this series of experiments, the concentration of PONPE-9 was 2.5 % (w/v) and gold concentration was 5 ppm. The temperature was maintained at 65 ^{o}C. The results are presented in Figure 4.9. $C_{Au,w}$ is the concentration of gold ion in the water-rich phase, and $C_{Au,o}$ is the initial concentration of gold ion in the solution. From Figure 4.9, the ratio of $C_{Au,w}/C_{Au,o}$ decrease rapidly with time in the same manner as that for the experiment performed in 25-cm^3 graduated cylinder (see Figure 4.3). The curve suggests the required time of 6 h for the complete separation between phases in 1-liter column.

As the result of the effect of variation of solution pH, large amount of gold is extracted into the surfactant-rich phase at pH 7 while the amount extracted is very small at pH 7. The result at pH 7 suggested the condition being suitable for separating gold from gold-entrapped surfactant. The process scheme was designed and named as the pH-switching method for recovering gold as shown in Figure 4.10. The process mainly consists of three steps: (i) extraction of gold ion from multimetals solution into the surfactant-rich phase in column No.1 (ii) separation of gold from gold-entrapped surfactant in column No.2 (iii) precipitation of gold metal.

Figure 4.11 shows the gold extraction in the extraction column No.1. The mixed solution appears clear blue color of copper ion as shown in Figure 4.11a. It is noteworthy that the mixed metal solutions contain copper and nickel much larger amounts than gold. Figure 4.11b shows the turbid phenomena at pH 3 after the increase in temperature to CP (65^{o}C). Figure 4.11c and 4.11d illustrate the two phases at equilibrium separation after 6 h. Here, the gold ion is extracted into the surfactant-rich phase which shows yellow color of gold while other ions (Cu^{2+}, Ni^{2+}, and Zn^{2+}) exist in the water-rich phase which shows blue color.

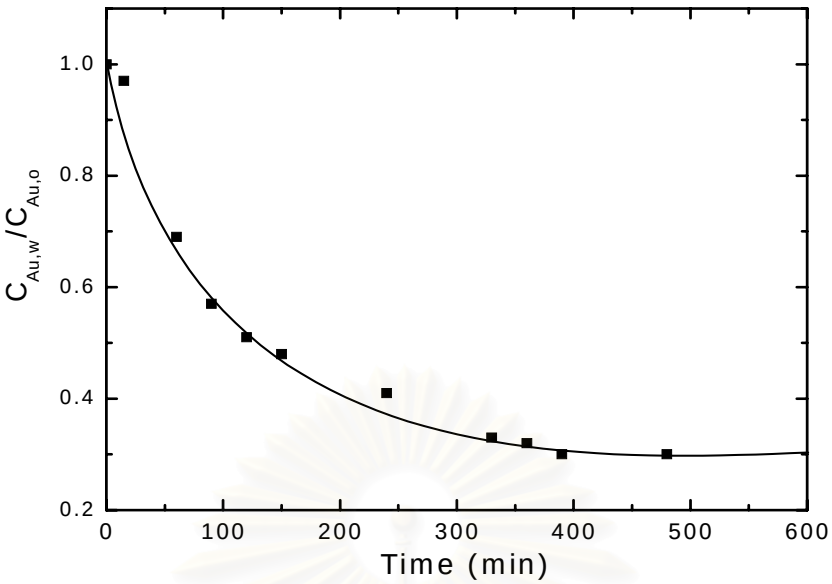

Figure 4.9 Ratio of $C_{Au,w}/C_{Au,o}$ as a function of time. $C_{Au,o}$ is the initial concentration of gold ion in the mixed solution, $C_{Au,w}$ is the concentration of gold ion in the water-rich phase at any time, [PONPE-9] = 2.5 % (w/v), $[Au^{3+}]_o$ = 5 ppm, pH = 3, T= 65 ^oC.

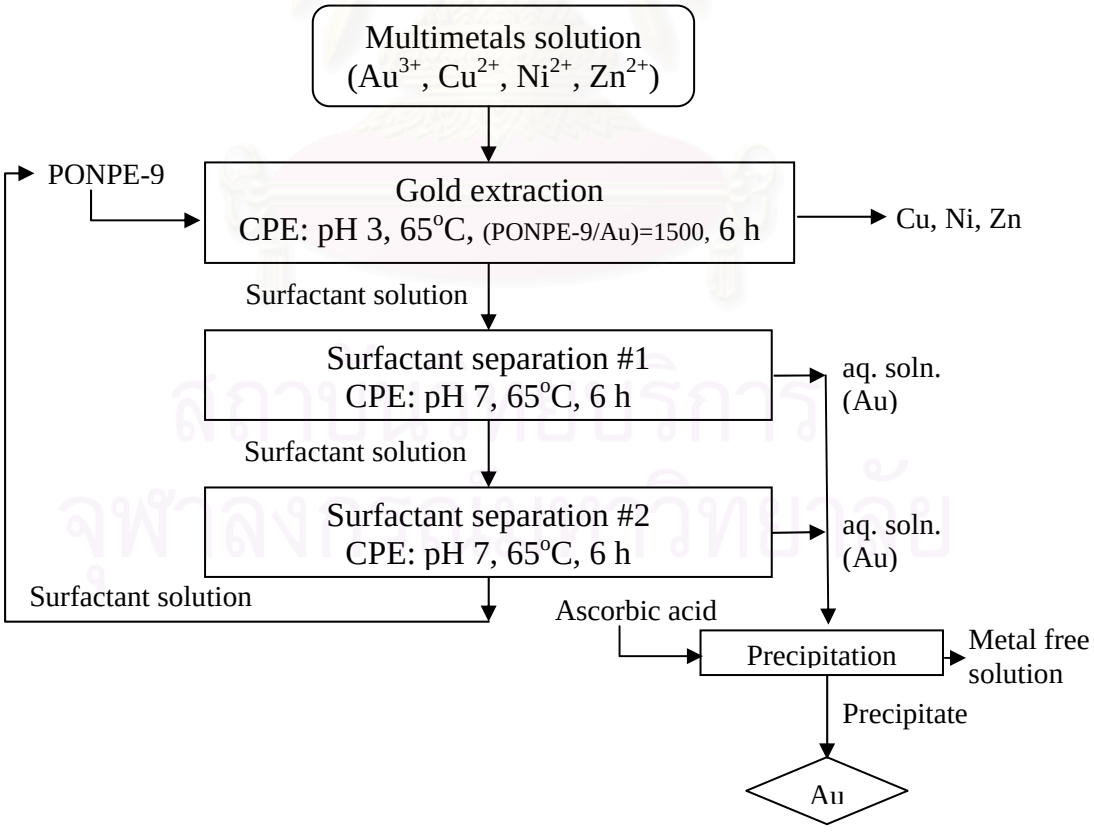

Figure 4.10 Process scheme of gold (III) ion recovery using CPE with PONPE-9.

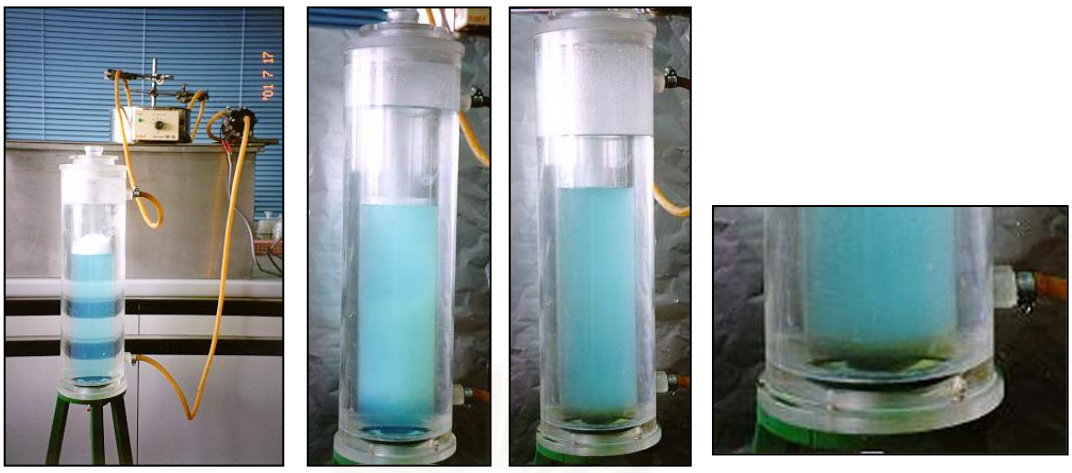

(a) (b) (c) (d)

Figure 4.11 Gold extraction from multimetal solution in 1-Liter column. (a) the initial multimetal solution in the extraction column No. 1 before heating, (b) turbid phenomena after increasing the temperature to CP, (c) the two phases after equilibrium separation, (d) close-up picture shows the interface between surfactant-rich phase and water-rich phase.

After the surfactant-rich phase was transferred into separation column No. 2, water was added and the solution pH was adjusted to pH 7 (see Figure 4.12a).The CPE was then applied at temperature of 65^{o}C for 6 h. It should be noted here that gold (III) ion surrounding with hydroxide ion in PONPE-9 shows purple color. Figure 4.12b illustrates the separation between phases after the CPE at pH 7. It shows purple color of the water-rich phase enriching with gold ion. The CPE of surfactant-rich phase was repeated at pH 7 (see Figure 4.10). It is clearly shown that the gold-free surfactant settles in the surfactant-rich phase of white color. Therefore, total percent recovery of gold in the water-rich phase was 63.3%.

The gold solution was then transferred to the precipitation bath and precipitated by ascorbic acid as reducing agent. The percentage recovery of gold in each step is summarized in Table 4.2. The recovery of metallic gold was obtained with 98.01% purity determined by SEM mounted with EDX. Figure 4.13 shows the scanning electron micrograph of the surface of the high fineness gold powder precipitated.

(a) (b)

Figure 4.12 Phase separation after CPE in the column No. 2.

Table 4.2 Percent extraction of gold from the multimetal solution.

Column number	Operation	Condition	Cycle number	Percent of gold
Column 1	Gold extraction	pH = 3 T = 65 ^{o}C Time = 6 h [PONPE-9/Au^{3+}] = 1500	1	98.8
Column 2	Gold separation from surfactant-rich phase	pH = 7 T = 65 ^{o}C Time = 6 h	2	63.3

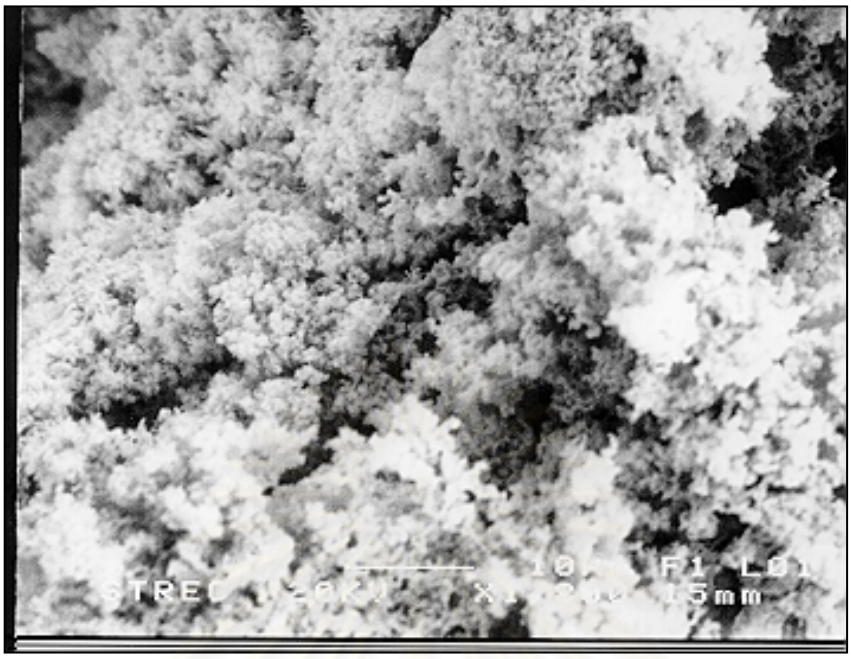

Figure 4.13 Scanning electron micrograph of precipitated gold metal (x 1000).

It should be noted here that relatively high loss of gold is occurred from the draining step of the thick solution of surfactant-rich phase from the column. It is possible that when the thick solution of surfactant-rich phase was drained off through the valve at the bottom of the column, the aqueous solution of water-rich phase which flows over the top moved through the lower phase due to its weight. Thus, the thick solution of surfactant-rich phase cannot be completely separated from the column, consequently, 63.3 percent gold recovery was obtained in this work.

4.4 Conclusion

PONPE-9 provides a good efficiency for recovering gold ion from multimetal solution. The proposed pH-switching process scheme consists of two batches of CPE performed at different solution pH. The first batch is to extract gold ion from other metal ions at pH 3. The second is conducted at pH 7 for separating gold ion from gold-entrapped surfactant. Metallic gold is finally precipitated. Advantages cited for the use of pH switching method include (i) the extraction can be carried out without organic solvent for metal stripping and (ii) after the extraction of gold from others metal ions by applying CPE at pH 3, it is much easier (compare to organic solvent

extraction) to separate gold by applying subsequently CPE at pH 7. Moreover, the separation efficiency can be improved by introducing a multistage process that deserves a further study. Therefore, it can be a choice for the gold ion recovery from expired electronic parts under the environmental saving concept.

CHAPTER 5

INTERACTION BETWEEN PONPE-9 AND GOLD (III) ION IN ADSORBED FILM AND MICELLE

5.1 Introduction

By means of the extraction of gold with PONPE-9 via cloud point extraction, gold (III) ion was incoorporated into micelle of PONPE-9 and concentrated into the surfactant-rich phase. The existence of the interaction between gold (III) ion and surfactant imposes the percent extraction of gold. It is under curiosity whether the changes in adsorption and micelle formation studied by thermodynamic approach can suggest the interaction between gold ion and PONPE-9. Hence, the thermodynamic equations are developed and proposed to study the interaction between gold ion and PONPE-9.

In the study on CPE of gold (III) ion using PONPE-9 in chapter 4, the remarkable dependence of the extraction efficiency on pH is shown that it is very high not only in acidic condition around pH 3 but also in basic one around pH 10, and is the lowest around pH 7 (see Figure 4.6). Presented is the study on interaction between PONPE-9 and $HAuCl_4$ in adsorbed films and micelles in the solution of some pH values by applying the thermodynamic method developed previously for mixed surfactant systems [4,5,50-53].

In the previous studies on mixed surfactant systems, on the other hand, it has been shown that the thermodynamic analysis of the surface tension data is useful to elucidate the interaction between ionic and nonionic surfactant, nonionic surfactant and some electrolytes such as HCl and NaCl [5]. Then, also in this study, the thermodynamic method [4,51] is applied to examine whether there exists the interaction between PONPE-9 and gold and also to shed light on the correlation between the results from the CPE and those from the surface tension measurements.

The thermodynamic equations were applied to the surface tension data of the aqueous solution of the PONPE-9 and $HAuCl_4$ mixtures at pH 3, pH 7, and pH 10. The results were discussed from the viewpoint of the interaction between PONPE-9

and gold not only in the adsorbed film but also in the micelle. The comparison among the results at three pH values of the solution was performed and provides satisfactory correspondence to the results of the extraction efficiency.

5.2 Experimental

5.2.1 Materials

PONPE-9 was obtained from Rhodia (Thailand) Limited., and used without further purification. Hydrogen tetrachloroaurate (III) tetrahydrate ($HAuCl_4.4H_2O$) was purchased from Nacalai Tesque, Inc., Japan. Water used in the surface tension measurement was purified by the distillation of three times from alkaline permanganate solution. NaOH and HCl solution were used for pH adjustment.

5.2.2 Surface Tension Measurement

The surface tension of the aqueous solution of PONPE-9 and the mixture were measured as a function of the total molarity m at pH 3, 7 and 10 by the drop volume technique at 298.15 K under atmospheric pressure [41,42] (detail in Chapter 2.2.2). The temperature was controlled within ±0.01 K by a controlled temperature water bath. The experimental error of the surface tension was within 0.05 mN m^{-1}.

5.2.3 Cloud Point Extraction Procedure

The cloud point extraction of gold (III) ion was carried out as follows: an aqueous solution containing given amount of PONPE-9 and gold (III) ion was prepared at the specified pH at room temperature. Then the solution was heated to a desired temperature at which the solution was separated into the water-rich and surfactant-rich phases. After the separation reaches the equilibrium, the concentration of gold in the water-rich phase C_w was determined by atomic absorption instrument (AA) and then that in the surfactant-rich phase C_s was calculated on the basis of mass

balance. The percent extraction, %E, were calculated by using the gold concentrations and the equilibration volumes of both the surfactant-rich and water-rich phases, V_s and V_w, as

$$E(\%) = 100\, V_s C_s / (V_s C_s + V_w C_w). \quad (5.1)$$

5.3 Results and disscussion

5.3.1 Thermodynamic Equations

The studied systems were composed of PONPE-9, $HAuCl_4$, and HCl at pH 3, and on the other hand PONPE-9, $HAuCl_4$, and NaOH at pH 7 and 10, respectively. According to the potential-pH equilibrium diagram of the gold-water system [49], it is said that gold is dissolved as hydroxide $Au(OH)_3$ in the pH range from 2 - 11. However, the visual observation under the presence of PONPE-9 showed that the color of the aqueous mixture was pale yellow at pH 3 and purple at pH 7 and 10. Therefore, we looked on the dissolved species of gold as $AuCl_4^-$ at pH 3 and $Au(OH)_3$ in the colloidal form stabilized by PONPE-9 molecules at pH 7 and 10, respectively.

At pH 3, therefore, the total molality of the solution m defined by

$$m = m_{H^+} + m_{AuCl_4^-} + m_{PO} = 2m_{Au} + m_{PO} \quad (5.2)$$

and the mole fraction of PONPE-9 and gold in the mixture by

$$X_{PO} = m_{PO}/m \quad (5.3)$$

and

$$X_{Au} = 2\, m_{Au} / m \quad (5.4)$$

are employed as the concentration variables according to the thermodynamic viewpoints [4,51]. Here m_{Au} and m_{PO} are the molalities of $HAuCl_4$ and PONPE-9, respectively.

At pH 3 the chemical species in the air/aqueous solution system are air, H^+, Cl^-, $AuCl_4^-$, PONPE, OH^-, and H_2O, and then

$$-\mathrm{d}\gamma/RT = (\Gamma_{H^+}/m_{H^+})\,\mathrm{d}m_{H^+} + (\Gamma_{Cl^-}/m_{Cl^-})\,\mathrm{d}m_{Cl^-} + (\Gamma_{AuCl_4^-}/m_{AuCl_4^-})\,\mathrm{d}m_{AuCl_4^-} + (\Gamma_{PO}/m_{PO})\,\mathrm{d}m_{PO} + (\Gamma_{OH^-}/m_{OH^-})\,\mathrm{d}m_{OH^-} + (\Gamma_{air}/m_{air})\,/\,\mathrm{d}m_{air} + (\Gamma_{H_2O}/m_{H_2O})\,/\,\mathrm{d}m_{H_2O} \quad (5.5)$$

According to the two dividing surface convention, $\Gamma_{air} = 0$ and $\Gamma_{H_2O} = 0$, and the very small concentration ($\approx 10^{-11}$) at this pH, the fourth term $(\Gamma_{OH^-}/m_{OH^-})\,\mathrm{d}m_{OH^-}$ is negligible. Using the concentration of gold complex, m_{Au} and that of HCl for adjusting pH, m_{HCl}, and assuming the complete dissociation of gold complex, we have the relation

$$m_{H^+} = m_{HCl} + m_{Au},\ m_{Cl^-} = m_{HCl},\ m_{AuCl_4^-} = m_{Au} \quad (5.6)$$

Since the concentration of HCl m_{HCl} is kept constant, then

$$\mathrm{d}m_{H^+} = \mathrm{d}(m_{HCl} + m_{Au}) = \mathrm{d}m_{Au},\ \mathrm{d}m_{Cl^-} = \mathrm{d}m_{HCl} = 0 \quad (5.7)$$

Therefore, the interfacial tension is given as a function of the concentrations of the gold complex and the PONPE at constant HCl concentration,

$$-\mathrm{d}\gamma/RT = (\Gamma_{H^+}/m_{H^+})\,\mathrm{d}m_{Au} + (\Gamma_{AuCl_4^-}/m_{AuCl_4^-})\,\mathrm{d}m_{Au} + (\Gamma_{PO}/m_{PO})\,\mathrm{d}m_{PO} \quad (5.8)$$

Here, the surface density of gold is defined by

$$\Gamma_{Au} = \frac{\Gamma_{Cl^-}}{(1 + m_{HCl}/m_{Au})} + \Gamma_{AuCl_4^-} \quad (5.9)$$

Then, the Eq. 5.8 is simplified as

$$-\mathrm{d}\gamma/RT = (\Gamma_{Au}/m_{Au})\,d\,m_{Au} + (\Gamma_{PO}/m_{PO})\,d\,m_{PO}. \quad (5.10)$$

At pH 7 and 10, the chemical species are air, H^+, Na^+, Cl^-, OH^-, $Au(OH)_3$, and H_2O, and then by using the two dividing surface convention, we have

$$-\mathrm{d}\gamma/RT = (\Gamma_{H^+}/m_{H^+})\,\mathrm{d}m_{H^+} + (\Gamma_{Na^+}/m_{Na^+})\,\mathrm{d}m_{Na^+} + (\Gamma_{Cl^-}/m_{Cl^-})\,\mathrm{d}m_{Cl^-} + (\Gamma_{Au(OH)_3}/m_{Au(OH)_3})\,\mathrm{d}m_{Au(OH)_3} + (\Gamma_{PO}/m_{PO})\,\mathrm{d}m_{PO} + (\Gamma_{OH^-}/m_{OH^-})\,\mathrm{d}m_{OH^-} \quad (5.11)$$

Now m_{H^+} is very small ($\approx 10^{-7}$ at pH7, $\approx 10^{-10}$ at pH10) irrespective of the m_{Au} value, and the concentration of the chemical species are

$$m_{Na^+} = m_{NaOH},\ m_{Cl^-} = 4\,m_{Au},\ m_{Au(OH)_3} = m_{Au},\ m_{OH^-} = m_{NaOH}. \quad (5.12)$$

Since the concentration of NaOH m_{NaOH} is kept constant, then

$$\mathrm{d}\,m_{Na^+} = \mathrm{d}\,m_{NaOH} = 0,\ \mathrm{d}\,m_{OH^-} = \mathrm{d}\,m_{NaOH} = 0. \quad (5.13)$$

Then, the surface tension at constant NaOH concentration is given by

$$-\mathrm{d}\gamma / RT = (\Gamma_{Cl^-} / m_{Au})\,\mathrm{d}\,m_{Au} + (\Gamma_{Au(OH)_3} / m_{Au})\,\mathrm{d}\,m_{Au} + (\Gamma_{PO} / m_{PO})\,\mathrm{d}\,m_{PO}. \quad (5.14)$$

Here, the surface density of gold is defined by

$$\Gamma_{Au} = \Gamma_{Cl^-} + \Gamma_{Au(OH)_3} \quad (5.15)$$

Then, the Eq. 5.14 is simplified as

$$-\mathrm{d}\gamma / RT = (\Gamma_{Au}/m_{Au})d\,m_{Au} + (\Gamma_{PO}/m_{PO})d\,m_{PO}. \quad (5.16)$$

Comparing Eqs. 5.9 and 5.10 to Eqs. 5.15 and 5.16, it should be noted that we have apparently the same equation at different pH, although Γ_{Au} consists of a surface density of different type of ions, H^+ or Cl^-, besides the surface density of gold.

Here, m and X_{PO} at pH 7 and 10 are also defined according to Eqs. 5.3 and 5.4, respectively for the convenience, although it is not necessary to use these definitions because gold is dissolved as nonionic hydroxide [4,51].

5.3.2 Effect of pH and Surfactant Concentration

The experiments were carried out in the solution of pH 3, 7 and 10. In this series of experiments, the surface tension of the solution of PONPE-9 in the absence and in the presence of $HAuCl_4$ was measured. The concentration of PONPE-9 was

varied over the range of 0 to 0.12 mmol.kg^{-1} and mole fraction of gold, X_{Au}, was fixed at 0.47. The surface tension of PONPE-9 solution was plotted against PONPE-9 molality, m_{PO}, as shown in Figure 5.1. Hereafter, the solutions in the absence of $HAuCl_4$ and in the presence of $HAuCl_4$ are called the reference and the mixture, respectively. It is seen that the surface tension decreases with increasing the molality m_{PO} and there is a distinct break point at the critical micelle concentrations (cmc). It should be noted that there exists the appreciable difference between the two curves at pH 3 and pH 10, but no appreciable one at pH 7.

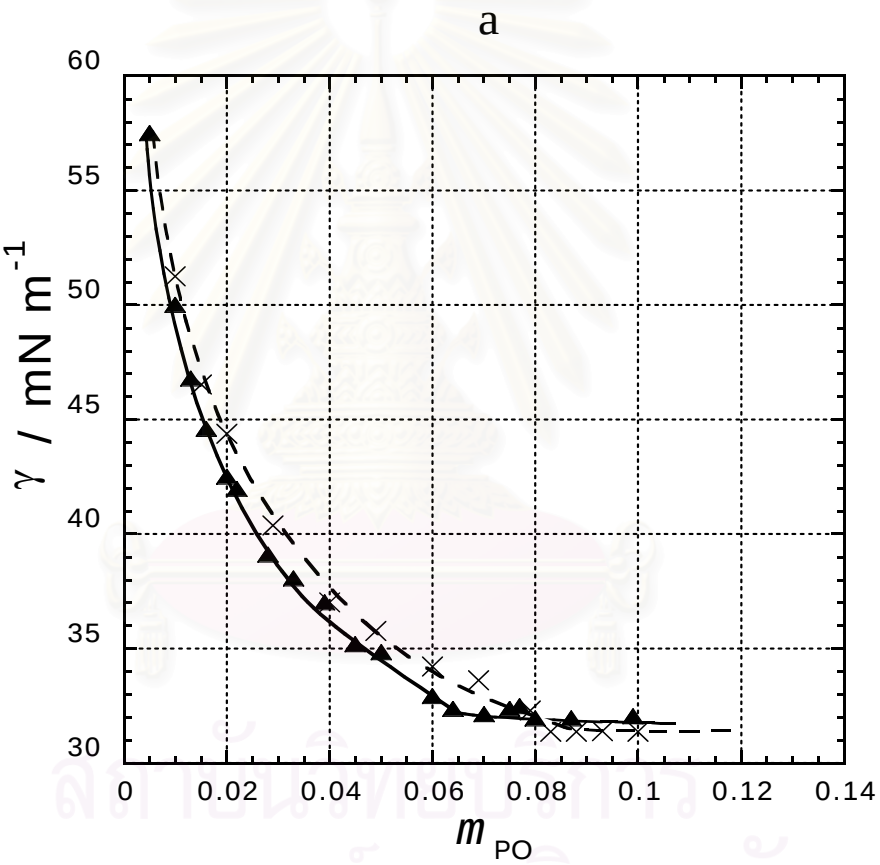

Figure 5.1a Surface tension versus surfactant molality curves of the mixture at pH 3 (▲) and the reference (×).

b

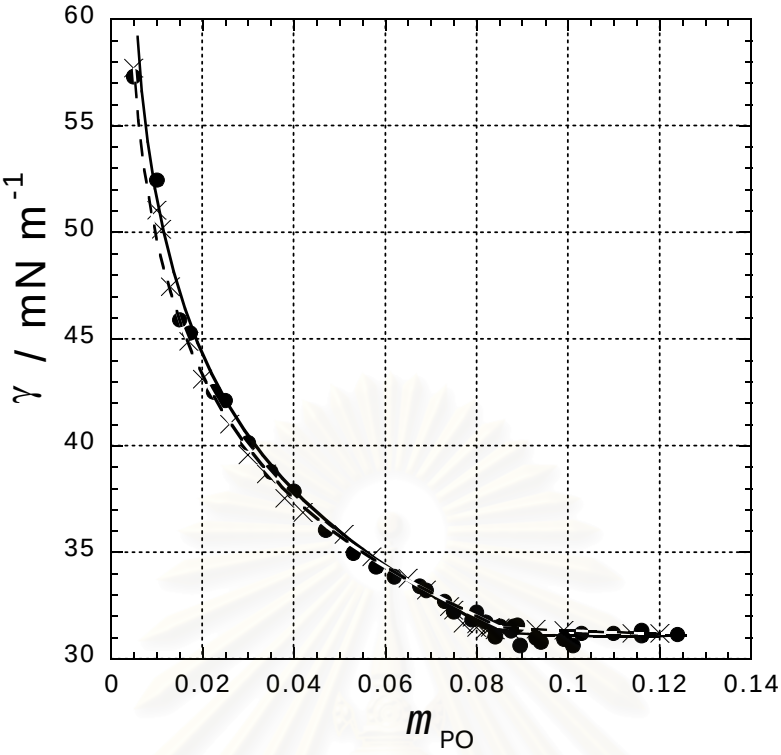

Figure 5.1b Surface tension versus surfactant molality curves of the mixture at pH 7 (●) and the reference (×).

c

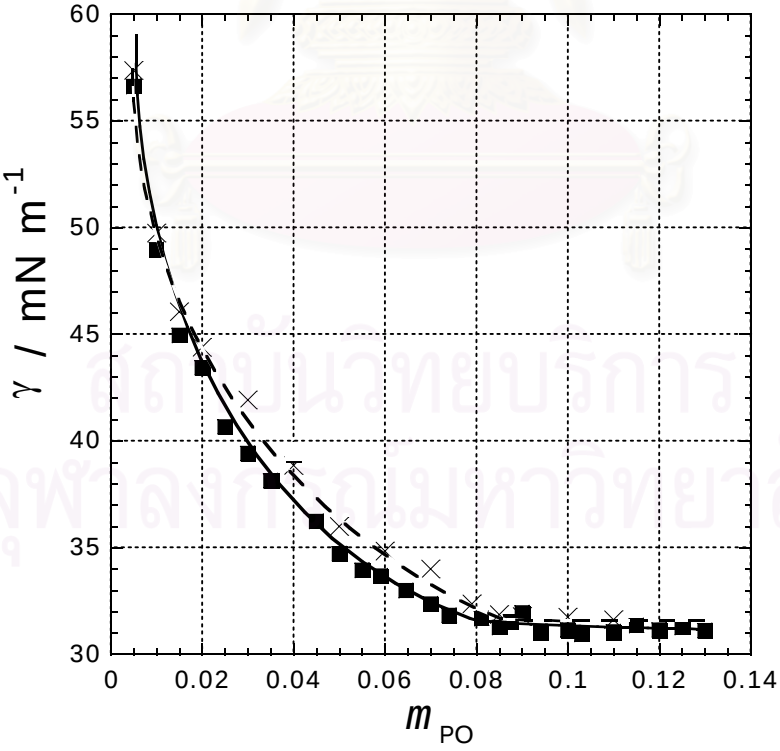

Figure 5.1c Surface tension versus surfactant molality curves of the mixture at pH 10 (■) and the reference (×).

Figure 5.2 shows the γ vs the total concentration m plots of the mixtures and the references at the three pH values of the solution. The cmc was determined from Figures 5.1 and 5.2; let C ,C_{Au}, and C_{PO} are referred to the total molality, gold and surfactant molality at the cmc of the mixture and $C_{\mathrm{PO}}^{\mathrm{o}}$ is referred to the surfactant molality at the cmc of the reference, respectively. The numerical values are summarized together with the surface tension at the cmc, γ^{C}, in Table 5.1. It is important to note that the cmc of the mixtures are in the order of

$$C_{\mathrm{PO}}\,(\mathrm{pH}\,3) \;<\; C_{\mathrm{PO}}\,(\mathrm{pH}\,10) \;<\; C_{\mathrm{PO}}\,(\mathrm{pH}\,7)$$

and furthermore, $C_{\mathrm{PO}} < C_{\mathrm{PO}}^{\mathrm{o}}$ at pH 3 and pH 10, while $C_{\mathrm{PO}} \cong C_{\mathrm{PO}}^{\mathrm{o}}$ at pH 7.

Table 5.1 The cmc and surface tension at the cmc at the three pH values of the solution.

pH		C	C_{Au}	C_{PO}	$C_{\mathrm{PO}}^{\mathrm{o}}$	γ^{C}	$\gamma^{C,\mathrm{o}}$
		mmol kg^{-1}				[mN m^{-1}]	
3	mixture	1.030	0.479	0.065	—	32.1	—
	reference	—	—	—	0.083	—	31.4
7	mixture	1.350	0.620	0.084	—	31.2	—
	reference	—	—	—	0.082	—	31.4
10	mixture	1.225	0.575	0.078	—	31.3	—
	reference	—	—	—	0.085	—	31.8

a

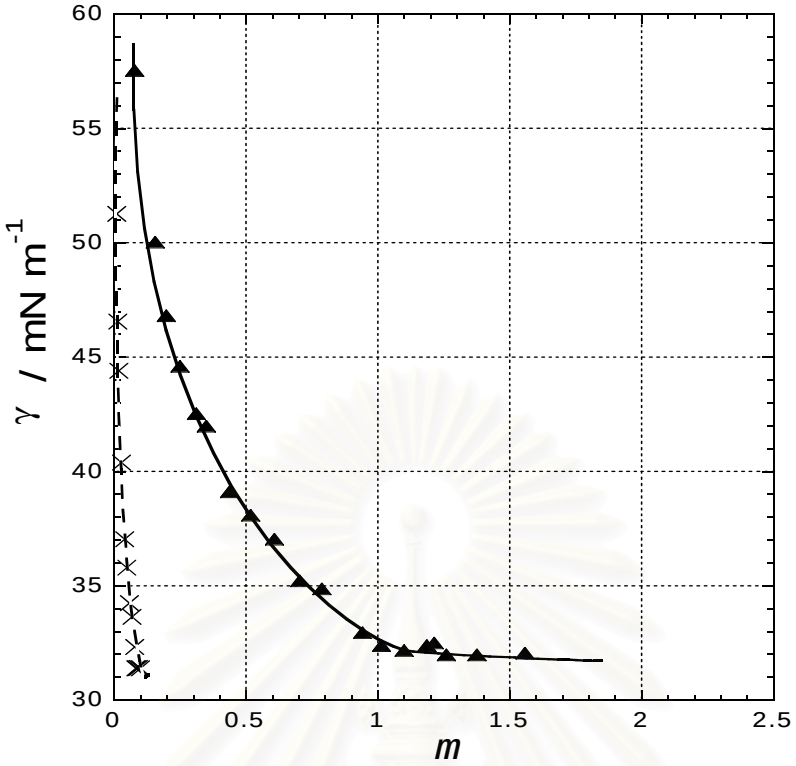

Figure 5.2a Surface tension versus total molality curves of the mixture at pH 3 (▲) and the reference (×).

b

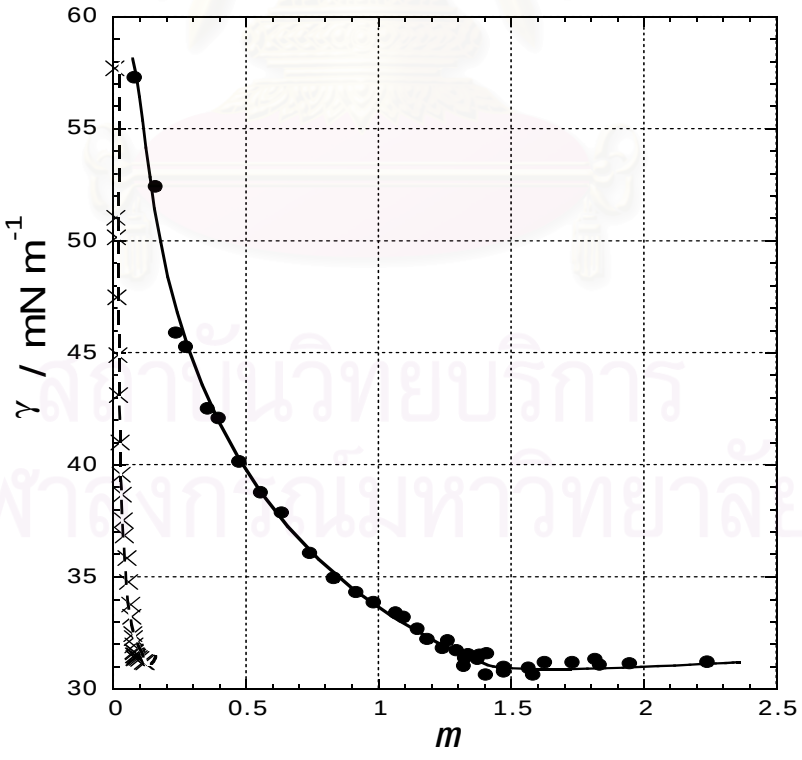

Figure 5.2b Surface tension versus total molality curves of the mixture at pH 7 (●) and the reference (×).

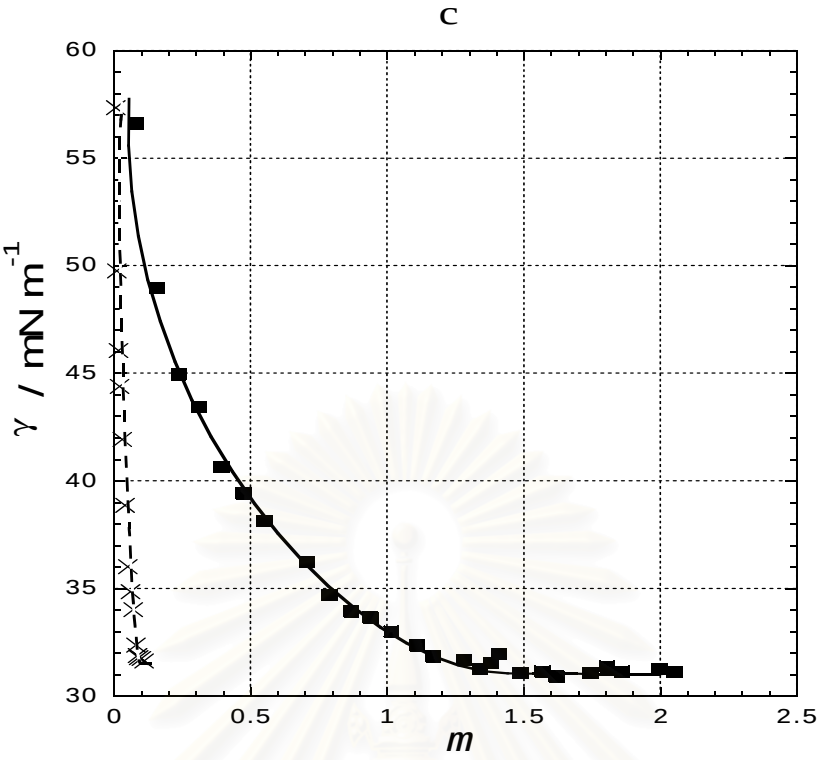

Figure 5.2c Surface tension versus total molality curves of the mixture at pH 10 (■) and the reference (×).

The interaction between gold and surfactant from the two aspects was explored in both the adsorbed film and in the micelle. With respect to the adsorbed films, the surface densities of components and their compositions play an important role. Taking account of the experimental conditions that the OH^- concentration was negligibly small and HCl concentration for adjusting pH m_{HCl} was constant at pH 3, and that the H^+ concentration was negligibly small irrespective of m_{Au} and NaOH concentration for adjusting pH m_{NaOH} was kept constant at pH 10, the total differentials of the surface tension are expressed formally both at pH 3 and at pH 7 and 10 as

$$-\mathrm{d}\gamma / RT = (\Gamma_{Au} / m_{Au})\mathrm{d}m_{Au} + (\Gamma_{PO} / m_{PO})\mathrm{d}m_{PO} \qquad (5.17)$$

In the present experiments, however, since the surface tension was measured at a fixed composition X_{PO}, it is appropriate to employ X_{PO} as the one of the

thermodynamic independent variables and rewrite Eq. 5.17 as a function of X_{PO} and the total molality m as

$$-\mathrm{d}\gamma / RT = (\Gamma^{H} / m)\mathrm{d}m + (\Gamma^{H} / X_{Au} X_{PO})(X_{PO}^{H} - X_{PO})\mathrm{d}X_{PO} \qquad (5.18)$$

or as a function of X_{PO} and the molality of surfactant m_{PO} as

$$-\mathrm{d}\gamma / RT = (\Gamma^{H} / m_{PO})\mathrm{d}m_{PO} - (1/X_{Au}X_{PO})\Gamma_{Au}^{H}\,\mathrm{d}X_{PO} \qquad (5.19)$$

The total surface density Γ^{H} and the mole fraction of the surfactant in the adsorbed film X_{PO}^{H} are defined by

$$\Gamma^{H} = \Gamma_{Au}^{H} + \Gamma_{PO}^{H} \qquad (5.20)$$

and

$$X_{PO}^{H} = \Gamma_{PO}^{H} / \Gamma^{H}, \qquad (5.21)$$

respectively. Then the total surface density $\Gamma^{H}$is evaluated by applying either the equation

$$\Gamma^{H} = -(m/RT)(\partial\gamma / \partial m)_{T,p,X_{PO}} \qquad (5.22)$$

to the $\gamma - m$ plots in Figure 5.2 or the equation

$$\Gamma^{H} = -(m_{PO}/RT)(\partial\gamma / \partial m_{PO})_{T,p,X_{PO}} \qquad (5.23)$$

to the $\gamma - m_{PO}$ plots in Figure 5.1. Furthermore, the mole fraction X_{PO}^{H} and the surface density of gold are respectively evaluated from Eq. 5.18 by

$$X_{PO}^{H} = X_{PO} - (X_{Au}X_{PO}/m)(\partial m / \partial X_{PO})_{T,p,\gamma} \qquad (5.24)$$

and from Eq. 5.19 by

$$\Gamma^{H}_{Au} = (X_{Au}X_{PO}/RT)(\partial\gamma / \partial X_{PO})_{T,p,m_{PO}} \quad (5.25)$$

The surface density of PONPE-9 of the reference $\Gamma^{H,o}_{PO}$ and the total surface density of the mixture Γ^{H} are plotted against the surfactant molality m_{PO} at different pH values in Figure 5.3. It is clearly demonstrated that the surface density increases both at pH 3 and 10 ($\Gamma^{H} > \Gamma^{H,o}_{PO}$), but does not change at pH 7 ($\Gamma^{H} \approx \Gamma^{H,o}_{PO}$) by adding the gold complexes into the surfactant solutions.

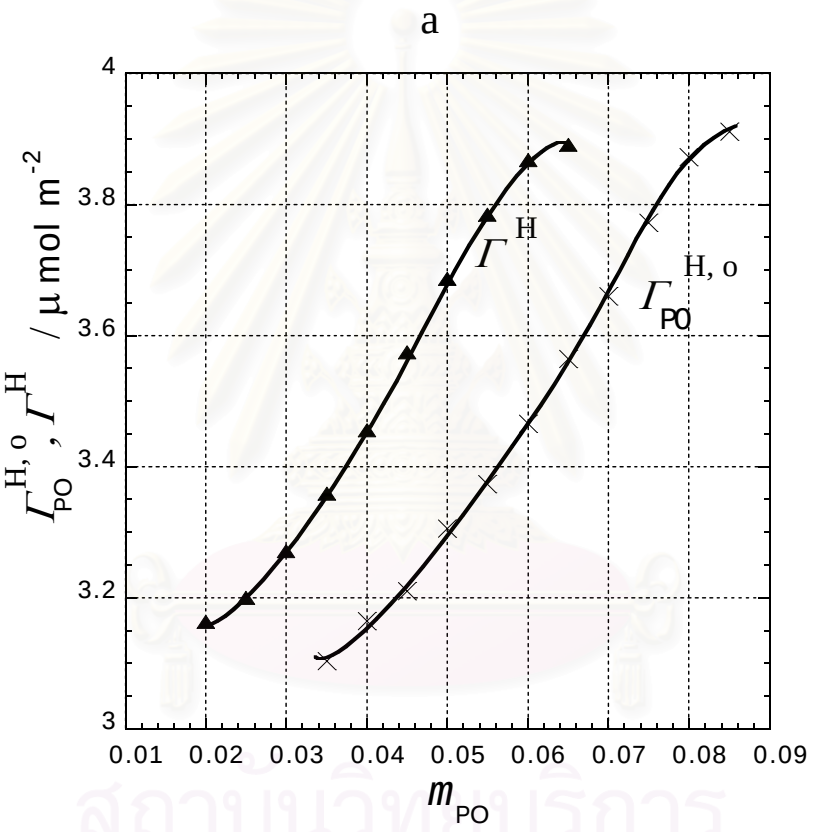

Figure 5.3a Surface density versus surfactant molality curves of the mixture at pH 3 (▲) and the reference $\Gamma^{H,o}_{PO}$ (×).

b

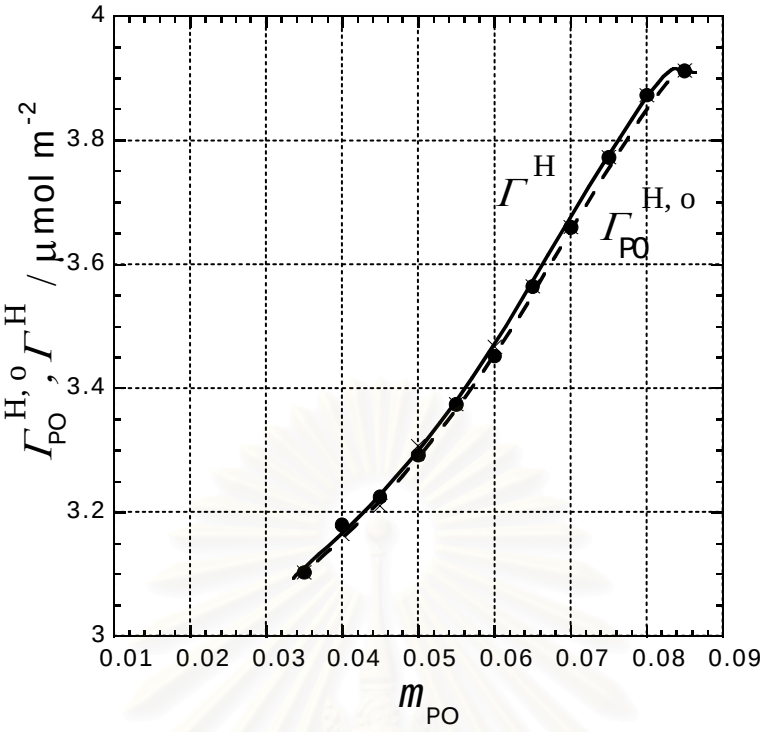

Figure 5.3b Surface density versus surfactant molality curves of the mixture at pH 7 (●) and the reference $\Gamma_{PO}^{H,o}$ (×).

c

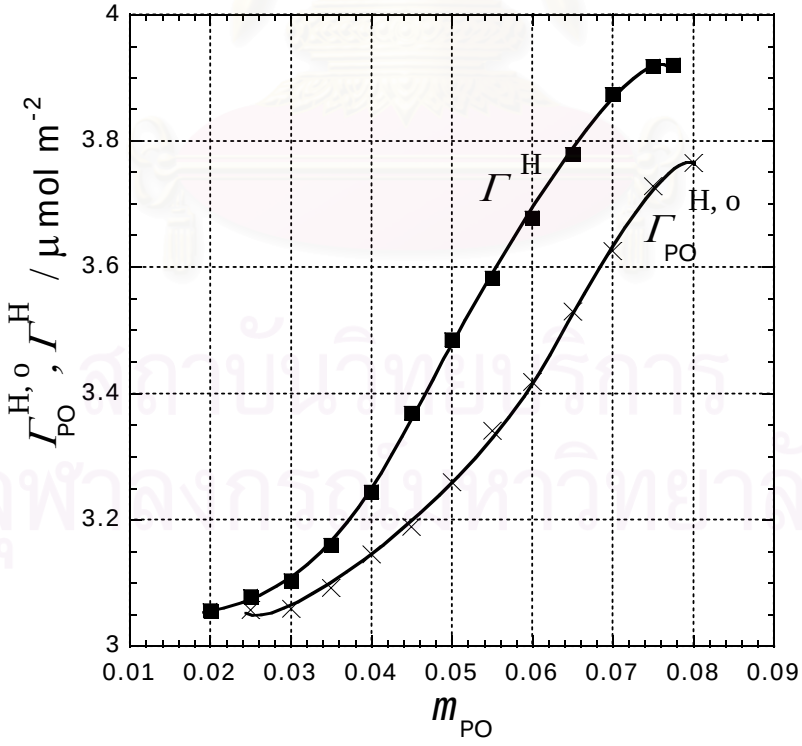

Figure 5.3c Surface density versus surfactant molality curves of the mixture at pH 10 (■) and the reference $\Gamma_{PO}^{H,o}$ (×).

Furthermore, Figure 5.4a and 5.4b reveal that the magnitude of the increase, $\Gamma^{H} - \Gamma_{PO}^{H,o}$, goes up at pH 3 and 10, while keeps almost zero at pH 7, with increasing not only the gold concentration m_{Au} but also the surfactant concentration m_{PO}. These findings strongly suggest an existence of interaction between gold and PONPE-9 at pH 3 and pH 10.

Taking account of the definition $\Gamma^{H} = \Gamma_{Au}^{H} + \Gamma_{PO}^{H}$ given by Eqs. 5.10 and 5.16 and the surface densities of H^+ and Cl^- are negligibly small even in the presence of the adsorbed film of ethylene oxide groups [5], it is said that the change in $\Gamma^{H} - \Gamma_{PO}^{H,o}$ may involve two contributions: the change in surface density of PONPE-9, Γ_{PO}^{H}, and that of gold, $\Gamma_{AuCl_4^-}^{H}$ or $\Gamma_{Au(OH)_3}^{H}$. The surface tension measurements confirmed that the surface density of the gold complexes was slightly negative in the absence of PONPE-9. Therefore, if the salting-out effect on the adsorption of PONPE-9 due to the presence of gold in the aqueous solution is responsible for the increase in $\Gamma^{H} - \Gamma_{PO}^{H,o}$, the surface density of gold, $\Gamma_{AuCl_4^-}^{H}$ or $\Gamma_{Au(OH)_3}^{H}$ remains zero or even negative.

On the other hand, if the interaction between PONPE-9 and gold in the adsorbed films is responsible for the increase in $\Gamma^{H} - \Gamma_{PO}^{H,o}$, $\Gamma_{AuCl_4^-}^{H}$ or $\Gamma_{Au(OH)_3}^{H}$ should take positive values. Looking at Figure 5.1, It is noticed that the surface tension decreases with decreasing X_{PO} at a given m_{PO} below the cmc at pH 3 and 10, but it does not change or even increases very slightly at pH 7. This means from Eq. 5.25 that the Γ_{Au}^{H} value is definitely positive at pH 3 and 10 but almost zero or very slightly negative at pH 7. Therefore it is concluded that an attractive interaction between PONPE-9 and gold in the adsorbed film is responsible for the increase of $\Gamma^{H} - \Gamma_{PO}^{H,o}$ and enhances the adsorption of PONPE-9 and gold ions at pH 3 and pH 10. Furthermore, the larger increase in $\Gamma^{H} - \Gamma_{PO}^{H,o}$ at pH 3 than at pH 10 suggests the stronger interaction at pH 3 than at pH 10.

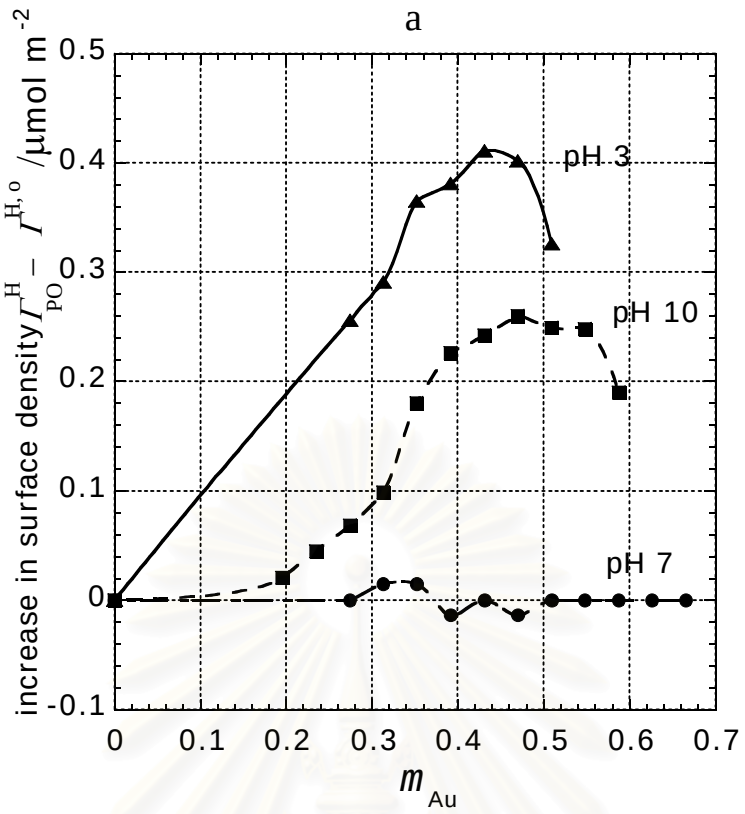

Figure 5.4a Increase in surface density versus molality $\Gamma^{H} - \Gamma^{H,o}_{PO}$ vs m_{Au}. pH 3 (▲), pH 7 (•), pH 10 (■).

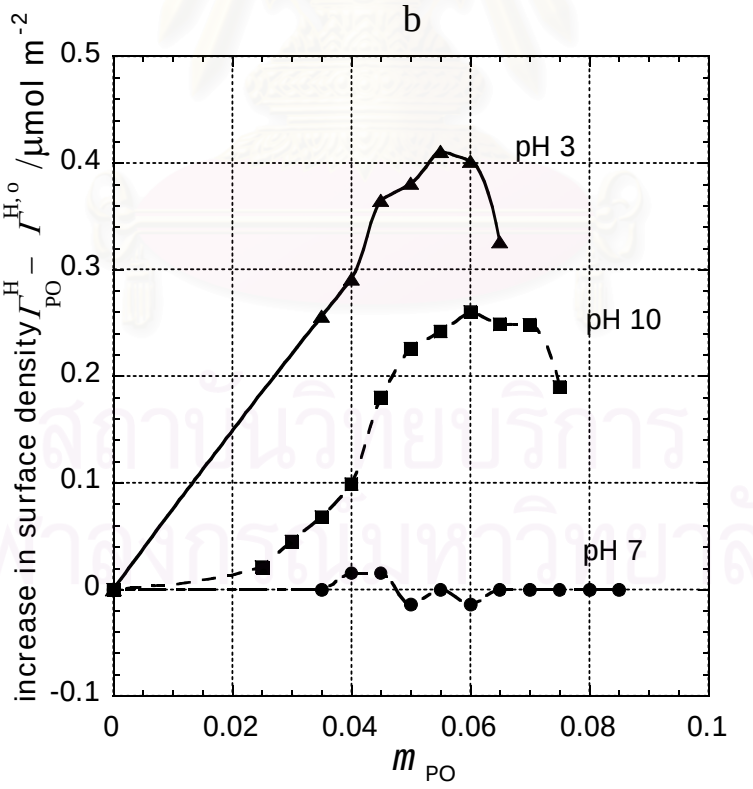

Figure 5.4b Increase in surface density versus molality $\Gamma^{H} - \Gamma^{H,o}_{PO}$ vs m_{PO}. pH 3 (▲), pH 7 (•), pH 10 (■).

The interaction in micelle particles is examined by using the thermodynamic relation

$$X_{\mathrm{PO}}^{\mathrm{M}} = \frac{1}{1-\frac{C_{\mathrm{Au}}}{C_{\mathrm{PO}}}\left(\frac{\partial C_{\mathrm{PO}}}{\partial C_{\mathrm{Au}}}\right)_{T,\,p}} \tag{5.26}$$

which is derived from the Gibbs-Duhem equation of the mixed micelle [4,51]. It is note worthy that this equation can be applied to suggest the difference among the $X_{\mathrm{PO}}^{\mathrm{M}}$ value between mixture solution and reference for each pH value of the solution. By referring the C_{Au} and C_{PO} values in Table 5.1, C_{PO} is smaller than $C_{\mathrm{PO}}^{\mathrm{o}}$ and give the trend that $\left(\partial C_{\mathrm{PO}}/\partial C_{\mathrm{Au}}\right)< 0$ and $X_{\mathrm{PO}}^{\mathrm{M}}<1$ consequently. Therefore gold are incorporated into micelle at pH 3 and pH 10. On the other hand, it is suggested that $X_{\mathrm{PO}}^{\mathrm{M}} \geq 1$ and therefore no gold is incorporated into micelle at pH 7. These findings undoubtedly correspond to the extraction results demonstrated in Figure 5.6. Furthermore the equation [4,51]

$$X_{\mathrm{PO}}^{\mathrm{H},C} = X_{\mathrm{PO}}^{\mathrm{M}} - (X_{\mathrm{Au}}X_{\mathrm{PO}} / RT\Gamma^{\mathrm{H},C})(\partial\gamma^{C} / \partial X_{\mathrm{PO}})_{T,\,p} \tag{5.27}$$

and the γ^{C} value in table 5.1 give the results on the relation between the composition of adsorbed film $X_{\mathrm{PO}}^{\mathrm{H},C}$ and that of micelle $X_{\mathrm{PO}}^{\mathrm{M}}$ at the cmc as

$X_{\mathrm{PO}}^{\mathrm{H},C} > X_{\mathrm{PO}}^{\mathrm{M}}$ at pH 3, $X_{\mathrm{PO}}^{\mathrm{H},C} \approx X_{\mathrm{PO}}^{\mathrm{M}}$ at pH 7, $X_{\mathrm{PO}}^{\mathrm{H},C} < X_{\mathrm{PO}}^{\mathrm{M}}$ at pH 10.

It is important to note that $X_{\mathrm{PO}}^{\mathrm{H},C}$ and $X_{\mathrm{PO}}^{\mathrm{M}}$ are different from each other at pH 3 and pH 10, while almost the same as each other at pH 7. Although the reason for the difference between pH 3 and pH 10 is obscure, the existence of the difference itself makes it decisive that there exists interaction between gold and surfactant both in the adsorbed film and in the micelle.

5.4 Conclusion

The important points about whether there exists the attractive interaction between gold and PONPE-9 in the adsorbed film and in micelle are as followed.

1. An appreciable difference of the $\gamma - m_{\mathrm{PO}}$ curves between the mixture and the reference was observed at pH 3 and pH 10, but it was not observed at pH 7.

2. The increase of the surface density of PONPE-9 and the decrease of the cmc by adding the gold to the reference were observed at pH 3 and pH 10 and larger at pH 3 than at pH 10. But they were not observed at pH 7.
3. The compositions of PONPE-9 both in adsorbed film and micelle were smaller than unity at pH 3 and pH 10, but they were almost equal to or even slightly larger than unity at pH 7.
4. The composition in the adsorbed film was different from that in micelle at pH 3 and pH 10, but almost the same (unity) at pH 7.

These points make it certain that there exists attractive interaction between gold and PONPE-9 in the adsorbed film and micelle at pH 3 and pH 10 and the interaction is stronger in the order of pH 3 > pH 10 > pH 7.

The percent extraction of gold via CPE using PONPE-9 as a separation media is in the order of pH 3 > pH 10 > pH 7 as demonstrated in Figure 4.6 and coincides with the order of the interaction between gold and PONPE-9 in the adsorbed film and micelle. Therefore, although the surfactant rich phase under the actual extraction condition is not simple spherical micellar solution, but more complex fluids containing self-organized surfactant assemblies like liquid crystals, the efficiency on CPE is probably dominated by the interaction between gold and PONPE-9 in the organized surfactant layers from which all the self-organized assemblies are constructed.

Judging from the experimental finding that the composition in the adsorbed film having flat interface and that micelle having curved one is different from each other, the structure of the assemblies is expected to be influential in the efficiency on CPE. Furthermore the dissolution states of gold in the aqueous solution may change with the solution conditions, like pH, the concentration of surfactants, and temperature, and therefore affect on the efficiency of CPE. Actually, the color of the mixture changes from pale yellow at pH 3 to purple at pH10; and therefore gold complex ion $AuCl_4^-$ is predominant at pH 3 and maybe gold colloidal particle stabilized by PONPE-9 molecules at pH 10. The structure of the surfactant-rich phase and the dissolution state of gold are still open questions in this study but may help to understand the extraction process, efficiency, and mechanisms.

CHAPTER 6

CONCLUSION AND RECOMMENDATION

6.1 Conclusion

Gold recovery is one effort of saving valuable materials. Many efficient extraction techniques, less expensive and reusable work substance and minimal energy consumption have been investigated. Cloud point extraction (CPE) is a relative novel separation method based on an aqueous two-phase system with polyoxyethylene nonionic surfactants. CPE utilizes partitioning of the solute between surfactant-rich phase and water-rich phase. If an aqueous solution containing a nonionic surfactant and solute is subjected to phase separation upon temperature alteration, then the solutes is distributed between the two phases by some interactions with the surfactant.

In this work, the thermodynamic quantity changes associated with the adsorption and micelle formation of nonionic surfactant were investigated in the theoretical and experimental viewpoints. Polyethylene glycol monoalkyl ether C_iE_j of various hydrophobic chain lengths were employed to study the temperature effect on dehydration. It was found that the increasing temperature strongly influences amount of the dehydration and then results in the increasing surface density at the interface. The increase of entropy changes along the increase of adsorption was acquired by the priority of dehydration over orientation effect, which was opposite to an ionic surfactant. Those results supported much intrinsic information which was described in Chapter 2.

In Chapter 3, cloud point extraction technique to recover gold from the aqueous solution of HCl and from the solution leached from printed substrate that contains copper, nickel, zinc, and gold ions was investigated. Before starting the experiment on CPE of gold, the study on properties of PONPE-9 which was used as a separation media had been carried out to support the information of that surfactant. It was found that many inorganic salts and some organic substance decreases cloud point temperature of PONPE-9 as stated in Chapter 3. The declining of CP was also observed in the mixture of PONPE-9 and gold (III) ion that supported a good understanding on the basic physical properties of nonionic surfactant.

In Chapter 4, the CPE of gold using PONPE-9 was investigated. It was found that, in HCl media, the maximum percent extraction of 98.78% was obtained at 65 ^{o}C, solution pH of 3, equilibration time of 6 hours, and the ratio of 1500 : 1 for PONPE-9 to gold ion. The selective cloud point extraction of gold (III) ion from several heavy metals was achieved with 98.8, 4.3, 10.0 and 0.0 % for gold, copper, nickel and zinc ions, respectively. The optimum experimental results obtained were applied to design the process scheme to overcome the drawback of the difficulty to separate gold from gold-entrapped surfactant. The process scheme has two CPE batches at two different pH values. The first batch is for extracting gold from others metal ions at pH 3. The second is conducted at pH 7 for separating gold ion from gold-entrapped surfactant. This process thus can be called the pH-switching method for gold (III) ion recovery by the CPE technique. The precipitation of metallic gold was obtained by using ascorbic acid as a reducing agent. By introducing this proposed scheme to recover gold from multimetal solution in a small-scale of 25 cm^3 of solution, satisfactory of gold with a high yield of 63.3% and purity of 98.01% could be obtained. Presented also substantiated feasibility of the process scheme by making a scale-up settling column (1-liter capacity) and the acceptable percent recovery of gold was 68%. It has been acceptable for the preliminary column design. As mentioned in Chapter 4 that a relatively high loss of gold was occurred from the transferring step due to that high weight of an aqueous solution of water-rich phase, which loads on the top, causes an incomplete taking target solution.

In Chapter 5, the interesting result was obtained by applying the thermodynamic equations to describe the interaction between gold (III) ion and PONPE-9 in various solution pH and compared the results to the experimental extraction studies from Chapter 4. The increase of the surface density of PONPE-9 and the decrease of the cmc by adding the gold ions to the PONPE-9 solution were observed at pH 3 and pH 10 and larger at pH 3 than at pH 10. But they were not observed at pH 7. The composition in the adsorbed film was different from that in micelle at pH 3 and pH 10, but almost the same at pH 7. Those can make a conclusion that the interaction between PONPE-9 and gold (III) ion is stronger in the order of pH 3 > pH 10 > pH 7.

Finally, it should be stated here that CPE is such a comparative technique to those conventional techniques. The advantageous of this process scheme are that the procedure is simple, easy to handle without an employment of toxic organic solvent

and supports the scale-up with capable of high selectivity. Therefore, it can be an alternative for the gold ion recovery from expired electronic parts under the environmental protection concept.

6.2 Recommendation

For the improving of percent gold recovery and the understanding on the conformation of surfactant structure including the interaction between PONPE-9 and gold (III) ion, further study should be given to the following aspects.

1. A modification on the settling column that suitable for draining the aqueous solution (upper phase) which is much easier than the concentrated surfactant phase (bottom phase). That will promote the percent recovery of gold to the utmost.
2. The study on NMR spectrum of the mixture of PONPE-9 and gold (III) ion. The adsorption shifts of oxygen atom response if there are the interaction between gold (III) ion and the oxygen atom in polyoxyethylene.
3. The feasibility of using of PONPE-9 to extract gold from underground soil exits in the Petchaboon province via CPE approach.
4. The recovery process for others precious metals contained in the leaching solution from printed substrate, copper, nickel, and zinc ions. Those may encourage an ideal process for taking care of world environment.

REFERENCES

1. Frankewich R. P. and Hinze W. L. Evaluation and Optimization of Factors Affecting Nonionic Surfactant-Mediated Phase Separation. Anal. Chem. 66 (1994): 944-954.
2. Schick M. J. Nonionic Surfactants, Surfactant Science Series. Vol.23. New York: Marcel Dekker, 1987.
3. Evans D.F. and Wennerstrom H. The Colloidal Domains; Where Physics, Chemisrty, Biology and Technology Meet 2nd ed. New York: Wiley-VCH, 1999. pp. 1-96.
4. Motomura K. and Aratono M. Miscibility in Binary Mixtures of Surfactants. Ogino K., Abe M. (Eds). Mixed Surfactant Systems Surfactant Science Ser. 46. New York: Marcel Dekker. 1993.
5. Matsubara H., Ohta A., Kameda M., Villeneuve M., Ikeda N., Aratono M. Interaction Between Ionic and Nonionic Surfactants in Adsorbed Film and Micelle: Hydrochloric Acid, Sodium Chloride and Tetraethylene Glycol Monooctyl Ether. Langmuir. 15 (1999**)**: 5496-5499.
6. Jin X., Xhu M., Conte E. D. Surfactant-Mediated Extraction Technique Using Alkyl Trimethylammonium Surfactants: Extraction of Selected Chlorophenols from River Water. Anal. Chem. 71 (1999): 514-517.
7. Lee C. K. and Su W. D. Separation Phenylaacetic Acid from 6-Aminopenicilin Acid via Cloud Point Extraction with N-Decyltetra(Ethylene Oxide) Nonionic Surfactant. Sep. Sci. Technol. 33 (1998): 1003-1021.
8. Porter M. R. Handbook of Surfactant. 2nd ed. Glasgow: Blackie Academic & Professional, 1994.
9. Attwood D. and Florence A. T. Surfactant Systems. London: Chapman and Hall, 1983**.**
10. Rosen M. J. Surfactants and Interfacial Phenomena. 2nd ed. New York: John Willey & Sons, 1989. pp 191-195.
11. Schick M. J. Nonionic Surfactants. Surfactant Science Series. Vol. 1. New York: Marcel Dekker, 1967.
12. Watanabe H. Nonionic Surfactants in Photometric Determination of Trace Metals. Mittal K. L. and Fedler E. J. (Eds). Solution Behavior of Surfactant Vol. 2. New York: Marcel Dekker, 1996. Vol. 2. pp. 1305-1313.

13. Bordier C. J. Phase Separation of Integral Membrane Proteins in Triton X-114 Solution. J. Biol. Chem. 25 (1981): 1604-1607.

14. Alecaraz G., Kinet J.-P., Kumar N., Wank S. A., Metzger H. Phase Separation of the Receptor for Immunoglobulin E and Its Subunits in Triton X-114. J. Biol. Chem. 259 (1984): 14922-14927.

15. Ganong B. R. and Delmove J. P. Phase Separation Temperatures of Mixtures of Triton X-114 and Triton X-45: Application to Protein Separation. Anal. Biochem. 193 (1991): 35-37.

16. Ahel M. and Giger W. Determination of Alkylphenols and Alkylphenol Mono- and Diethoxylates in Environmental Sample by High-Performance Liquid Chromotography. Anal. Chem. 57(1985): 1577-1583.

17. Garcia Pinto C., Perez Pavon J. L., Moreno Cordero B. Cloud Point Pre-concentration and High-Performance Liquid Chromatographic Determination of Polycyclic Aromatic Hydrocarbons with Fluorescence Detection. Anal. Chem. 66 (1994): 874-871.

18. Garcia Pinto C., Perez Pavon J., Moreno Cordero B. Cloud Point Preconcentration and High-Performance Liquid Chromatographic Determination of Organophosphorus Pesticides with Dual Electrochemical Detection. Anal. Chem. 67 (1995): 2606-2612.

19. Sirimanne S. R., Bar J. R., Patterson D. G. Quantification of Polycyclic Aromatic Hydrocarbons and Polychlorinated Dibenzo-p-dioxins in Human Serum by Combinded Micelle-Mediated Extraction (CPE) and HPLC. Anal. Chem. 68 (1996): 1556-1560.

20. Akita S. and Takeuchi H. Equilibrium Distribution of Aromatic Compounds between Aqueous Solution and Coacervate of Nonionic Surfactant. Sep. Sci. Technol. 31 (1996): 401-412.

21. Akita S. and Takeuchi H. Cloud Point Extraction of Organic Compounds from Aqueous Solutions with Nonionic Surfactant. Sep. Sci. Technol. 30 (1995): 833-846.

22. Garcia Pinto C., Perez Pavon J. L., Moreno Cordero B., Beato E. R., Sanchez S. G. Cloud Point Preconcentration and Flame Atomic Absorption Spectrometry: Application to the Determination of Cadmium. J. Anal. At. Spectrom. 11 (1996): 37-41.

23. Fernandez Laespada M. E., Perez Pavon J. L., Moreno Cordero B. Micelle-mediated Methodology for the Preconcentration of Uranium Prior to its Determination by Flow Injection. Analyst. 118 (1993): 209-212.

24. Oliveros M. C. C., Jimenez de Blas O., Perez Pavon J. L., Moreno Cordero B. Cloud Point Preconcentration and Atomic Absorption Spectroscopy: Application to the Determination of Nickel and Zinc. J. Anal. At. Spectrom. 13 (1998): 547-550.

25. Silva M. F., Fernandez L., Olsina R. A., Stacchiola D. Cloud Point Extraction, Preconcentration and Spectrophotometric Determination of Erbium (III)–2-(3,5-dichloro-2-pyridylazo)-5-dimethylaminophenol. Anal. Chim. Acta. 342 (1997): 229-238.

26. Vaidya B. and Porter M. D. Selective Determination of Cadmium in Water Using a Chromogenic Crown Ether in a Mixed Micellar Solution. Anal. Chem. 69 (1997): 2688-2693.

27. Mesquita de Silva M. A., Frescura V. L. A., Aguilera F. J. N., Curtius A. J. Determination of Ag and Au in Geological Samples by Flame 16. Atomic Absorption Spectrometry after Cloud Point Extraction. J. Anal. At. Spectrom. 13 (1998): 1369-1373.

28. Akita S., Rovira M., Sastra A. M., Takeuchi H. Cloud Point Extraction of Gold (III) with Nonionic Surfactant – Fundamental Studies and Application to Gold Recovery from Printed Substrate. Sep. Sci. Technol. 33 (1998): 2159-2177.

29. Aratono M., Shimada K., Ikeda M., Takiue T., Motomura, K. Enthalpies of Adsorption and Micelle Formation of Octyl Methyl Sulfoxide. Netsu Sokutei. 22 (1995): 131-136.

30. Scamehorn J.F. (Ed.) Phenomena in Mixed Surfactant Systems. ACS Symp Ser. 311. Washington DC.: Amer. Chem. Soc., 1986.

31. Hayami Y., Ichikawa H., Someya A., Aratono M., Motomura K. Thermodynamic Studies on Adsorption and Micelle Formation of Long Chain Alkyltrimethyl Ammonium Chlorides. Colloids Polym Sci. 276 (1998): 595-600.

32. Motomura K., Iwanaga S., Uryu S., Matsukiko H., Yamamaka M., Matuura R.Thermodynamic. Study of the Adsorption of Octylsulfinylethanol at the Micellar Solution/Air Interface. Colloids and Surfaces. 9 (1984): 19.

33. Corkill J. M., Goodman J. F. Haisman D. R., Harrold S. P. The Thickness and

Composition of Thin Detergent Films. Trans. Faraday. 57 (1961): 821-828.

34. Schick, M. Surface Films of Nonionic Detergents-I. Surface Tension Study. J. Colloid Sci. 17 (1962): 801.

35. Rosen M. J., Anna A. W., Dahanayake M., Hua X. Relation of Structure to Properties in Surfactants. 10. Surface and Thermodynamic Properties of 2-Dodecyloxypoly (ethenoxyethanol)s, $C_{12}H_{25}(OC_2H_4)_xOH$, in Aqueous Solution. J. Phys. Chem. 86 (1982): 541-545.

36. Lu J. R., Li Z. X., Thomas R. K., Staples E. J., Thompson L., Tucker I., Penfold J. Neutron Reflection from A Layer of Monododecyl Octaethylene Glycol Adsorbed at the Air-Water Interface: The Structure of the Layer and the Effects of Temperature. J. Phys. Chem. 98 (1994): 6559-6567.

37. Motomura K., Iwanaga S., Yamamaka M., Aratono M., Matuura R. Thermodynamic Studies on Adsorption at Interface V. Adsorption from Micellar Solution. J. Colloid Interface Sci. 86 (1984): 151-157.

38. Motomura K. Thermodynamic Studies on Adsorption at Interfaces. I. General Formulation. J. Colloid Interface Sci. 64 (1978): 348.

39. Lando J. L., Oakley H. T., Tabulated Convection Factor for the Drop–Weight Volume Determination of Surface and Interfacial Tensions. 25(1967): 526-530.

40. Ohta A., Murakami R., Takiue T., Ikeda N., Aratono M. Calorimetric Study of Micellear Solutions of Petaethylene Glycol Monooctyl and Monodecyl Ethers. J. Phys. Chem. B. 104 (2000): 8592.

41. Matuski H., Kaneshina S., Yamashita Y., Motomura. K. Automatic Surface Tension Measurements of Aqueous Surfactant Solutions by the Drop Volume Method. Langmuir.10 (1994): 4394.

42. Aratono M., Ohta A., Minamizawa H., Ikeda N., Iyota H., Takiue T. The Excess Thermodynamic Quantities of Adsorption of a Binary Nonionic Surfactant Mixture. J. Colloid Interface Sci. 217 (1999): 128.

43. Motomura K., Iwanaga S., Hayami Y., Uryu S., Matuura R. Thermodynamic Studies on Adsorption at Interface IV. Dodecyl Ammonium Chloride at Water/Air Interface. J. Colloid Interface Sci. 80 (1981): 32-38.

44. Aratono M., Okamoto T., Motomura K. Adsorption of Dodecyltrimethylammonium Chloride from the Micellar Solution at Water/Air Interface. Bull. Chem. Soc. Jpn. 60 (1987): 2361.

45. Aratono M., Okamoto T., Ikeda N., Motomura, K. Effect of the N-Methylation of Dodecylammonium Chloride on the Adsorption from its Micellar Solution.Bull. Chem. Soc. Jpn. 61 (1988): 2773.

46. Gullockson N.D. In Surfactant-Based Separation Processes. Scamehorn J. F., Harwell J. H. (Eds.). New York: Marcel Dekker, 1989. pp 139-152.

47. Schmitt T. M. Analysis of Surfactants. New York: Marcel Dekker, 1992. pp. 289-300.

48. Perkampus H. H. UV-Vis Spectroscopy. Berlin: Springer-Verlag, 1992. p. 26- 30.

49. Marsden J. and House L. The Chemistry of Gold Extraction. New York: Eltis Horwood. 1992. pp142, 158.

50. Iyota H. and Motomura K. Miscibility of Ethanol and 2-(Octylsulfinyl)Ethanol in the Adsorbed Film at Water/Air Interface and Micelle. J. Colloid Interface Sci. 148 (1992): 369.

51. Aratono M., Villeneuve M., Takiue T., Ikeda N., Iyota H. Thermodynamic Consideration of Mixtures of Surfactants in Adsorbed Films and Micelle. J. Colloid Interface Sci . 200 (1998):161-171.

52. Iyota H. , Tomimitsu T., Motomura K., Aratono M. Miscibility and Nonideality of Mixing of Hepatanol and Octylsulfinylethanol in the Adsorbed Film and Micelle. Langmuir. 14 (1998): 5347.

53. Matsubara H., Ohta A., Kameda M., Ikeda N., Aratono M. Interaction between Ionic and Nonionic Surfactants in the Adsorbed Film and Micelle, Dodecylammonium Chloride and Tetraethyleneglycol Monooctyl Ether. Langmuir. 16 (2000): 7589.

54. Christian D. S., Scamehorn J.F. (Eds). Solubilization in Surfactant Aggregates. Surfactant Science Series Vol. 55. New York: Marcel Dekker, 1995. pp.146-184.

55. Adamson A. W. Physical Chemistry of Surfaces. 5th. New York: John Wiley& Sons, 1990. pp. 77-84.

56. Motomora K., Ando N., Matsuki H., Aratono M. Thermodynamic Studies on Adsorption at Interfaces. J. Colloid Interface. Sci. 139 (1990): 188-197.

57. Aratono M., Ikeda N. Structure-Performance Relationships in Surfactants. Esumi K., Ueno M. (Eds.). New York: Dekker, 1997. pp 83-108.

58. Tanford C. The Hydrophobic Effect. New York: John Wiley& Son, 1980.

APPENDICES

Table A-1 Raw data of PONPE-9 in water-rich phase after CPE at various (Chapter 3)

T (^{o}C)	$[PONPE-9]_w$						
	1	2	3	4	5	mean	SD
56	0.108	0.104	0.116	0.08	0.096	0.1008	0.0137
60	0.025	0.02	0.025	0.02	0.025	0.0230	0.0027
65	0.02	0.016	0.02	0.014	0.02	0.0180	0.0028
70	0.018	0.018	0.01	0.008	0.008	0.0124	0.0052
75	0.012	0.012	0.012	0.012	0.008	0.0112	0.0018
80	0.02	0.01	0.016	0.014	0.018	0.0156	0.0038

Table A-2 Raw data of phase diagram determination (Chapter 3)

T1	T2	T(mean)	SD	%w/w
56.1	56.4	56.25	0.212132	0.94
54.6	54.4	54.5	0.141421	1.85
53.7	53.4	53.55	0.212132	2.25
53.5	53.5	53.5	0	2.82
53.3	53.4	53.35	0.070711	3.46
53.3	53.4	53.35	0.070711	3.92
53.3	53.3	53.3	0	4.45
53.2	53.6	53.4	0.2	4.94

T1	T2	T(mean)	SD	%w/w
53.7	53.6	53.65	0.070711	5.77
53.7	53.5	53.6	0.141421	6.62
53.6	53.4	53.5	0.141421	6.89
53.6	53.8	53.7	0	7.35
54.5	54.6	54.55	0.070711	7.86
55.2	55.3	55.25	0.070711	9.8
55.5	55.5	55.5	0	10.87

Table A-3 Raw data of phase diagram determination for mixture PONPE-9 + $HAuCl_4$ (Chapter 3)

T1	T2	T(mean)	SD	%w/w
53.9	54.1	54	0.141421	0.065
53.1	53.7	53.26667	0.378594	0.24
52.9	52.7	52.66667	0.251661	0.69
52.4	52.4	52.4	0	1.17
52.2	52.3	52.25	0.070711	1.9
52.3	52.3	52.3	0	3.09
52.5	52.4	52.45	0.070711	3.48
52.4	52.4	52.4	0	3.96
52.4	52.3	52.35	0.070711	4.35
52.5	52.5	52.5	0	5.13
51.8	51.7	51.85	0.129099	5.47
52	52.7	52.4	0.360555	6.17
52.6	52.7	52.65	0.070711	6.57
52.7	52.7	52.7	0	7.02
52.6	52.6	52.5	0.173205	7.46

T1	T2	T(mean)	SD	%w/w
52.7	53.5	53.13333	0.404145	7.91
53.9	53.8	53.85	0.070711	9.09
55.5	55.4	55.36667	0.152753	10.88
56.5	56.5	56.5	0	12.95

Table A-4 Raw data of effect of organic substance on cloud point temperature of PONPE-9 (Chapter 3)

Glycerol %	CP (^{o}C)	EG %	CP (^{o}C)	PVA %	CP (^{o}C)	SLS %	CP (^{o}C)	PEG %	CP (^{o}C)	EG %	CP (^{o}C)	Butanol %	CP (^{o}C)
0	52	0	52	0	50	0	52	0	50	0	52	0.52	52
6.305	48.5	5.545	54	0.1	50	0.356	48	0.1	49	0.1	60	486	14
12.61	46.5	11.09	54.5	0.2	51	0.712	47.5	0.2	47	0.2	72		
25.22	43	22.18	58	0.4	51	1.068	46.5	0.4	45	0.3	82		
27.742	39	33.27	67	0.6	53	1.424	45	0.6	43.5				
50.44	28.5	44.36	73	0.8	54	1.78	44.5	0.8	42				
63.05	18					2.492	44						

Table A-5 Raw data of effect of organic substance on cloud point temperature of PONPE-9 (Chapter 3)

$NaC_2H_3O_2$ M	CP (^oC)	$Na_3C_6H_6O_5$ M	CP (^oC)	$Na_2C_2O_4$ M	CP (^oC)	$(NH)_4C_2O_4$ M	CP (^oC)	NaCl M	CP (^oC)	Na_2CO_3 M	CP (^oC)	Na_2SO_4 M	CP (^oC)	Na_3PO_4 M	CP (^oC)
0	50	0	50	0	50	0	50	0	52	0	52	0	52	0	52
0.010545	48.5	0.00697	48	0.00403	48.5	0.007095	48	0.1	45	0.05	41.5	0.0275	44	0.0103	44
0.04218	48	0.02788	45.5	0.01612	47	0.02838	46.5	0.2	42	0.1	38.5	0.055	31	0.0205	36
0.08436	46	0.05576	42	0.03224	45	0.05676	43	0.3	41	0.15	32	0.1375	29	0.0615	34
0.12654	44.5	0.08364	40	0.04836	43	0.08514	42	0.4	38.5	0.25	28.5	0.22	24	0.1025	29
0.16872	43.5	0.11152	37.5	0.06448	42	0.11352	40	0.6	37	0.4	18	0.275	22	0.164	27
								0.8	34	0.5	13			0.205	22
								1	32.5						
								1.3	30						
								1.5	27.5						

Table A-6 Raw data of effect of organic substance on cloud point temperature of PONPE-9 (Chapter 3)

NH_4Cl M	CP (^oC)	LiCl M	CP (^oC)	$NaHCO_3$ M	CP (^oC)	$(NH_4)_2CO_3$ M	CP (^oC)
0	52	3.7164	32	0.9378	30	0	52
0.336	42	3.22088	32	0.87528	31	0.0250725	49
0.56	41	2.72536	33	0.81276	33	0.050145	48
0.784	36	2.22984	34	0.75024	34	0.10029	46
1.12	34	1.73432	35	0.68772	34.5	0.150435	44
1.68	32	1.2388	37	0.6252	36	0.250725	41.5
		0.74328	41.5	0.56268	36.5	0.351015	40
		0.24776	44	0.50016	38	0.451305	36
		0	52	0.37512	41.5	0.551595	34
				0.25008	43	0.651885	33.5
				0.12504	47	0.752175	32
				0	52		

Table A-7 Raw data of effect of organic substance on cloud point temperature of PONPE-9 (Chapter 3)

Ratio [PONPE-9/Au^{3+}]	CP (^{o}C)	pH
3198.05	48.5	2.77
2132.03	48.0	2.51
1599.03	47.9	2.29
1279.22	48.5	2.44
999.39	48.0	1.96
799.51	47.7	2.09
666.26	48.5	1.87
639.61	48.8	2.13
571.08	48.5	1.84
499.70	48.5	1.79
444.17	47.8	1.74
399.76	48.0	1.77
363.41	47.8	1.70

Table A-8 Raw data of CPE at 53 ^{o}C, PONPE-9 = 2.5% w/v (Chapter 4)

(%)	(mg)	(mole)	(ppm)	(mg)	(mole)		(^{o}C)		(ppm)	(mg)	(Molar)	(mole)	
PO	PO	PO	Au_o	Au_o	Au_o	pH	CP	$(PO/Au)_o$	Au_w	Au_w	Au_w	Au_w	%E
2.5	250	4.058E-04	5	0.05	2.538E-07	2.05	48	1599.03	1.3934	0.0111	7.073E-06	5.659E-08	77.71
2.5	250	4.058E-04	8	0.08	4.061E-07	1.96	48	999.39	1.8579	0.0149	9.431E-06	7.545E-08	81.42
2.5	250	4.058E-04	10	0.1	5.076E-07	1.89	48.5	799.51	1.9772	0.0154	1.004E-05	7.828E-08	84.58
2.5	250	4.058E-04	10	0.1	5.076E-07	1.89	48.5	799.51	1.8956	0.0148	9.622E-06	7.505E-08	85.21
2.5	250	4.058E-04	12	0.12	6.091E-07	1.87	48.5	666.26	2.1529	0.0168	1.093E-05	8.513E-08	86.02
2.5	250	4.058E-04	12	0.12	6.091E-07	1.87	48.5	666.26	2.1152	0.0165	1.074E-05	8.364E-08	86.27
2.5	250	4.058E-04	14	0.14	7.107E-07	1.84	48.5	571.08	2.2948	0.0179	1.165E-05	9.086E-08	87.21
2.5	250	4.058E-04	14	0.14	7.107E-07	1.84	48.5	571.08	2.0537	0.0160	1.043E-05	8.132E-08	88.56
2.5	250	4.058E-04	16	0.16	8.122E-07	1.66	48	499.70	2.4253	0.0189	1.231E-05	9.603E-08	88.18
2.5	250	4.058E-04	16	0.16	8.122E-07	1.66	48	499.70	2.3098	0.0180	1.172E-05	9.145E-08	88.74
2.5	250	4.058E-04	18	0.18	9.137E-07	1.74	47.5	444.17	2.2931	0.0179	1.164E-05	9.079E-08	90.06
2.5	250	4.058E-04	18	0.18	9.137E-07	1.74	47.5	444.17	2.3977	0.0187	1.217E-05	9.493E-08	89.61
2.5	250	4.058E-04	20	0.2	1.015E-06	1.59	47.5	399.76	2.4981	0.0195	1.268E-05	9.891E-08	90.26
2.5	250	4.058E-04	20	0.2	1.015E-06	1.59	47.5	399.76	2.7032	0.0211	1.372E-05	1.070E-07	89.46
2.5	250	4.058E-04	22	0.22	1.117E-06	1.7	47.5	363.41	2.6320	0.0205	1.336E-05	1.042E-07	90.67

Table A-9 Raw data of CPE at 56 ^{o}C, PONPE-9 = 2.5% w/v (Chapter 4)

(%)	(mg)	(mole)	(ppm)	(mg)	(mole)		(^{o}C)		(ppm)	(mg)	(M)	(mole)	
PO	PO	PO	Au_o	Au_o	Au_o	pH	CP	$(PO/Au)_o$	Au_w	Au_w	Au_w	Au_w	%E
2.5	250	4.058E-04	5	0.05	2.538E-07	2.17	46.5	1599.03	0.2675	0.0022	1.358E-06	1.113E-08	95.61
2.5	250	4.058E-04	5	0.05	2.538E-07	2.17	46.5	1599.03	0.1895	0.0016	9.617E-07	7.886E-09	96.89
2.5	250	4.058E-04	10	0.1	5.076E-07	1.97	47	799.51	2.1007	0.0172	1.066E-05	8.744E-08	82.77
2.5	250	4.058E-04	10	0.1	5.076E-07	1.97	47	799.51	1.7274	0.0142	8.769E-06	7.190E-08	85.84
2.5	250	4.058E-04	16	0.16	8.122E-07	1.82	46.5	499.70	1.1312	0.0094	5.742E-06	4.766E-08	94.13
2.5	250	4.058E-04	16	0.16	8.122E-07	1.82	46.5	499.70	1.0587	0.0088	5.374E-06	4.461E-08	94.51
2.5	250	4.058E-04	20	0.2	1.015E-06	1.74	45.5	399.76	1.4042	0.0115	7.128E-06	5.845E-08	94.24
2.5	250	4.058E-04	20	0.2	1.015E-06	1.74	45.5	399.76	1.2761	0.0105	6.477E-06	5.311E-08	94.77

Table A-10 Raw data of CPE at 60 ^{o}C, PONPE-9 = 2.5% w/v (Chapter 4)

(%)	(mg)	(mole)	(ppm)	(mg)	(mole)		(^{o}C)		(ppm)	(mg)	(Molar)	(mole)	
PO	PO	PO	Au_o	Au_o	Au_o	pH	CP	$(PO/Au)_o$	Au_w	Au_w	Au_w	Au_w	%E
2.5	250	4.058E-04	5	0.05	2.538E-07	2.17	46.5	1599.03	0.0613	0.0005	3.111E-07	2.738E-09	98.92
2.5	250	4.058E-04	5	0.05	2.538E-07	2.17	46.5	1599.03	0.1839	0.0016	9.334E-07	8.214E-09	96.76
2.5	250	4.058E-04	10	0.1	5.076E-07	1.97	47	799.51	0.6241	0.0054	3.168E-06	2.724E-08	94.63
2.5	250	4.058E-04	10	0.1	5.076E-07	1.97	47	799.51	0.5294	0.0046	2.687E-06	2.311E-08	95.45
2.5	250	4.058E-04	16	0.16	8.122E-07	1.82	46.5	499.70	0.8358	0.0072	4.243E-06	3.649E-08	95.51
2.5	250	4.058E-04	16	0.16	8.122E-07	1.82	46.5	499.70	0.9584	0.0082	4.865E-06	4.184E-08	94.85
2.5	250	4.058E-04	20	0.2	1.015E-06	1.74	45.5	399.76	1.1869	0.0102	6.025E-06	5.181E-08	94.90
2.5	250	4.058E-04	20	0.2	1.015E-06	1.74	45.5	399.76	1.1590	0.0100	5.883E-06	5.060E-08	95.02

Table A-11 Raw data of CPE at 70 ^{o}C, PONPE-9 = 2.5% w/v (Chapter 4)

(%)	(mg)	(mole)	(ppm)	(mg)	(mole)		(^{o}C)		(ppm)	(mg)	(M)	(mole)	
PO	PO	PO	Au_o	Au_o	Au_o	pH	CP	$(PO/Au)_o$	Au_w	Au_w	Au_w	Au_w	%E
2.5	250	4.058E-04	5	0.05	2.538E-07	2.22	48.5	1599.03	0.5020	0.0046	2.548E-06	2.345E-08	90.76
2.5	250	4.058E-04	5	0.05	2.538E-07	2.22	48.5	1599.03	0.4145	0.0038	2.104E-06	1.946E-08	92.33
2.5	250	4.058E-04	10	0.1	5.076E-07	2.04	48	799.51	1.8593	0.0171	9.438E-06	8.683E-08	82.89
2.5	250	4.058E-04	10	0.1	5.076E-07	2.04	48	799.51	1.4302	0.0130	7.260E-06	6.607E-08	86.98
2.5	250	4.058E-04	16	0.16	8.122E-07	1.89	49	499.70	3.1319	0.0285	1.590E-05	1.447E-07	82.19
2.5	250	4.058E-04	16	0.16	8.122E-07	1.89	49	499.70	2.9451	0.0271	1.495E-05	1.375E-07	83.07
2.5	250	4.058E-04	20	0.2	1.015E-06	1.78	48.5	399.76	3.2137	0.0294	1.631E-05	1.493E-07	85.30
2.5	250	4.058E-04	20	0.2	1.015E-06	1.78	48.5	399.76	3.0123	0.0277	1.529E-05	1.407E-07	86.14

Table A-12 Raw data of CPE at 80 ^{o}C, PONPE-9 = 2.5% w/v (Chapter 4)

(%)	(mg)	(mole)	(ppm)	(mg)	(mole)		(^{o}C)		(ppm)	(mg)	(M)	(mole)	
PO	PO	PO	Au_o	Au_o	Au_o	pH	CP	$(PO/Au)_o$	Au_w	Au_w	Au_w	Au_w	%E
2.5	250	4.058E-04	5	0.05	2.538E-07	2.22	48.5	1599.03	0.1109	0.0010	5.630E-07	5.236E-09	97.94
2.5	250	4.058E-04	5	0.05	2.538E-07	2.22	48.5	1599.03	0.0584	0.0005	2.963E-07	2.756E-09	98.91
2.5	250	4.058E-04	10	0.1	5.076E-07	2.04	48	799.51	1.0741	0.0099	5.452E-06	5.044E-08	90.06
2.5	250	4.058E-04	10	0.1	5.076E-07	2.04	48	799.51	1.2055	0.0112	6.119E-06	5.660E-08	88.85
2.5	250	4.058E-04	16	0.16	8.122E-07	1.89	49	499.70	3.2341	0.0301	1.642E-05	1.527E-07	81.20
2.5	250	4.058E-04	16	0.16	8.122E-07	1.89	49	499.70	3.3275	0.0309	1.689E-05	1.571E-07	80.66
2.5	250	4.058E-04	20	0.2	1.015E-06	1.78	48.5	399.76	4.5593	0.0424	2.314E-05	2.152E-07	78.80
2.5	250	4.058E-04	20	0.2	1.015E-06	1.78	48.5	399.76	4.4308	0.0412	2.249E-05	2.092E-07	79.40

Table A-13 Raw data of CPE at 53 ^{o}C, PONPE-9 = 1% w/v (Chapter 4)

(%)	(mg)	(mole)	(ppm)	(mg)	(mole)		(^{o}C)	(mL)	(mL)		(ppm)	(Molar)	
PO	PO	PO	Au_o	Au_o	Au_o	pH	CP	Vs	Vw	(NP/Au)o	Au_w	Au_w	%E
1	100	1.623E-04	1	0.01	5.076E-08	2.85	49	0.8	9.2	3198.05	0.2452	2.663E-07	95.17373
1	100	1.623E-04	1	0.01	5.076E-08	2.85	49	0.8	9.2	3198.05	0.1895	1.003E-07	98.18263
1	100	1.623E-04	2.5	0.025	1.269E-07	2.52	48	1	9	1279.22	0.8626	1.013E-06	92.81446
1	100	1.623E-04	2.5	0.025	1.269E-07	2.52	48	1	9	1279.22	0.9584	1.379E-06	90.22345
1	100	1.623E-04	5	0.05	2.538E-07	2.06	49	0.85	9.15	639.61	3.1205	9.62E-06	65.31898
1	100	1.623E-04	5	0.05	2.538E-07	2.06	49	0.85	9.15	639.61	3.1260	9.641E-06	65.24241
1	100	1.623E-04	10	0.1	5.076E-07	1.88	48.5	0.8	9.2	319.81	3.9719	1.287E-05	76.6824
1	100	1.623E-04	10	0.1	5.076E-07	1.88	48.5	0.8	9.2	319.81	3.7864	1.216E-05	77.96435

Table A-14 Raw data of CPE at 56 ^{o}C, PONPE-9 = 1% w/v (Chapter 4)

(%)	(mg)	(mole)	(ppm)	(mg)	(mole)		(^{o}C)	(mL)	(mL)		(ppm)	(Molar)	
PO	PO	PO	Au_o	Au_o	Au_o	pH	CP	Vs	Vw	$(PO/Au)_o$	Au_w	Au_w	%E
1	100	1.623E-04	1	0.01	5.076E-08	2.93	48	0.7	9.3	3198.05	0.3455	1.754E-06	67.87
1	100	1.623E-04	1	0.01	5.076E-08	2.93	48	0.7	9.3	3198.05	0.3678	1.867E-06	65.80
1	100	1.623E-04	2.5	0.025	1.269E-07	2.47	47.5	0.7	9.3	1279.22	0.5015	2.546E-06	81.34
1	100	1.623E-04	2.5	0.025	1.269E-07	2.47	47.5	0.7	9.3	1279.22	0.3566	1.810E-06	86.73
1	100	1.623E-04	5	0.05	2.538E-07	2.12	48	0.7	9.3	639.61	0.9640	4.893E-06	82.07
1	100	1.623E-04	5	0.05	2.538E-07	2.12	48	0.7	9.3	639.61	0.9027	4.582E-06	83.21
1	100	1.623E-04	10	0.1	5.076E-07	1.91	47.5	0.7	9.3	319.81	1.6382	8.316E-06	84.76
1	100	1.623E-04	10	0.1	5.076E-07	1.91	47.5	0.7	9.3	319.81	1.6550	8.401E-06	84.61

Table A-15 Raw data of CPE at 60 ^{o}C, PONPE-9 = 1% w/v (Chapter 4)

(%)	(mg)	(mole)	(ppm)	(mg)	(mole)		(^{o}C)	(mL)	(mL)		(ppm)	(M)	
PO	PO	PO	Au_o	Au_o	Au_o	pH	CP	V_s	V_w	$(PO/Au)_o$	Au_w	Au_w	%E
1	100	1.623E-04	1	0.01	5.07614E-08	2.93	48	0.45	9.55	3198.05	0.1282	6.506E-07	87.76
1	100	1.623E-04	1	0.01	5.07614E-08	2.93	48	0.45	9.55	3198.05	0.1282	6.506E-07	87.76
1	100	1.623E-04	2.5	0.025	1.26904E-07	2.47	47.5	0.45	9.55	1279.22	0.4736	2.404E-06	81.91
1	100	1.623E-04	2.5	0.025	1.26904E-07	2.47	47.5	0.45	9.55	1279.22	0.4681	2.376E-06	82.12
1	100	1.623E-04	5	0.05	2.53807E-07	2.12	48	0.35	9.65	639.61	1.3652	6.930E-06	73.65
1	100	1.623E-04	5	0.05	2.53807E-07	2.12	48	0.35	9.65	639.61	1.5580	7.909E-06	69.93
1	100	1.623E-04	10	0.1	5.07614E-07	1.91	47.5	0.3	9.7	319.81	1.6048	8.146E-06	84.43
1	100	1.623E-04	10	0.1	5.07614E-07	1.91	47.5	0.3	9.7	319.81	1.6382	8.316E-06	84.11

Table A-16 Raw data of CPE at 70 ^{o}C, PONPE-9 = 1% w/v (Chapter 4)

(%)	(mg)	(mole)	(ppm)	(mg)	(mole)		(^{o}C)	(mL)	(mL)		(ppm)	(M)	
PO	PO	PO	Au_o	Au_o	Au_o	pH	CP	Vs	Vw	$(PO/Au)_o$	Au_w	Au_w	%E
1	100	1.623E-04	1	0.01	5.076E-08	2.85	49	0.3	9.7	3198.05	0.0780	3.960E-07	92.43
1	100	1.623E-04	1	0.01	5.076E-08	2.85	49	0.3	9.7	3198.05	0.0390	1.980E-07	96.22
1	100	1.623E-04	2.5	0.025	1.269E-07	2.34	50	0.3	9.7	1279.22	0.5405	2.744E-06	79.03
1	100	1.623E-04	2.5	0.025	1.269E-07	2.34	50	0.3	9.7	1279.22	0.6018	3.055E-06	76.65
1	100	1.623E-04	5	0.05	2.538E-07	2.21	49.5	0.3	9.7	639.61	2.2456	1.140E-05	56.43
1	100	1.623E-04	5	0.05	2.538E-07	2.21	49.5	0.3	9.7	639.61	0.9083	4.611E-06	82.38
1	100	1.623E-04	10	0.1	5.076E-07	2.06	50	0.3	9.7	319.81	5.8899	2.990E-05	42.87
1	100	1.623E-04	10	0.1	5.076E-07	2.06	50	0.3	9.7	319.81	5.5890	2.837E-05	45.79

Table A-17 Raw data of CPE at 80 ^{o}C, PONPE-9 = 1% w/v (Chapter 4)

(%)	(mg)	(mole)	(ppm)	(mg)	(mole)		(^{o}C)	(mL)	(mL)		(ppm)	(M)	
PO	PO	PO	Au_o	Au_o	Au_o	pH	CP	Vs	Vw	$(PO/Au)_o$	Au_w	Au_w	%E
1	100	1.623E-04	1	0.01	5.076E-08	2.85	49	0.3	9.7	3198.05	0.0056	2.829E-08	99.46
1	100	1.623E-04	1	0.01	5.076E-08	2.85	49	0.3	9.7	3198.05	0.0000	0.000E+00	100.00
1	100	1.623E-04	2.5	0.025	1.269E-07	2.34	50	0.3	9.7	1279.22	0.1003	5.091E-07	96.11
1	100	1.623E-04	2.5	0.025	1.269E-07	2.34	50	0.3	9.7	1279.22	0.1616	8.203E-07	93.73
1	100	1.623E-04	5	0.05	2.538E-07	2.21	49.5	0.3	9.7	639.61	1.0086	5.120E-06	80.43
1	100	1.623E-04	5	0.05	2.538E-07	2.21	49.5	0.3	9.7	639.61	0.5684	2.885E-06	88.97
1	100	1.623E-04	10	0.1	5.076E-07	2.06	50	0.3	9.7	319.81	5.4330	2.758E-05	47.30
1	100	1.623E-04	10	0.1	5.076E-07	2.06	50	0.3	9.7	319.81	5.4553	2.769E-05	47.08

Table A-18 Raw data of temperature effect on percent extraction of gold (Chapter 4)

Settling Temperature = 60°C		Settling Temperature = 65°C	
Time	Ci/Co	Time	Ci/Co
0.00	1.000	0	1
0.50	0.444	0.5	0.3226
1.00	0.112	1	0.1094
1.50	0.114	1.5	0.0802
2.00	0.163	2	0.0663
2.50	0.137	2.5	0.03
3.00	0.148	3	0.0286
6.00	0.070	3.5	0.0202
11.00	0.065	6	0
		11	0

Table A-19 Raw data of NaCl concentration effect on percent extraction of multimetals (Chapter 4)

[NaCl] M	Percent Extraction			
	Zn^{2+}	Cu^{2+}	Au^{3+}	Ni^{2+}
0	0	0	84.005	1.68999
0.2446	0	0	87.225	1.52028
0.4891	0	0.045	83.5	1.64049
0.7337	0	0.04	77.695	2.36881

Table A-20 Raw data of NaCl concentration effect on percent extraction of multimetals (Chapter 4)

pH	Percent Extraction			
	Au^{3+}	Cu^{2+}	Ni^{2+}	Zn^{2+}
2.935	92.39	0	12.8	0
3.9	96.47	0	10	0
3.085	96.8	4.29	10	0
2.065	94.77	2.8	10	0
1.41	85.87	0	9.98	0
0.97	81.35	0	9.97	0

Table A-21 Raw data of surface tention of PONPE-9 in the absence of gold (III) ion (Chapter 5), syringe information, r=0.10425 mm and V^3/L = 0.01138586 cm^3/mm

m_{PO}	m	Surface Tension
0.005	0.005	57.69
0.01	0.01	51.02
0.011	0.011	50.14
0.013	0.013	47.46
0.017	0.017	44.90
0.02	0.02	43.11
0.026	0.026	41.00
0.03	0.03	39.56
0.034	0.034	38.66
0.038	0.038	37.53
0.042	0.042	36.85
0.051	0.051	35.84
0.057	0.057	34.77
0.065	0.065	33.77
0.069	0.069	33.22
0.074	0.074	32.45
0.075	0.075	32.27
0.077	0.077	31.68
0.079	0.079	31.94
0.08	0.08	31.64
0.08	0.08	31.49
0.082	0.082	31.38

m_{PO}	m	Surface Tension
0.083	0.083	31.49
0.084	0.084	31.36
0.085	0.085	31.45
0.087	0.087	31.43
0.093	0.093	31.38
0.099	0.099	31.34
0.114	0.114	31.21
0.12	0.12	31.19

Table A-22 Raw data of surface tention of PONPE-9 in the presence of gold (III) ion at pH = 3, syringe information, r=0.10425 mm and V^3/L = 0.01138586 cm^3/mm (Chapter 5)

m_{PO}	m	Surface Tension
0.005	0.079	57.52
0.01	0.158	50.02
0.013	0.198	46.80
0.016	0.251	44.59
0.02	0.313	42.52
0.022	0.351	41.97
0.028	0.439	39.10
0.033	0.519	38.08
0.039	0.608	37.02
0.045	0.704	35.19
0.05	0.788	34.85
0.06	0.942	32.93
0.064	1.014	32.38
0.07	1.101	32.15
0.075	1.185	32.38
0.077	1.214	32.48
0.08	1.259	31.96
0.087	1.377	31.96
0.099	1.557	32.04

Table A-23 Raw data of surface tension of PONPE-9 in the presence of gold (III) ion at pH = 10, syringe information, r=0.10425 mm and V^3/L = 0.01138586 cm^3/mm (Chapter 5)

m_{PO}	m	Surface Tension	m_{PO}	m	Surface Tension
0.005	0.078	58.03603	0.062	0.981	34.10961
0.005	0.079	56.61055	0.0645	1.016	33.00218
0.01	0.157	55.59978	0.065	1.026	34.0405
0.01	0.156	48.9758	0.07	1.109	32.36607
0.015	0.238	47.52756	0.074	1.166	31.84469
0.015	0.236	44.95503	0.078	1.227	32.19237
0.0176	0.277	44.70825	0.08	1.256	33.09461
0.02	0.31	43.43863	0.081	1.282	31.68231
0.025	0.394	42.35725	0.085	1.34	31.25277
0.025	0.392	40.66227	0.0875	1.38	31.54306
0.03	0.474	39.42633	0.09	1.412	31.96063
0.034	0.539	39.81225	0.094	1.486	31.05521
0.035	0.55	38.14109	0.1	1.577	32.53968
0.0395	0.623	39.3014	0.1	1.568	31.1482
0.04	0.629	39.38091	0.103	1.619	30.92732
0.045	0.712	36.26824	0.11	1.745	31.05521
0.045	0.705	36.24535	0.115	1.805	31.36892
0.05	0.788	34.70798	0.12	1.9	31.56628
0.055	0.868	35.19055	0.12	1.859	31.1482
0.055	0.867	33.93681	0.125	1.996	31.276
0.059	0.937	33.67168	0.13	2.053	31.12495
0.062	0.981	34.10961			

Table A-24 Raw data of surface tension of PONPE-9 in the presence of gold (III) ion at pH = 7, syringe information, r=0.10425 mm and V^3/L = 0.01138586 cm^3/mm (Chapter 5)

m_{PO}	m	Surface Tension	m_{PO}	m	Surface Tension
0.005	0.079	57.309	0.08	1.26	32.182
0.01	0.157	52.435	0.082	1.292	31.728714
0.015	0.235	45.907	0.084	1.323	31.392
0.0173	0.273	45.279	0.084	1.32	31.055214
0.0225	0.355	42.532	0.085	1.337	31.543
0.025	0.394	42.103	0.0875	1.372	31.334078
0.03	0.473	40.155	0.088	1.38	31.532
0.035	0.555	38.790	0.089	1.406	31.590
0.04	0.633	37.878	0.0895	1.403	30.648089
0.047	0.738	36.069	0.093	1.47	30.996
0.053	0.829	34.966	0.094	1.47	30.787735
0.058	0.913	34.321	0.099	1.565	30.950
0.062	0.979	33.871	0.101	1.58	30.648089
0.0675	1.063	33.421	0.103	1.624	31.206
0.069	1.092	33.213	0.11	1.729	31.194
0.073	1.145	32.704	0.116	1.832	31.090
0.075	1.182	32.240	0.116	1.816	31.334078
0.079	1.241	31.844691	0.124	1.946	31.148
0.08	1.26	32.182	0.143	2.239	31.217915

APPENDIX B
Thermodynamic Relation for Surface Adsorption and Micelle Formation of Surfactant.

Since the system under consideration consists of air and the aqueous solution of nonionic surfactant 1, the Gibbs-Duhem equation of the system is given by

$$sdT - vdP + Ad\gamma + n_W d\mu_W + n_1 d\mu_1 + n_a d\mu_a = 0 \qquad \text{(B1)}$$

where γ = surface tension
A = area of plane surface
s = entropy
v = volume
n = number of mole
μ = chemical potential

Subscript w, 1 and a designate water, surfactant 1 and air, respectively.

The fundamental equation describing adsorption behavior of the surfactant at the water/air interface is written in the following form

$$d\gamma = -s^H dT + v^H dp - \Gamma_1^H d\mu_1 \qquad \text{(B2)}$$

where y^H is the surface excess quantity per unit area and defined with respect to the two dividing planes making the excess numbers of mole of water and air zero simultaneously, and Γ_1^H is the surface density of surfactant. Assuming the aqueous solution of surfactant to be ideally at a concentration around the cmc and adopting T, p and the molality of monomeric surfactant m_1 as the independent variables, the total differential of the chemical potential of surfactant μ_1 is expressed as

$$d\mu_1 = -s_1 dT + v_1 dp + (RT / m_1^w) dm_1^w, \qquad \text{(B3)}$$

where y_1 is the partial molar thermodynamic quality of monomeric surfactant in the solution. Substituting of Eq. B3 into Eq. B2 and gives

$$d\gamma = -\Delta s(1) dT + \Delta v(1) dp + \frac{RT}{m_1^w} \Gamma_1^H dm_1^w \qquad \text{(B4)}$$

where

$$\Delta y\,(1) \;=\; y^{\mathrm{H}} \;-\; \Gamma_1^{\mathrm{H}}\, y_1 \qquad \text{(B5)}$$

Since m_1^{w} is equal to the total molality of surfactant m_1, below the cmc, Γ_1^{H} value is calculated by applying the following equation to the γ versus m_1 curve.

$$\Gamma^{\mathrm{H}} \;=\; -\frac{m_1}{RT}\left(\frac{\partial\gamma}{\partial m_1}\right)_{T,p} \qquad \text{(B6)}$$

Entropy Change Associated with the Adsorption of Surfactant Δs

From the experimental viewpoint, the total molality of surfactant m_1 is more appropriate than m_1^{w} as the variable. From Eq.B4, therefore, $\Delta s\,(1)$ relates to the derivative of γ against T at constant m_1 under atmospheric pressure:

$$(\partial\gamma \,/\, \partial T)_{p,m_1} \;=\; -\Delta s\,(1) \;+\; (RT \,/\, m_1^{\mathrm{w}})\,\Gamma_1^{\mathrm{w}}\,(\partial m_1^{\mathrm{w}} \,/\, \partial T)_{p,m_1} \qquad \text{(B7)}$$

Since the micelles are not expected to exist in the solution at concentrations below the cmc (C), m_1^{w} is equal to m_1, and Eq. B7 is reduced to

$$(\partial\gamma \,/\, \partial T)_{p,m_1} \;=\; -\Delta s\,(1) \qquad\qquad m_1 < C \qquad \text{(B8)}$$

At concentration above the cmc, since the m_1^{w} value is approximately equal to molality at the cmc, then

$$(\partial\gamma \,/\, \partial T)_{p,m_1} \;=\; -\Delta s\,(1) \;+\; (RT \,/\, C)\,\Gamma_1^{\mathrm{w}}\,(\partial C \,/\, \partial T)_{p,m_1} \qquad\qquad m_1 \geq C \qquad \text{(B9)}$$

When micelle is assumed to be treated thermodynamically as a macroscopic phase, the behavior of micelles in a limited concentration range near the cmc is determined solely by T and p. So the total differential of the chemical potential of micelle μ^{M} is expressed as

$$d\mu^{\mathrm{M}} \;=\; -s^{\mathrm{M}}\,dT \;+\; v^{\mathrm{M}}\,dp\;, \qquad \text{(B10)}$$

where y^{M} is the excess thermodynamic quantity of micelle which is defined with reference to spherical dividing surface, making the excess number of moles of water zero. Since the monomeric surfactants are in equilibrium with surfactants in micellar state, chemical potential of micelle μ^{M} is given by

$$\mu^{\mathrm{M}} \;=\; N_1^{\mathrm{M}}\,\mu_1\,, \qquad \text{(B11)}$$

where N_1^{M} is the number of surfactant molecules in the micelle.

Substituting Eqs. B10 and B11 into Eqs B2, then, gives

$$d\gamma \;=\; -\Delta s\,(\mathrm{M})\,dT \;+\; \Delta v\,(\mathrm{M})\,dp\;, \qquad \text{(B12)}$$

where $\Delta y\,(\mathrm{M})$ is the thermodynamic quantity of adsorption of surfactant from the micellear state per unit surface area defined by

$$\Delta y\,(\mathrm{M}) = y^{\mathrm{H}} - \Gamma_1^{\mathrm{H}}(y^{\mathrm{M}} / N_1^{\mathrm{M}}) \,. \qquad \text{(B13)}$$

The temperature dependence of surface tension gives $\Delta s\,(\mathrm{M})$ at concentration above the cmc, therefore the following equation is obtained

$$(\partial\gamma / \partial T)_{p,m_1} = -\Delta s\,(\mathrm{M}) \qquad \text{(B14)}$$

Consequently, from Eqs. B8 and B14, the value of $(-\partial\gamma / \partial T)$ provides $\Delta s\,(1)$ below the cmc and $\Delta s\,(M)$ above the cmc. The $\Delta s\,(1)$ value and $\Delta s\,(\mathrm{M})$ value, which are respectively estimated by applying Eqs. B8 and B14 to the γ versus T curves.

The entropy change associated with the micelle formation $\Delta_{\mathrm{w}}^{\mathrm{M}}s$ defined by

$$\Delta_{\mathrm{W}}^{\mathrm{M}}s = s^{\mathrm{M}} / N_1^{\mathrm{M}} - s_1 \,. \qquad \text{(B15)}$$

Combination of Eqs. B5, B13, and B15 results on the relation of

$$\Delta_{\mathrm{W}}^{\mathrm{M}}s = [\Delta s\,(1) - \Delta s\,(\mathrm{M})] / \Gamma_1^{\mathrm{H}} \,. \qquad \text{(B16)}$$

Comparing Eqs.B9 and B14, it is found that the difference between $\Delta s\,(1)$ and $\Delta s\,(\mathrm{M})$ at the cmc is related to the temperature dependence of cmc by the equation

$$[\Delta s\,(1) - \Delta s\,(\mathrm{M})] / \Gamma_1^{\mathrm{H}} = -(RT / C)(\partial C / \partial T)_p \qquad \text{(B17)}$$

As a consequence, the $\Delta_{\mathrm{w}}^{\mathrm{M}}s$ value can be evaluated by two ways, that is, one way is by use of the left hand side of Eq. B17, the other is by use of the right hand side of Eq. B17.

APPENDIX C

The Calculation of PONPE-9 in Surfactant-Rich Phase

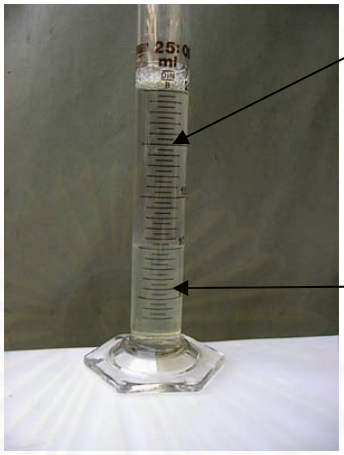

$$[PONPE]_s = \left(\frac{V_t [PONPE - 9]_o - V_w [PONPE - 9]_w}{V_s} \right) 100$$

where $[PONPE\text{-}9]_o$ = initial PONPE-9 concentration

$[PONPE\text{-}9]_w$ = PONPE-9 concentration in water-rich phase after CPE (%(w/v))

$[PONPE\text{-}9]_s$ = PONPE-9 concentration in surfactant-rich phase after CPE

V_t = total volume (cm^3)

V_s = the volume of surfactant-rich phase (cm^3)

V_s = $V_t - V_s$ (cm^3)

VITA

Kanda Wongwailikhit was born on January 28, 1961, in Petchabun province, Thailand. She received the Bachelor's Degree in Chemistry from the Faculty of Science, Mahidol University in 1981 and Master's Degree in Energy Technology, Faculty of Energy and Material, King Mongkut's Institute of Technology in 1984.